STARS

Electronic Theses and Dissertations

2017

Chaperonin Containing TCP1 (CCT) as a Target for Cancer Therapy

Ana Carr
University of Central Florida

STARS Citation

University of Central Florida

STARS
Showcase of Text, Archives, Research & Scholarship

CHAPERONIN CONTAINING TCP1 (CCT) AS A
TARGET FOR CANCER THERAPY

by

ANA CAROLINA CARR
B.S. University of Central Florida, 2012

A dissertation submitted in partial fulfillment of the requirements
for the degree of Doctor of Philosophy
in the Cancer Division
of the Burnett School of Biomedical Sciences
in the College of Medicine
at the University of Central Florida
Orlando, Florida

Fall Term
2017

Major Professor: Annette Khaled

ABSTRACT

Treatments for aggressive cancers like triple negative breast cancer (TNBC) and small-cell lung cancer (SCLC) have not improved and remain associated with debilitating side effects. There is an unmet medical need for better, druggable targets and improved therapeutics. To this end, we investigated the role of Chaperonin-Containing TCP1 (CCT), an evolutionarily conserved protein-folding complex composed of eight subunits (CCT1-8), in oncogenesis. Our laboratory was the first to report that the CCT2 subunit is highly expressed in breast cancer and could be therapeutically targeted. To determine whether CCT is a marker of disease progression in other cancers, we analyzed CCT2 gene expression in liver, prostate and lung cancer, using publicly available genetic databases, and confirmed findings by assessing CCT2 and client proteins, like STAT3, in tumor tissues by immunohistochemistry. We found that CCT2 was high in all cancers, especially SCLC, and correlated with decreased patient survival. We tested CT20p, the peptide therapeutic developed by our laboratory to inhibit CCT, on SCLC and primary lung cells, finding that CT20p was cytotoxic to SCLC cells. Since SCLC currently lacks targeted therapeutics, our work yielded a new targeted agent that could improve lung cancer mortality. To establish a mechanism of action for CT20p, we partially knocked out CCT2 in TNBC cells, which decreased tumorigenicity in mice and reduced levels of essential proteins like STAT3. To confirm, we overexpressed CCT2 in non-tumorigenic cells and conferred tumor-like characteristics such as increased migration and elevated STAT3. These studies positioned us to develop and validate a strategy for discovery of new small molecule inhibitors of CCT. We thus advanced the field of cancer research by

demonstrating that CCT could have diagnostic potential for cancers, such as SCLC and TNBC, that are a significant cause of human death and showed that targeting CCT is a promising therapeutic approach.

Dedicated to

my daughter and my son

ACKNOWLEDGMENTS

TABLE OF CONTENT

LIST OF FIGURES

LIST OF TABLES

LIST OF ABBREVIATIONS

ANOVA   analysis of variance

ATCC   American Type Culture Collection

ATP   adenosine triphosphate

CCT   chaperonin containing TCP1, with subunits denoted by number

CT20p   CT20 peptide

CT20p-NPs   CT20p encapsulated in nanoparticle

DiI   1,1'-dioctadecyl-3,3,3'3'-tetramethylindocarbocyanine perchlorate

DMEM   Dulbecco's modified Eagle's Media

DMSO   dimethyl sulfoxide

DNA   deoxyribonucleic acid

EDTA   Ethylenediaminetetraacetic acid

EGF   epidermal growth factor

EMT   epithelial-mesenchymal transition

ER   estrogen receptor

ER stress   endoplasmic reticulum stress

FBS   fetal bovine serum

H & E   hemotoxylin and eosin

HBPE-NPs   hyperbranced polyester nanoparticles

HCC   hepatocellular carcinoma

HEPES   4-(2-hydroxyethyl)-1-piperazineethanesulfonic acid

Her2   human epidermal growth factor receptor 2

HSP90 heat shock protein 90

IACUC Institutional Animal Care and Use Committee

IDC invasive ductal carcinoma

IRB Institutional Review Board

I-Trp N-iodoacetyl-tryptophan

MCF-10A Michigan Cancer Foundation 10A, human breast epithelial cell line

MCF-10A(CCT) MCF-10A cells transiently transfected to overexpress CCTβ

MCF-10A(T) MCF-10A cells that have undergone spontaneous EMT-like transformation

MDA-MB-231 MD Anderson metastatic breast 231, human carcinoma cell line

NPs nanoparticles

NP-40 nonyl phenoxypolyethoxylethanol

PBS phosphate-buffered saline

PVDF polyvinylidene difluoride

mRNA messenger RNA

RPMI Roswell Park Memorial Institute media

SDS-PAGE sodium dodecyl sulfate polyacrylamide gel electrophoresis

SCLC small-cell lung cancer

SqCLC squamous cell lung canrcinoma

STAT3 Signal transducer and activator of transcription 3

TMA tissue microarray

TNBC triple negative breast cancer

TNM The TNM Classification of Malignant Tumors

WT wild-type;

CHAPTER 1:INTRODUCTION

<u>Preface</u>

This chapter was composed entirely by A.C.C. Comments from A.K. were incorporated into the final version presented here.

The Burden of Cancer

Cancer is the second leading cause of death in the United States and accounts for nearly 1 in every 4 fatalities [1, 2]. For the year of 2017, it is estimated that 600,920 people will die due to cancer in the United States alone (Table1), that's equivalent to 1,650 deaths per day [3]. In regards to cancer incidence, it is estimated that 1,688,780 people will be diagnosed with cancer in 2017, that equates to over 4,600 people being diagnosed with cancer daily [3]. The most commonly diagnosed type of cancer in women is breast cancer. In the U.S., the chances of a woman being diagnosed with breast cancer during her lifetime is 1 in 8 or 12.4% [4]. That's an increase from the 9.09% 1970's rate. Part of this increase is due to longer life expectancy in addition to increased incidence [4]. The most commonly diagnosed type of cancer in men is prostate cancer. The lifetime risk of a man developing prostate cancer is 11.6% based on 2012-2014 data. Overall, rate of cancer incidence is 20% higher in men than in women, while rate of cancer fatalities is 40% higher [5]

Lung Cancer

Lung cancer is the deadliest type of cancer in the United States and Worldwide, being responsible for more deaths than prostate, breast and colorectal cancer combined [6]. There are two major classes of lung cancer: non-small cell lung cancer (NSCLC) and small cell lung cancer (SCLC). NSCLC is responsible for more than 80% of cases and its

further subdivide into three subtypes based on histological characteristics: adenocarcinoma (AdC), squamous cell carcinoma (SqCLC) and large cell carcinoma (LCC). SCLC accounts for 10 to 15% of cases. SCLC is more aggressive, faster spreading, and more likely to recur than NSCLC. It is associated with a 5-year survival rate of only 6%, compared to 21% for NSCLC [6]. The 5- year survival rate of lung cancer is only 17.8%, which is much lower than the 90.5% and 99.6% survival rates for breast and prostate cancer, respectively [2]. Frequently, the symptoms associated with lung cancer do not appear until the cancer is advanced, a factor that contributes to the severity of this disease. Over 50% of lung cancers are only detected after the tumor has metastasized from the primary site, and the 5-year survival rate for these cases are 4% [2]. SCLC is a carcinoma of neuroendocrine origin and it is characterized by aggressive behavior, fast growth and high metastatic spread [7]. Treatments for SCLC include cisplatin and etoposide and although about 75% of tumors respond to chemotherapy, only 25% show complete response and most patients experience disease relapse [8, 9]. Attempts to improve outcome using combination therapy or prolonged regimens, have not been successful.

Breast Cancer

Breast cancer is the second leading cause of death in women [3]. There's a 12.4% risk of a woman developing breast cancer during her lifetime, that is one in eight women will be diagnosed with breast cancer [1, 6]. About 90% of deaths caused by breast cancer are due to metastatic disease [10]. Metastasis occurs when tumor cells leave the primary

site and invade distant, vital organs such as lungs, brain and liver, in which case, currently available chemotherapeutics are no longer effective. Breast cancer is a heterogeneous disease and while certain subtypes of breast cancer, such as ER+, benefit from hormone therapy and are associated with better prognosis, subtypes such as triple negative breast cancer (TNBC) are associated with lower survival rate and poor prognosis [11]. TNBC affects 17% of breast cancer patients and it is characterized by the absence of estrogen (ER) and progesterone (PR) hormone receptors, as well human epidermal growth factor receptor 2 (Her2) so patients diagnosed with TNBC cannot benefit from hormone therapies or Her2 inhibitors [11]. TNBC is the most aggressive form of breast cancer, marked by genomic instability, heterogeneity, high incidence of drug resistance, high recurrence rates and increased risk of metastasis. The aggressive biology of TNBC and the lack of approved targeted agents have contributed to the challenges associated with treating this disease successfully [12].

<u>The challenge</u>

Current treatment strategies for patients diagnosed with cancer include surgery, radiation therapy and chemotherapy. Surgery is usually recommended for patients with solid tumors that are limited to one area and it is not an option in patients with metastatic disease. Radiation therapy can be given with curative, palliative intent or as a prophylactic measurement as exemplified by small cell lung cancer patients who often

receive prophylactic cranial irradiation to reduce the risk of brain metastases [Takahashi, 2017 #165]. Traditional chemotherapeutic agents, or cytotoxics, can target the cell cycle in a specific manner, being most effective during S or M phase, or in a non-specific manner (independent of cell cycle phase). Side effects associated with traditional chemotherapy are debilitating and often have a negative impact on the patient's quality of life. Additionally, due to tumor heterogeneity, positive selection of drug-resistant tumor subpopulation tumor may lead to tumor recurrence. Resistance to chemotherapies and targeted therapies limits the effectiveness of current cancer treatments Oncology drugs that go into clinical trial have poor success rates, being three times lower than that of cardiovascular disease [13]. There is a fundamental flaw in the way we have looked at cancer treatments so far. How can we redefine our approach?

The dynamic duo

CT20p: the rationally developed peptide

CT20p is an amphipathic peptide derived from the last twenty amino acids in the C-terminus of the pro-apoptotic Bax [14] (Fig. 1). CT20p had cytotoxicity activity that was independent of the parent protein or Bcl-2 overexpression and caused cytoskeletal disorganization, loss of adhesion, and cell death [14, 15]. CT20p is membrane impermeable but can be encapsulated for delivery to cancer cells in nanoparticles (NPs) made from a hyperbranched, polyester polymer (HBPE) [16, 17]. The resulting HBPE-

CT20p has increased serum half-life in addition to having the potential of being modified to contain different groups, which allows targeting of tumor cells. In animal models of breast and prostate cancer, treatment with CT20p-NPs caused significant tumor regression [18, 19]. In order to determine the target of CT20p, a pull down experiment was performed and the target proteins were subjected to mass spectroscopy analysis (Fig. 2). The top results from the pull down experiment are shown in Table 2 and indicate that CT20p interacts with 7 out 8 subunits (numbers 5-11 on the list) of the chaperonin containing TCP1 (CCT). Transient overexpression of CCT2 (denoted CCTβ in figure 3) in cells with low CCT2 levels, increased susceptibility to the peptide (Fig. 3). Conversely, silencing the CCT2 gene in cells highly susceptible to the peptide, decreased susceptibility [18].
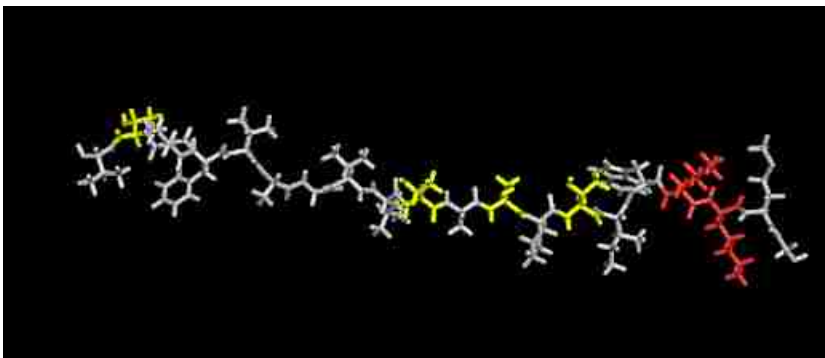
Figure 1: Amino acid sequence and structure of CT20p

This figure illustrates the amphipathic nature of CT20p. Polar residues are shown in yellow, hydrophobic residues are shown in light grey and basic residues are shown in red. CT20p structure was rendered using PyMol by the author.
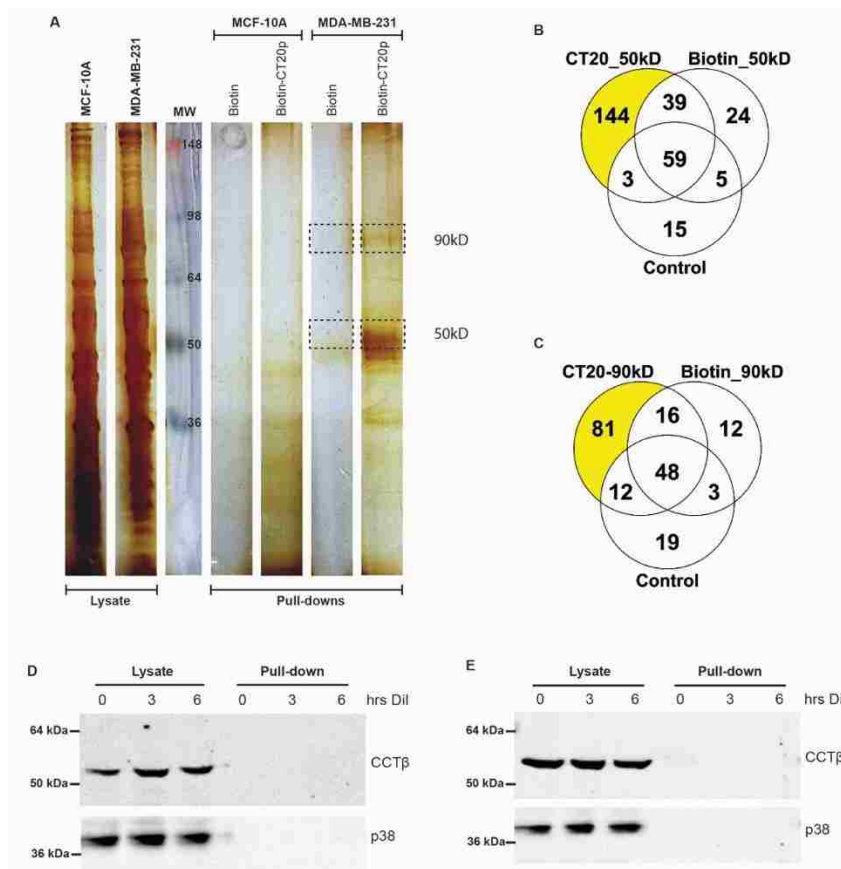
Figure 2: Biotin-CT20p pull down

(A) Biotin-CT20p was used to pull down interaction proteins in MCF-10A and MDA-MB-231 lysates. Lysates were run on SDS-PAGE, and the gel was silver stained to visualize bands. Molecular weights (MW) indicated are in kDa. Four bands, indicated by boxes, were excised from MDA-MB-231 Biotin-CT20p and biotin pull downs and analyzed by mass spectrometry. All lanes presented were originally run on the same gel, but have been rearranged for clarity in this figure. (B-C) To analyze true binding to CT20p, proteins also identified in the biotin pull down or control gel sample were excluded. This resulted in 114 true binding partners in the 50 kDa band (B), and 81 in the 90 kDa band (C). (D-E) As a control for the "in-cell" pull down, DiI dye encapulated in HBPE-nanoparticles was delivered to viable MCF-10A (D) and MDA-MB-231 (E) cells, followed by cell lysis and recovery of bound proteins. CCTβ and p38 were detected by Western blot - Reprinted from Clinical Cancer Research, 2016, Volume 22, Issue 17, Rania Bassiouni et al., "Chaperonin Containing-TCP-1 Protein Level in Breast Cancer Cells Predicts Therapeutic Application of a Cytotoxic Peptide", with permission from AACR
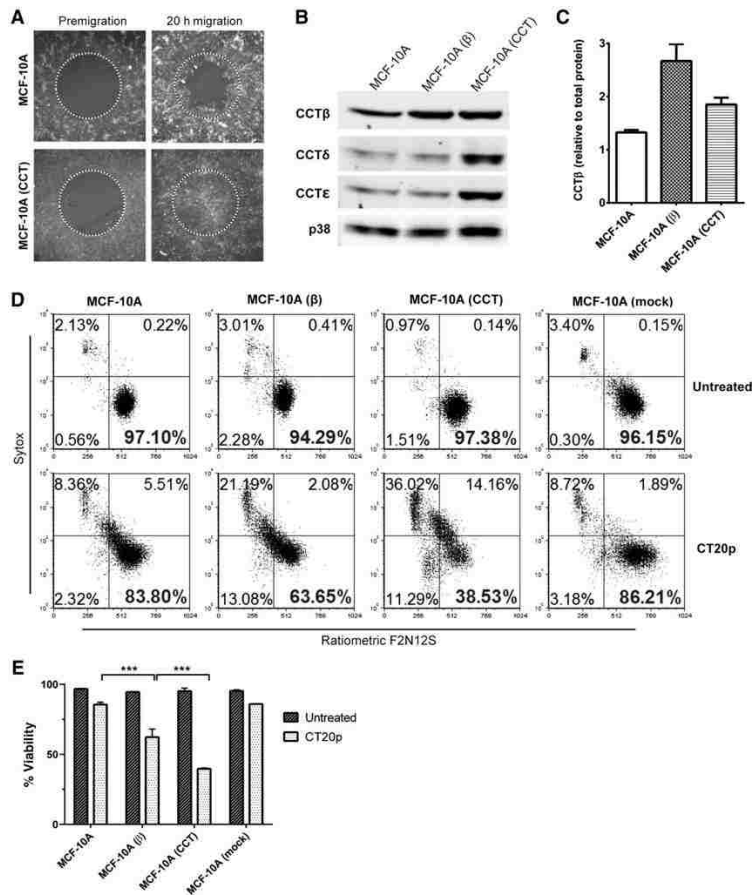
Figure 3: CCT overexpression increases the susceptibility of MCF-10A cells to CT20p

(A) MCF-10A and MCF-10A (CCT) cells were subjected to a migration assay for 20 hours. The premigration area is outlined. (B) MCF-10A cells were transfected to overexpress CCTb are denoted here as MCF-10A (b). The levels of CCT subunits were examined by immunoblotting in these cells, as well as in MCF-10A and MCF-10A (CCT) cells. p38 MAPK is used as a loading control. (C) level of CCTb relative to total protein was quantified in the three MCF-10A variants. (D) MCF-10A variants were treated with CT20p at a dose of 75 mg/mL for 24 hours. Cell death discrimination was determined by staining with Sytox AADvanced and F2N12S, followed by flow cytometry. The viable cells are in the lower-right quadrant, and their percentage is displayed in bold. As a control, mock-transfected MCF-10A were similarly analyzed. E, viability data of the MCF-10A variants was quantified. = *** = p<0.001, **** = p<0.0001- Reprinted from Clinical Cancer Research, 2016, Volume 22, Issue 17, Rania Bassiouni et al., "Chaperonin Containing-TCP-1 Protein Level in Breast Cancer Cells Predicts Therapeutic Application of a Cytotoxic Peptide", with permission from AACR.

CCT: the intracellular target

Chaperones are a group of proteins essential for maintaining proteostasis by stabilizing other proteins and helping them reach their native conformation [20]. Chaperonins (a class of chaperones) are formed by two rings stacked back-to-back, forming a central cavity in which unfolded client proteins are sequestered into and can reach native conformation isolated from the cytosol [21]. Chaperonins are further subdivided into Group I, present in bacteria, mitochondria and chloroplast, and Group II, found in archaea and eukaryotes [21]. The eukaryotic chaperonin containing TCP1 (CCT), also known as TriC, is a type II chaperonin composed of two stacked rings, each ring consisting of eight paralogous subunits (Fig. 4). Subunits of the mammalian CCT are named using Greek letters (CCTα - CCTθ) and subunits in yeast are denoted using numbers (CCT1-CCT8). Subunits range from 50kDa-60kDa [21, 22].

CCT subunits are structural homologues and each subunit comprises an apical substrate binding domain, an equatorial ATP binding domain and an intermediate domain linking the other two domains (Fig. 5). CCT's ATP binding domain is extensively conserved among the subunits, in contrast with the apical substrate binding domain, which is the most convergent [23]. This 1MDa complex folds about 10% of the eukaryotic proteome in a ATP dependent manner [24]. The nascent peptide is sequestered into the cavity of CCT partially or entirely where energy derived from ATP hydrolysis allows the substrate to achieve native conformation [25].
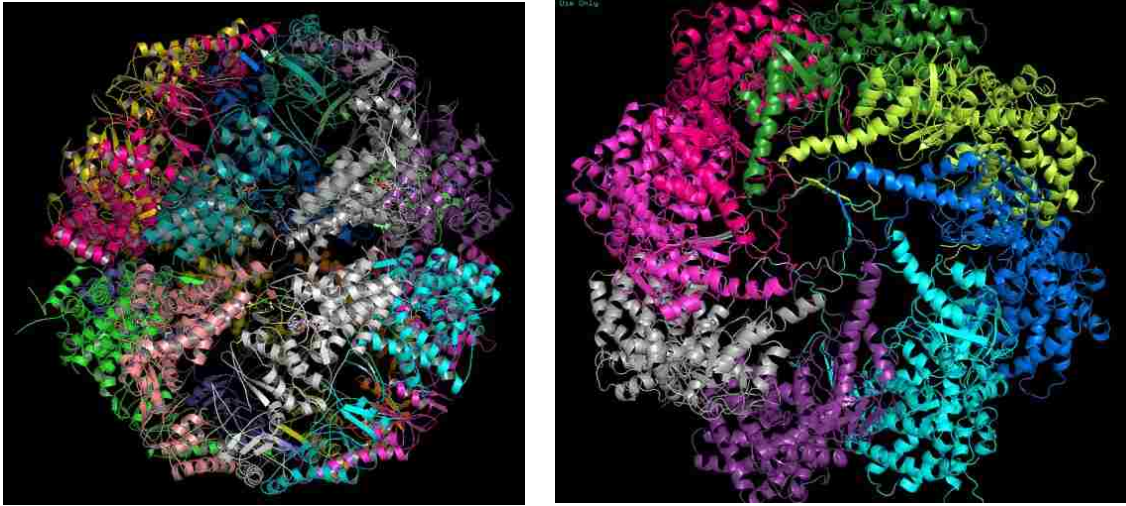
Figure 4: Overall structure of CCT

Structure of yeast CCT showing the closed conformation of the chaperonin and top view showing the arrangement of all eight paralogous subunits. PDB accession number 4V94. Image downloaded and rendered in PyMol by the author [21]
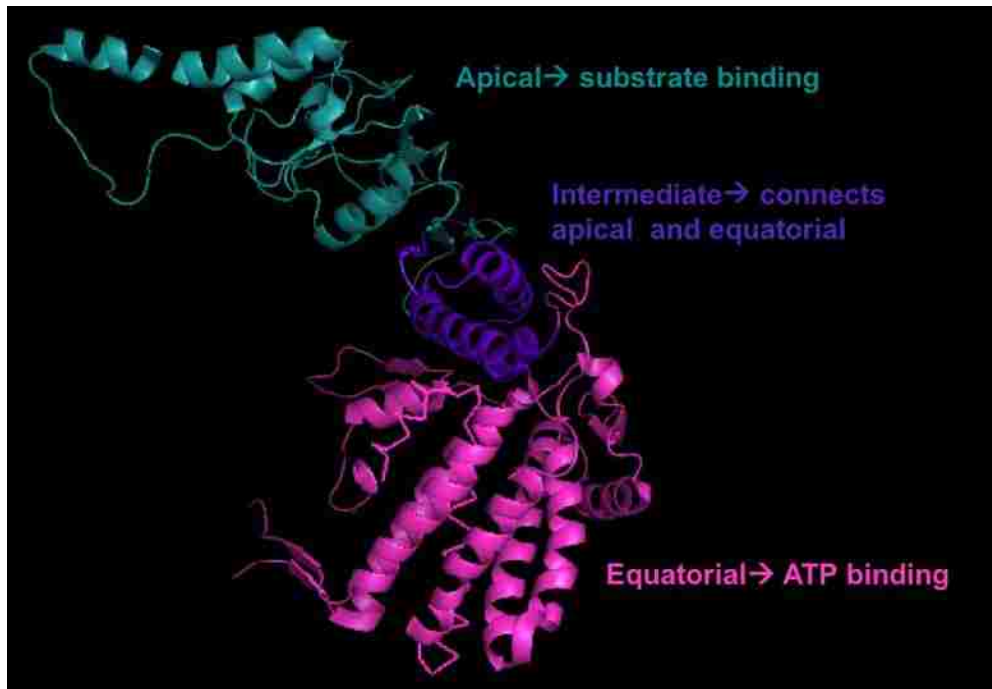
Figure 5: Ribbon diagram of bovine CCT2 subunit

General architecture of CCT subunits exemplified by CCT2 from *bos tauros*. The substrate binding apical domain (teal) is linked to the equatorial, ATP binding domain (fuchsia) by the intermediate domain, a flexible linker that allows CCT transition from open (substrate binding) to closed (ATP binding) forms. Image generated by A.C.C. using structure PDB number 3KTT

CCT clients

Although there is much to be learned in regards to CCT's substrate specificity, a study have showed that about 40% of CCT's substrates are essential and about 90% are oligomeric complexes [24]. Studies on CCT client's diversity using NMR, modeling, XL-MS and mutagenesis suggest that client proteins contact CCT subunits in their apical domain on the same loop [26]. The eight human CCT subunits share 30% homology and are most divergent at the apical domain, indicating subunit specialization acquired through evolution. Cytoskeletal proteins such as actins and tubulins, can only reach their native conformation if CCT mediated [22]. Notably, many of CCT's client proteins are involved in oncogenesis, including Von Hippel-Lindau (VHL), p53, cyclin B and E, Cdc20, Myc and Stat3 [27, 28]. Von Hippel-Lindau protein (VHL) is a tumor suppressor E3 ligase, crucial to the hypoxia response pathway [29]. Loss of function mutations have been associated with hemangioblastomas, retinal angiomas, clear cell renal cell carcinoma, pheochromocytoma; pancreatic neuroendocrine tumor [27, 30]. VHL was the first non-cytoskeletal protein shown to be a CCT client [31]. The tumor suppressor gene TP53 is the most commonly mutated gene in cancers and recent evidence indicates p53 needs CCT for proper folding [32, 33]. CCT also folds and regulates many cell cycle regulatory proteins such as Cyclin E [34], Cyclin B and Cdc20 [35, 36]. Myc is an oncogene involved in the onset of many cancers [37], also folded by CCT. Signal transducer and activator of transcription 3 (Stat3) transduces signals of over 40 peptide hormones from the cell surface to the nucleus and acts as an oncoprotein in several cancers types [28, 38]. Taken together, this indicates that CCT is a key regulator of many proteins necessary for the development of several cancers.

CCT levels in cancer

In addition to assisting in the folding of many proteins involved in oncogenesis and cancer progression, CCT levels are elevated in many cancer types. As an example, the CCT8 subunit was upregulated in hepatocellular carcinoma and played an important role in the proliferation of these cells [39]. A similar correlation was observed with CCT1 (TCP1) and CCT2 in both hepatocellular carcinoma and colonic carcinoma [40] and with CCT2 in colorectal carcinoma. CCT1 and CCT2 may be upregulated by driver oncogenes that are responsible for tumorigenesis in breast cancer [41]. Our own published studies provided evidence that CCT2 is significantly overexpressed in invasive ductal breast carcinoma (IDC) and in TNBC cell lines, like MDA-MB-231 [18], as well as prostate cancer cell lines [19], suggesting the CCT2 levels could correspond to increased disease severity. The elevated levels of CCT subunits in cancer is important in two aspects. Firstly, CCT levels can be used as a biomarker in the clinical setting for early diagnosis of multiple types of cancer as well as a potential marker of disease severity. Secondly, due to its elevated levels in cancer cells compared to normal ones, CCT is also a promising target for cancer therapy.

We suggest that by targeting multiple aspects involved in cancer progression (versus a single mutation or pathway) the probability of recurrence and resistance is greatly diminished. Cancer cells have higher demand for many of CCT's client proteins, therefore CCT inhibition will prevent the proper folding of key cancer related proteins, halting cancer progression.

Table 1: Estimated new cases and deaths due to cancer for 2017

Primary site	Estimated New Cases			Estimated Deaths		
	Total	Males	Females	Total	Males	Females
All sites	1,688,780	836,150	852,630	600,920	318,418	282,500
Breast	255,180	2,470	252,710	41,070	460	40,610
Prostate	161,360	161,360	-	26,730	26,730	-
Lung and Bronchus	222,500	116,990	105,510	155,870	84,590	71,280

Table reproduced from numbers published in Cancer statistics, 2017 [5]

Table 2: Proteins identified by mass spectrometry to interact with CT20p

Number	Identified protein	Accession number	MW (kDa)	No. of unique peptides
1	Reticulocalbin-2	RCN2_HUMAN	37	10
2	Signal transducer and activator of transcription 1-alpha/beta	STAT1_HUMAN	87	7
3	Coatomer subunit gamma-1	COPG1_HUMAN	98	6
4	Coatomer subunit beta	COPB2_HUMAN	102	6
5	T-complex protein 1 subunit beta	TCPB_HUMAN	57	6
6	T-complex protein 1 subunit delta	TCPD_HUMAN	58	4
7	T-complex protein 1 subunit gamma	TCPG_HUMAN	61	3
8	T-complex protein 1 subunit eta	TCPH_HUMAN	59	3
9	T-complex protein 1 subunit zeta	TCPZ_HUMAN	58	2
10	T-complex protein 1 subunit alpha	TCPA_HUMAN	60	2
11	T-complex protein 1 subunit epsilon	TCPE_HUMAN	60	2
12	Signal transducer and activator of transcription 3	STAT3_HUMAN	88	2
13	Hsp90 co-chaperone Cdc37	CDC37_HUMAN	44	2
14	Cellular tumor antigen p53	P53_HUMAN	44	1
15	Huntingtin	HD_HUMAN	348	1

CHAPTER 2: TARGETING THE CHAPERONIN CONTAINING TCP1 (CCT) AS A THERAPEUTIC FOR SMALL CELL LUNG CANCER

<u>Preface</u>

The work presented in this chapter has material accepted for publication in Oncotarget, Impact Journals, LLC expected publication month is November 2017. The material is reprinted here under the Creative Commons CC BY NC license which permits non-commercial use, distribution and reproduction in any medium, of the original work

Ana C. Carr, Amr S. Khaled, Rania Bassiouni, Orielyz Flores, Daniel Niernenberg, Hammad Bhatti, Priya Vishnubhotla, J. Manuel Perez, Santimukul Santra, and Annette R. Khaled. Targeting the Chaperonin Containing TCP1 (CCT) as a Therapeutic for Small Cell Lung Cancer *Oncotarget*

<u>Introduction</u>

Cancer remains a leading cause of death, with breast, lung, prostate, and colorectal among the top four cancers in terms of new cases diagnosed and estimated deaths [42]. Most cancer-related deaths are due to metastatic disease, when the primary cancer spreads to vital organs like the brain, bone, or liver. A significant impediment to finding effective treatments or better ways to detect and diagnose cancers, especially metastatic cancers, is tumor heterogeneity. Genomic instability, together with selection pressures from the tumor micro-environment, are among the factors that produce genetic and phenotypic differences in patients' tumors and even within the same tumor (intra-tumor heterogeneity). A case in point is small cell lung cancer (SCLC). SCLC accounts for about 15% of lung cancer cases and is characterized by genetic alterations and a high proliferative index as well as early metastatic spread [8]. SCLC is an aggressive disease, and while responsive to initial treatments, patients later succumb to the disease, which is associated with a high rate of relapse and recurrence [43, 44]. SCLC can be further classified as limited stage (LS-SCLC) if the disease is confined to one hemithorax and regional nodes, or as extensive disease (ES-SCLC) if the cancer has spread to distant sites [45, 46]. This classification helps determine the treatment plan for SCLC patients, whether surgery and/or prophylactic cranial irradiation (PCI) are recommended. The first-line treatment for any stage of SCLC is etoposide-platinum based chemotherapy; however, patient survival decreases upon disease recurrence, largely due to the development of chemoresistance [9, 11, 43]. Although SCLC is a good candidate for targeted therapies, clinical trials testing new targeted chemotherapeutics for SCLC

patients have been unsuccessful. As an example, a recent clinical trial using bevacizumab—an angiogenesis inhibitor targeting the vascular endothelial growth factor (VEGF)—in combination with etoposide-platinum based chemotherapy for SCLC patients, concluded that the addition of bevacizumab did not improve patient overall survival [47]. In comparison, in non-small cell lung cancer (NSCLC) patients, modest results were achieved with angiogenesis inhibitors like bevacizumab when used in combination with chemotherapeutics to treat metastatic patients [48, 49]. While there is renewed hope of developing new cancer drugs, especially with the recent focus on immunotherapies, the challenges of achieving a molecularly targeted treatment that provides real benefit for patients with cancers like SCLC are substantial. Central to these challenges is the need to identify druggable molecular alterations through a better understanding of the basic biology underlying these aggressive cancers.

The molecular landscape underlying the heterogeneity of cancers like SCLC is far from understood and complicates cancer drug discovery. While SCLC has not undergone extensive molecular subtyping, it is characterized by a high mutation rate and genomic instability. Inactivation of TP53 and RB1 [50], along with alterations of MYC, NOTCH, and the PI3K/AKT/mTOR pathways, are among the key genetic changes associated with SCLC [51]. Other genes less frequently mutated in SCLC include *EGFR* [52], *KIT* [53], *MET* [54, 55], and heat shock proteins [56]. These genes are also commonly mutated in other cancers. [57]. Using targeted agents to inhibit these pathways is the goal of many studies, but recent findings suggest that single target agents are less effective, and that combination therapies, hitting multiple pathways, are more successful in preventing cancer relapse and drug resistance in patients [58, 59]. A drawback for combination

18

approaches, however, is the potential for increased drug-related off-site toxicities. A rational approach would be to inhibit protein-folding, which could impact multiple pathways while using a single inhibitory agent. Chaperonin-containing TCP-1 (CCT) or T-complex 1 ring protein (TRiC) is an evolutionarily conserved macromolecular complex involved in folding about 10% of the cell proteome [21]. Many of the gene products deregulated in cancers such as SCLC (e.g., *MYC*, *TP53*, *CCNE, KRAS, HSP90, ESR1*, and *NOTCH*) are CCT client proteins [60], suggesting a role for the involvement of CCT in the development of cancer, driving the need to better understand its contribution to malignant transformation.

Collective evidence suggests that CCT may be upregulated in a broad range of cancers. CCT is a hetero-oligomeric complex composed of two rings formed by eight subunits [61]. Each CCT subunit, named CCT1-8 (or CCTα-θ), is found at a fixed position in the ring [21]. Protein folding occurs within a central chamber formed by the rings and is mediated through the opening and closing of a lid structure in an ATP-dependent fashion [62, 63]. A study examining CCT and its activity in cancer cell lines revealed that while these cell lines had varying reliance on the protein-folding activity of CCT, it was more impactful in cancer cells than in normal cells [64]. As an example, in hepatocellular (HCC) carcinoma, the CCT8 subunit was upregulated and played an important role in the proliferation of these cells [39]. A similar correlation was observed with CCT1 (TCP1) and CCT2 in both hepatocellular carcinoma and colonic carcinoma [40], as well as with CCT2 in colorectal carcinoma. In breast cancer, CCT1 and CCT2 may be upregulated by driver oncogenes that are responsible for tumorigenesis [41]. Our own published studies provided evidence that CCT2 is significantly overexpressed in

invasive ductal breast carcinoma and in triple-negative breast cancer (TNBC) cell lines, like MDA-MB-231 [18], as well as prostate cancer cell lines [19]. This suggests that the CCT2 levels could correspond to increased disease severity.

The elevated expression of different CCT subunits in cancer is intriguing on two fronts. First, CCT levels may be useful as a biomarker in clinical settings. Potentially, CCT could be detected as an early diagnostic marker in cancers such as SCLC. Or it could be used for the diagnosis of disease severity in cancers like breast cancer, in which levels of CCT2 correlated with disease progression, as we have previously demonstrated [18]. Second, CCT is a promising target for cancer therapy, as depletion of CCT in cancer cells caused cell cycle arrest and growth inhibition [39, 41]. In previous studies, we showed that an amphipathic peptide called CT20p, derived from the last twenty amino acids of Bax, had cytotoxicity activity that was independent of the parent protein or Bcl-2 overexpression and caused cytoskeletal disorganization, loss of adhesion, and cell death [14, 15]. CT20p, while being membrane impermeable, can be readily encapsulated for delivery to cancer cells in nanoparticles (NPs) made from a hyperbranched, polyester polymer [16, 17]. In animal models of breast and prostate cancer, treatment with CT20p-NPs caused significant tumor regression [18, 19]. The mechanism of action of CT20p is likely inhibition of CCT, as overexpression or deletion of the CCT2 subunit altered the capacity of the peptide to kill cells [18]. In the work presented herein, we examined the protein levels of CCT in tissue samples of liver, prostate, colon, and lung cancer to determine whether CCT subunits were highly expressed in these cancers. We also sought to determine whether inhibition of CCT through treatment with CT20p could impact CCT client proteins needed for cancer progression. To that end, we focused on STAT3, since

20

this transcription factor is a CCT client protein [28], is constitutively active in many tumors [38], and is a predictor of poor prognosis in cancer [38, 65]. Our analysis revealed SCLC to be a promising model to study the role of CCT in cancer, as well as a likely candidate to benefit from CCT-targeted therapy.

Materials & Methods

Immunohistochemistry

Tissue microarrays (TMAs) used in this study were obtained from US Biomax, Inc. Their catalog numbers are as follows: CO484a (colonic carcinoma), PR803b and PR631 (prostate carcinoma), BC03118 (hepatocellular carcinoma), LC726b, LC802a, LC802c, and BC041115a (lung carcinomas) and BN501 (normal tissue array). Each TMA contained varied numbers of patient tissue cores as well as normal tissue corresponding to the specific cancer type being analyzed. Please refer to Table 3 and 4 for the number of samples per cancer type. Information about the tissue type, TNM score, tumor grade, and stage were provided with the samples. TMAs were stained for CCT2 using anti-CCTβ antibody (LS-B4861; LifeSpan Biosciences). TMA LC802c was stained in parallel for CCT2 and Stat3 (anti-Stat3 antibody ab32500; Abcam). Primary antibodies were diluted 1:100 in Antibody Diluent (Leica). Staining of tissue arrays was performed by a Bond-Max Immunostainer (Leica), with an epitope retrieval buffer of EDTA pH 9.0 (Leica). Polymer Refine Detection reagents (Leica) were used, which

include a hematoxylin counterstain. Image acquisition and scoring of staining was performed by a surgical pathologist as previously published [18]

Cell lines and culture condition

NCI-H1882 (ATCC CRL-5903), NCI-H1048 (ATCC CRL-5853), NCI-H1105 (ATCC CRL-5856) and NCI-H719 (ATCC CRL-5837) were cultured in HITES medium supplemented with 5% FBS (Gemini). NCI-H1417 (ATCC CRL-5869) was cultured in RPMI-1640 in 10% FBS. MCF 10A (ATCC CRL-10317) cells were cultured in Mammary Epithelial Cell Growth Media using MEGM bullet kit (Lonza). THLE-2 (ATCC CRL-2706) cells were cultured in Bronchial Epithelial Cell Growth Media using BEGM bullet kit (Lonza) without the supplied epinephrine, supplemented with an extra 5 ng/mL EGF (Corning), 70 ng/mL phosphoethanolamine (Sigma) and 10% FBS. AC16 Human Cardiomyocyte Cell Line (Millipore-Sigma) was cultured in AC16 expansion medium [66]. All media contained 1% antibiotic antimycotic solution (Corning). Cells were grown in a humidified 37° incubator with 5% carbon dioxide. All experiments with listed cell lines were performed within 4 months of receiving them using low passage number cells. Viability was routinely assessed by trypan blue exclusion (Gibco). Table 5 provides additional cell line information as well as the lot number of all cells lines used in this study.

Reagents

CT20p (VTIFVAGVLTASLTIWKKMG) was commercially synthesized (Biopeptide Co., Inc) at >98% purity, with the N- and C- terminals capped with acetyl and amine groups, respectively. For cellular delivery, CT20p was encapsulated in hyperbranched polyester nanoparticles (HBPE-NPs) as previously described [14, 15, 17]. Typically, a peptide loading of 0.15 µg CT20p to 1 mg polymer is achieved. Stat3 inhibitor VI S31-201 (Calbiochem) was purchased already in solution.

Treatments

Cytotoxicity experiments: the indicated adherent cell lines were seeded in 96 well plates at the recommended seeding density and treated at 70-80% confluency. Suspension cell lines were transferred to a 96 well plates in 70% of final well volume, using fresh medium. Adherent cells were treated by replacing the well medium with medium containing CT20p-HBPE-NPs or Stat3 inhibitor VI at final treatment concentration. Suspension cells were treated in 30µLs (3.34X concentration), 24 hours after being transferred to 96 well plate. The concentrations selected for CT20p-HBPE-NPs treatments were 75 µg nanoparticle/mL 150 µg nanoparticle/mL. The concentrations of Stat3 inhibitor VI (S31-201) used were 50µM and 100µM, based on product description overview regarding effective concentration of < 100µM (Calbiochem, 573130). NCI-H1882 cells were treated for 16 hours with 150 µg/mL CT20p-HBPE-NPs, in parallel with untreated control, which received medium only. Cells were lifted, washed in

1XPBS and frozen at -80ºC until lysate preparation. NCI-H1048 cells were treated for 6 hours before being lifted for lysate preparation.

Measuring cell viability

Cytotoxicity of cells treated with CT20p-HBPE-NPs or Stat3 inhibitor VI was determined by adding Calcein-AM and ethidium homodimer (Live/Dead Thermofisher) 48 hours post treatment and measuring signal intensity using GFP and TexasRed filter cubes respectively. Signal intensity and image acquisition were obtained using Cytation5 (Biotek) and Gen5 software. Per well, three distinct, non-overlapping areas were imaged using a 4X phase objective without and with each appropriate filter. Because suspension cells grow in clusters, determining cell number using the "cellular analysis" feature is suboptimal. We use image analysis to determine GFP and TexasRed mean fluorescent intensity. Threshold values were employed when appropriate to eliminate background signal. All the data points generated per condition are averaged and used to calculate the ratio between intensity from GFP (live cells) and TexasRed (dead cells). Only unprocessed images were used for data analysis. Representative images are shown on figures.

Immunoblotting

Cell pellets used to make protein lysates were washed in 1X PBS (Corning) and frozen at -80º C for at least 1 hour prior to lysis. Lysates were obtained by quickly adding

ice cold NP-40 Lysis Buffer (50mM K$^+$HEPES pH 7.5, 150mM NaCl, 1% NP-40, 1mM

EDTA) with freshly added Halt protease inhibitor (Thermo, 78438) immediately after

pellets were removed from the -80° C. Lysis took place on ice for 20 minutes with gentle

and intermittent vortexing intervals. Lysates were cleared by centrifuging at 12,000 x g

for 10 minutes, at 4° C. Soluble lysates were stored at -20° C for no longer than 3 months.

Freeze/thaw cycles were minimized to avoid protein precipitation and degradation.

Proteins in the lysates were resolved by SDS-PAGE and transferred to Immobilon-FL

PVDF membrane (Millipore IPFL00010). Prior to blocking, membranes were stained for

total protein using Revert (LI-COR) and imaged on Odyssey (LI-COR) using the 700

channel. After blocking, blots were probed with primary antibodies against CCT2 (anti-

CCTβ, Millipore), CCT4 (anti-CCTΔ, Abcam), CCT5 (anti-CCTε, Abcam), and STAT3

(anti-Stat3, Abcam), followed by 1-hour incubation with secondary antibodies IRDye

800CW and/or IRDye 680CW (LI-COR) at a 1:10000 dilution. Bands were visualized by

NIR fluorescence detection using Odyssey (LI-COR). Relative protein quantification was

performed with Image Studio software (LI-COR). The signal obtained for proteins of

interest were normalized to total protein content using Revert (LI-COR) image as

follows: first, total protein quantification was performed using the 700nm channel, using

all the protein transferred onto the blot after Revert staining. Second, lane normalization

factor (LNF) was calculated by dividing the signal of each lane by the signal from the

lane with highest signal. Third, target signal was determined. Normalization was

performed by dividing the signal from each target by the LNS. Immunostaining was

performed with a minimum of two biological replicates and at least three technical

replicates per target.

Statistical analysis

Experiments were performed at least three times, in duplicates or triplicates, where appropriate. Data representative of experiments were selected for this publication. TMA data is expressed as means and standard deviation, whereas blots and Live/Dead assay data is represented as means and standard error. One-way ANOVA was used to compare mean scoring between the different groups defined by various tissue parameters as well as signal intensity ratio in treated cells. Tukey's multiple comparison test was used to compare significance between individual groups. For CT20p treatment analyzed by immunoblot, unpaired, two-tailed t-test was used to calculate significance between untreated and treated samples. Calculations were performed with GraphPad Prism software (GraphPad). Statistical significance was defined as $p < 0.05$. Datasets generated in the current study are available in the Kaplan-Meier Plotter (KMPlot) repository [67, 68] at http://kmplot.com/analysis/index.php?p=service&cancer=breast.

CCT2 is overexpressed in lung cancer patient tumors and correlates with decreased survival.

CCT is a macromolecular complex composed of eight subunits, which we will refer to by number (CCT1-8) hereinafter. Our previous studies with breast cancer [18] revealed that the CCT2 subunit was overexpressed in tumor tissues as compared to normal tissues, was increased with advanced disease, and was inversely correlated with patient survival. To determine whether CCT2 was elevated in other cancers, we evaluated CCT2 protein levels in several human tissue microarrays (TMAs) for lung, colon, hepatocellular, and prostate carcinomas by immunohistochemistry (IHC). We found that lung, liver, and prostate tissues had significantly higher levels of CCT2 as compared to matched normal tissue (Fig. 6A,B, and E,F Fig. 7A,B). Our findings for colon cancer were inconclusive due to high background staining of normal colon tissue (Fig. 6I). In liver carcinomas, CCT2 levels were higher in both subtypes analyzed (HCC and cholangiocellular carcinomas) as compared to normal hepatic tissue (Fig. 6A-B). This difference was statistically significant ($p<0.05$) in HCC. We also analyzed HCC according to grade, as high grade HCC is associated with poorer prognosis [69], and observed a progressive increase in CCT2 staining with increasing grade (Fig. 6A). In prostate adenocarcinoma, we observed significantly increased levels of CCT2 as compared to normal prostate tissue (Fig. 6E). Because increased stage indicates higher severity of disease and poorer prognosis, we also analyzed CCT2 levels in prostate cancer

by stage and observed a trend of increasing CCT2 staining with increasing stage (Fig. 6E). Mining databases like The Cancer Genome Atlas (TCGA) and the Human Protein Atlas confirmed our findings that high expression of CCT2 occurs in liver and prostate cancer and is associated with unfavorable prognosis (Fig. 6C,D and G,H). However, in colon cancer, high levels of CCT2 were associated with improved prognosis, although this result was not statistically significant (Fig. 6J).

We next assessed the levels of CCT2 in various subtypes of lung cancer by evaluating staining intensity in 236 tissue microarray cores containing cases of adenocarcinoma, carcinoid, SCLC, and squamous cell lung carcinoma (SqCLC) (Table 3). This was then compared to normal lung tissue. All lung cancer subtypes examined had significantly higher levels of CCT2 as compared to normal tissue (Fig. 7A). Representative images of CCT2 staining in normal lung tissue, SqCLC, and SCLC are provided in Figure 7B. We selected SqCLC and SCLC to study in greater detail because together, these two lung cancer types represent 35%-45% of all cases [3] and both scored significantly higher than normal tissue for CCT2 (Fig. 7A). To determine if CCT2 levels increased with disease progression in these two lung cancer subtypes, we grouped TMA cores according to their TNM classification (Figure 7C-D) or stage (data not shown) and found no statistically significant differences among the groups analyzed. Essentially, CCT2 levels were higher than normal lung in these lung cancer subtypes and independent of stage or grade. To investigate if CCT2 levels correlated with survival in lung cancer patients, we used the publicly available Kaplan-Meier plotter database to generate survival data in all lung cancer patients that expressed high levels of CCT2 mRNA. We found that there was a statistically significant correlation ($p = 0.0031$) between decreased

28

survival of grade III lung cancer patients and CCT2 expression, with a 30-month difference in survival between the higher expression patient cohort and the lower expression patient cohort (Fig. 7E). These results were confirmed with the TCGA database.

We and others previously reported a correlation between high levels of CCT subunits and disease progression in breast [18], hepatocellular and colonic carcinoma, and gallbladder squamous/adenosquamous carcinoma [70]. To our knowledge, however, no other groups have published a correlation between lung cancer and CCT levels. To address this gap, we selected this cancer type to investigate further

SCLC cell lines express varied levels of CCT2, CCT4, and CCT5 subunits and were susceptible to killing by CT20p.

About 95% of SCLC patients have TP53 mutations [71]; therefore, as representative cell lines for our studies, we chose four SCLC cell lines containing common TP53 mutations and one SCLC cell line with wild-type TP53 (Table 5). To assess CCT expression in the SCLC cell lines, we determined the basal protein levels of the subunits CCT2, CCT4, and CCT5 by immunoblot (Fig. 8A-C). The levels of assayed subunits were normalized to total protein by staining the membrane prior to blocking. Figure 8D provides a representative image of the membrane stained for total protein. The cell line NCI-H1048 had the highest level of all five cell lines assayed for CCT subunits (Fig. 8A-C). In contrast, NCI-H719 had the lowest level of CCT2, CCT4, and CCT5 (Fig. 8A-C). The levels of CCT subunits in cell lines NCI-H1882, NCI-H1417, and NCI-

H1105 were in between those of the highest and lowest SCLC cell lines (Fig. 8A-C). For a qualitative analysis of relative levels of the assayed CCT subunits, we normalized the signal from all cell lines to the signal from cell line NCI-H1048 for each CCT subunit assayed. We then combined the data into one graph to aid visualization (Fig. 8E). It is important to note that this comparison is only qualitative since different antibodies were used to detect each subunit. The relevant knowledge we gained from these experiments is that we can now detect protein level differences of each CCT subunit among the selected cell lines. As a quality control check for our protein lysates, we also assayed basal levels of wild-type (WT) or mutant p53 in these cell lines and found that NCI-H719 cells had the highest and NCI-H1417 cells had the lowest levels of mutant p53, which confirmed the data set available at the ATCC website (Fig. 9A-B).

Our previous published work showed that CT20p is selectively cytotoxic to breast cancer cells, and that modulating the levels of CCT2 by inhibition or overexpression regulated the susceptibility of cells to killing by CT20p [18]. Hence, it is likely that CT20p's primary mechanism of action is inhibition of CCT. To deliver CT20p to cells, we encapsulated the peptide in nanoparticles made from a hyperbranched polyester polymer (CT20p-NPs). These nanoparticles are approximately 80 nm in diameter, monodispersed and spherical as we have shown in our previous publications [14, 15, 18, 19]. Peptide loading efficiency was estimated to be 0.15 µg CT20p per mg polymer. These nanoparticles are negatively charged and we confirmed uptake by all SCLC cells, using nanoparticles loaded with the fluorescent dye DiI (Fig. 10). All cells were treated with 75 and 150 µg/mL of CT20p-NPs (based on polymer amounts) for 48 hours and live/dead cells detected with two probes to assess intracellular esterase activity (Calcein

AM) for live cells and plasma membrane integrity (ethidium homodimer) for dead cells. Live cells fluoresced green, while dead cells fluoresced red. The cell line most susceptible to CT20p treatment at the two doses tested was NCI-H1048 (Fig. 11B), which also displayed the highest levels of all three CCT subunits (Fig. 8A-C). The cell line with the lowest amount of all three CCT subunits, NCI-H719, was also killed by CT20p treatment but to a lesser extent (Fig. 11E). Interestingly, the only cell line with WT p53, NCI-H1882, had the second lowest levels of CCT subunits but was also highly susceptible to CT20p treatment (Fig. 11A) This suggests that loss of p53, a CCT client protein, could contribute to cell death in this line. Hence, total levels of CCT may not always be as important as the outcome of CCT protein folding activity. The two cell lines with high CCT2 levels but lower levels of the other subunits, NCI-H1417 and NCI-H1105, were susceptible to CT20p, more so for NCI-H1105 (Fig. 8C-D, Fig.11C-D). These results indicate that while all SCLC cell lines were killed by CT20p-NPs, those like NCI-H1048 that upregulated multiple CCT subunits were more sensitive to killing by the peptide. We also observed that in a number of these cell lines, the cells tended to aggregate or cluster (NCI-H719, NCI-H1882), which also decreased upon treatment with CT20p (Fig. 11E,A). This is important as we have shown that CCT inhibition through CT20p reduces actin and tubulin, which are cytoskeletal components that are CCT client proteins [15, 18]. Additionally, of the three SCLC cell lines with the highest levels of CCT subunits (NCI-H1048, NCI-H1417, and NCI-H1105), those derived from metastatic sources were more susceptible to killing by CT20p than those derived from a primary tumor source. These results are summarized in Table 7.

CCT2 levels correlate with STAT3 levels in SCLC patient tissues.

CCT is responsible for folding ~5-10% of the cell's proteome [24] and many of its client proteins are involved in oncogenesis; however, the full CCT interactome remains to be discovered [60]. To determine whether CT20p treatment results in decreased CCT client proteins, we evaluated STAT3 because this transcription factor is frequently involved in oncogenesis [72] and its biosynthesis and activity is directly regulated by CCT [28]. To demonstrate a correlation between STAT3 and the levels of CCT2 in tumors from SCLC patients, we used TMAs containing SCLC tumor cores (Table 3) for analysis of both CCT2 and STAT3. We found that the levels of STAT3 consistently correlated with CCT2 (Fig. 12A) in most SCLC patient tumor tissues. Representative images of two STAT3/CCT2 pairs showing lower score (score 2 and 3) and high (score 4) are in Figure 12B. Next, we assayed total STAT3 protein levels in SCLC cell lines and determined that STAT3 was detectable in all five cell lines with the highest levels in NCI-H719 (Fig. 14A). To investigate the effect of CT20p-NPs treatment on the levels of total STAT3, two adherent SCLC cell lines that were most sensitive to the peptide, NCI-H1882 and NCI-H1048, were subjected to treatment with the peptide for 16 hours and 6 hours respectively. These times were chosen in order to obtain enough viable cells for high quality cell lysates. Protein lysates were not effectively recovered from SCLC cells treated with CT20p-NPs beyond 16 hours, indicating that most cells after treatment are likely dead or dying. CCT2 and STAT3 protein levels were normalized to total protein to control for any proteolysis in the CT20p-treated cells. We found that in both SCLC cell lines, STAT3 levels decreased significantly, supporting the notion that CT20p could be inhibiting the protein-folding activity of CCT and causing

loss of client proteins like STAT3 (Fig. 13A). We also noted that the levels of CCT2 itself also decreased, but to a lesser extent. That CT20p could cause destabilization and cause the loss of CCT subunits is intriguing and indicates that more needs to be learned about the regulation and formation of the CCT complex.

We also treated the SCLC cell lines with a STAT3 inhibitor (STAT3 inhibitor VI) that binds to the SH2 domain and prevents STAT3 phosphorylation. Previous published studies showed a reduction in tumor cell growth in vitro at doses < 100 μM [73, 74]. SCLC cells were treated for 48 hours at 50 and 100 μM and viability assessed as in Figure 11. We found that other than the SCLC line, NCI-H719, the SCLC cells were minimally affected by the STAT3 inhibitor (Fig. 14B). This suggests that CT20p was more effective at reducing STAT3 levels and killing cells than a typical STAT3 inhibitor that targets only the phosphorylation and activation of the transcription factor.

Immortalized and actively dividing cells have high levels of CCT2.

To examine the broader effect of CT20p treatment on other cell lines, we selected three immortalized non-cancer cell lines that are typically used as controls for testing chemotherapeutics [75]. The AC16 and THLE-2 cell lines are used to examine cardio and liver toxicities. Based on our previously published work, the normal breast cell line MCF-10A was also selected. We first determined the basal levels of CCT2 (Fig. 15A) and STAT3 (Fig. 15B) and included two SCLC cell lines, NCI-H1048 and NCI-H719, for comparison since NCI-H1048 had the highest level of CCT2 and NCI-H719 had the lowest (Fig. 8A). Note that Figure 15C contains a representative image of one of the blots

used for relative quantification of the target levels as well as the total protein stain used for normalization. AC16 and THLE-2 cells had levels of CCT2 that were even higher than one of the SCLC cell lines, NCI-H719 (Fig. 15A). This was expected since both AC16 and THLE-2 cell lines were immortalized using SV40 oncogene [66, 76]. SV40 inhibits p53 and Rb1, inactivation of which are hallmarks of SCLC. The conditional inactivation of these alleles in mice was sufficient for the mice to develop SCLC [77]. We also observed a similar trend of high CCT2 levels when cells like the immortalized lung cancer cell line, BEAS-2B (data not shown), and normal bronchial epithelial (NHBE) or fibroblast cells (NHLF) (Fig. 16) were actively replicating in cell culture, likely due to the need for increased CCT client proteins like cyclins. Since it is known that NBE cells can cause phenotypic changes when co-cultured with cancer cells [78] future studies will investigate CCT levels under co-culture conditions and in senescent versus dividing cells to determine the involvement of the chaperonin in modulating the behavior of normal and cancer cells. In this regard, in our previous work [18], we found that MCF-10A cells can undergo spontaneous epithelial-to-mesenchymal (EMT) transformation and that transformed cells exhibit higher levels of CCT2 and are susceptible to CT20p treatment as shown in Figure 15D. Treatment with CT20p proved toxic to these immortalized cells given their high expression levels of CCT2 (Fig. 15A,D). Normal tissues, on the other hand, are not immortalized with oncogenes or actively dividing, so levels of CCT2 were lower, as we observed with normal lung tissue (Fig. 15E) and tissues from other organs such as the heart and liver (Fig. 15E). To examine any potential toxicities that could result from CT20p treatment, we performed a dose escalation study in mice. We observed no significant alternations in the liver and

34

kidney function of mice and all clinical chemistry values were within reference ranges (Fig. 17), nor were any changes in weight, blood in urine or necrosis of organs observed (Fig. 17). Hence, these studies suggest that CT20p's susceptibility is based on the expression levels of CCT, as well as the activity of the chaperonin. This could establish a therapeutic window that could be exploited to develop an effective treatment strategy.

Hepatocellular carcinoma
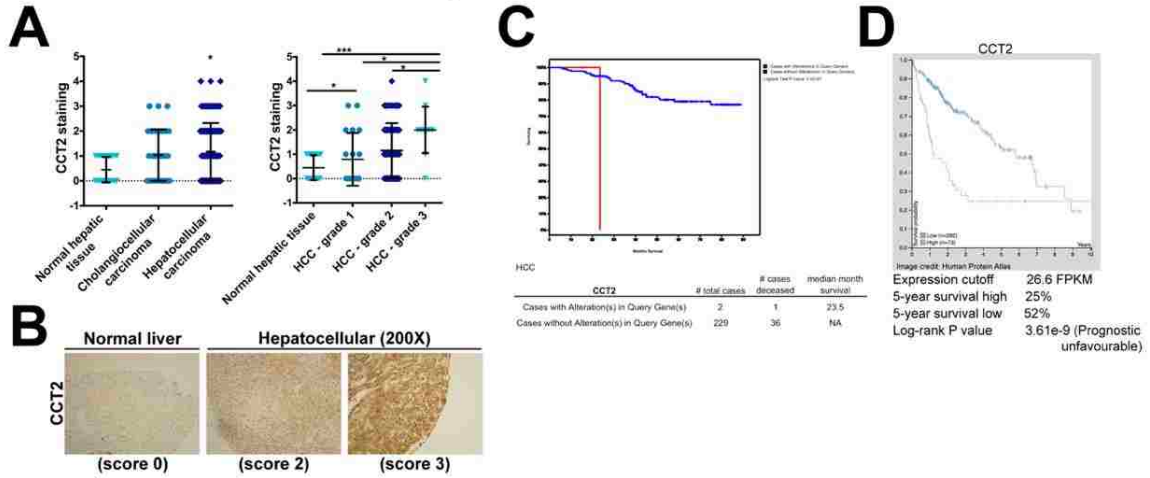
Prostate carcinoma
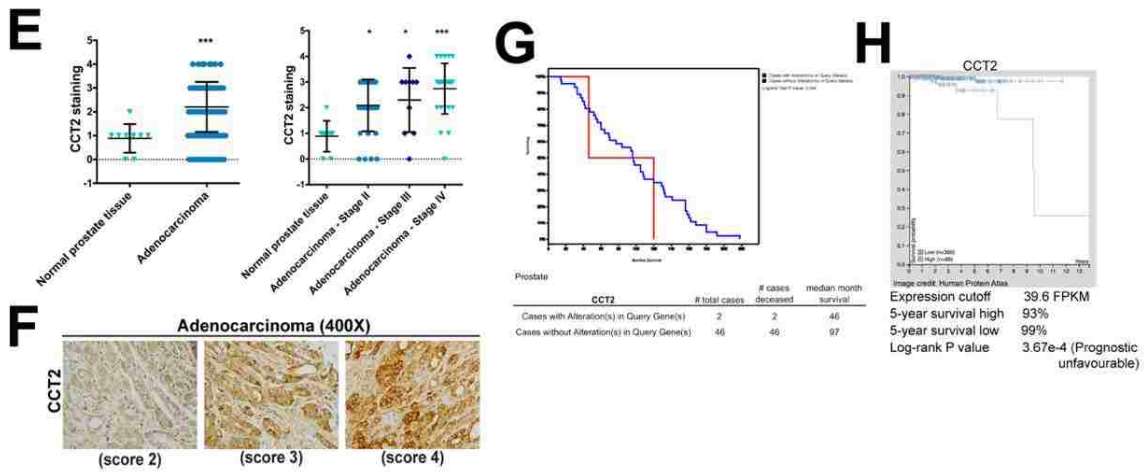
Colonic carcinoma
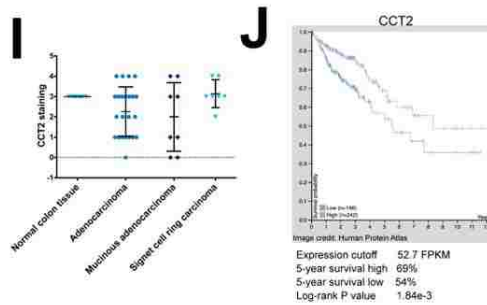
Figure 6: Effects of high levels of CCT2 in hepatocellular, prostate and colon cancers

(**A, E and I**) Levels of CCT2 were assayed in human tumor tissue samples of (**A**)hepatocellular, (**E**) prostate and (**I**) colon cancer by immunohistochemistry (IHC) as described in Supplemental Methods and Materials. Representative images of different staining intensities are shown for (**D**) hepatocellular (200X) and (**H**) prostate(400X) tissues. Images of stained tissues as well as analysis of staining intensity were performed by a pathologist For staining analysis a score between 0-4 was give following a scheme previously published in Bassiouni et al (2016). Significance was calculated in reference to normal tissue. $p < 0.05$, ** = $p < 0.01$, *** = $p < 0.001$, **** = $p < 0.0001$. (**B, F**) Survival data for patients with high and low levels of CCT2 were queried using the TCGA database trhough cBioPortal (repository can be found in Supplemental Methods and Materials). (**B**) Kaplan-Meyer plot for HCC patients showing that duplication of CCT2 gene decreases survival.(**F**) Kaplan-Meyer plot for prostate cancer patients showing that genomic alterations in CCT2 decreases median survival rate by half. (**C,G and J**) Survival data for patients with high levels of CCT2 was queried using The Human Protein Atlas database showing that (**C**) in HCC patients with high levels of CCT2 the 5-year survival rate is 25% compared to 52% in patients with low levels of CCT2. (**G**) In prostate cancer, patients with high levels of CCT2 have a 5-year survival rate of 93% and patients with low levels of CCT2 have 99% survival rate. (**J**) In colonic carcinoma, the 5-year survival rate for patients with high levels of CCT2 is 69% versus 54% for patients with low levels.
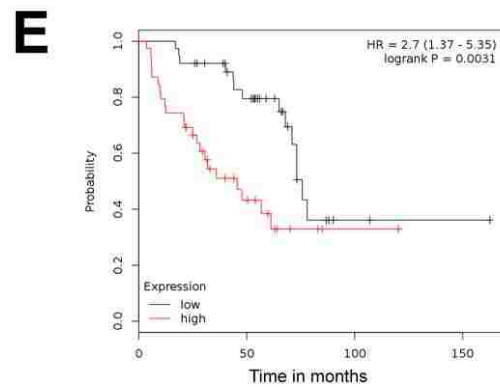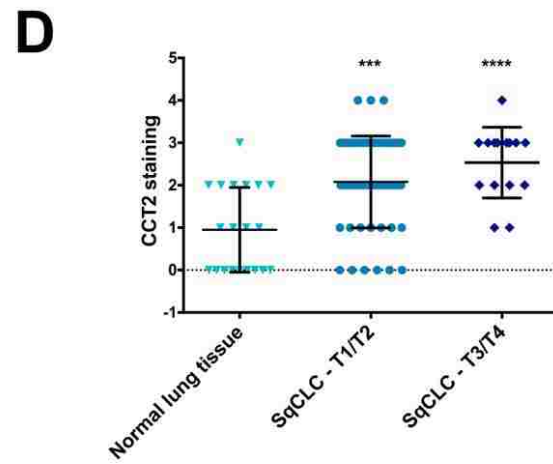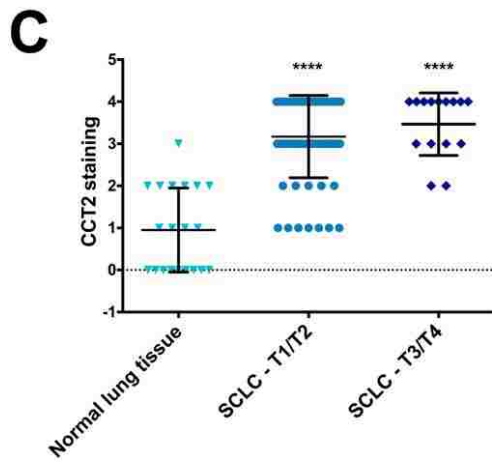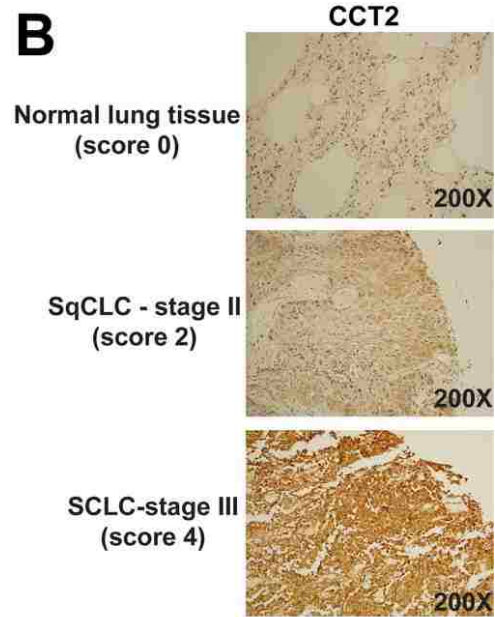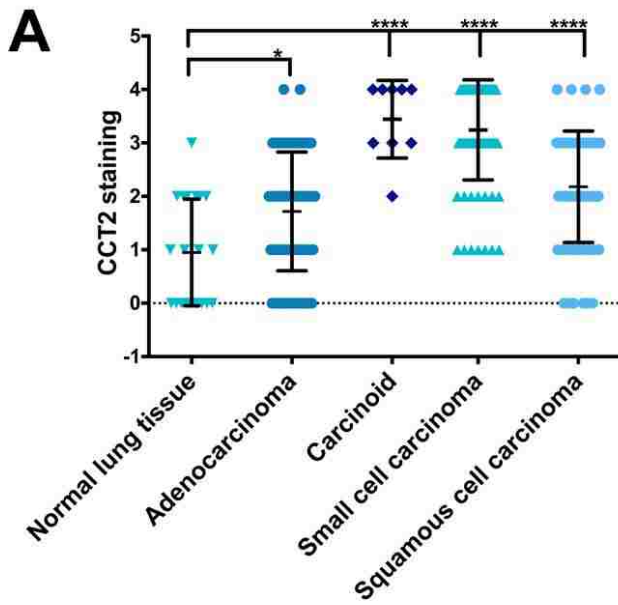
Figure 7: Analysis of CCT2 staining in lung cancer patient tissue

(A) The levels of CCT2 were assayed in human tumor tissue samples of different lung cancer subtypes by immunohistochemistry (IHC) as described in Materials and Methods. Tissue cores were analyzed by a pathologist according to stain intensity and given a score between 0-4 as previously published in Bassiouni et al (2016). Significance was calculated in reference to normal lung tissue. (B) Representative images of stained human tissue microarrays (TMAs) shows the elevated levels of CCT2 in both squamous cell carcinoma and small cell carcinoma compared to low levels in normal lung tissue. (C) Small cell lung cancer (SCLC) samples were grouped according to TNM score (T1/T2 and T3/T4) and stain intensity for CCT2 was compared between them. Significance indicated is in reference to normal lung tissue. (D) Squamous cell lung carcinoma (SqCLC) was also grouped by TNM score (T1/T2 and T3/T4) and CCT2 stain intensity was compared. Significance indicated is in reference to normal lung tissue. (E) Kaplan-Meier plot of lung cancer patients based on CCT2 expression. The survival graph was generated using publicly available database (KM plotter; www.kmplot.com). Data analysis was restricted to patients with grade III lung cancer (n=77). * = $p<0.05$, ** = $p<0.01$, *** = $p<0.001$, **** = $p<0.0001$
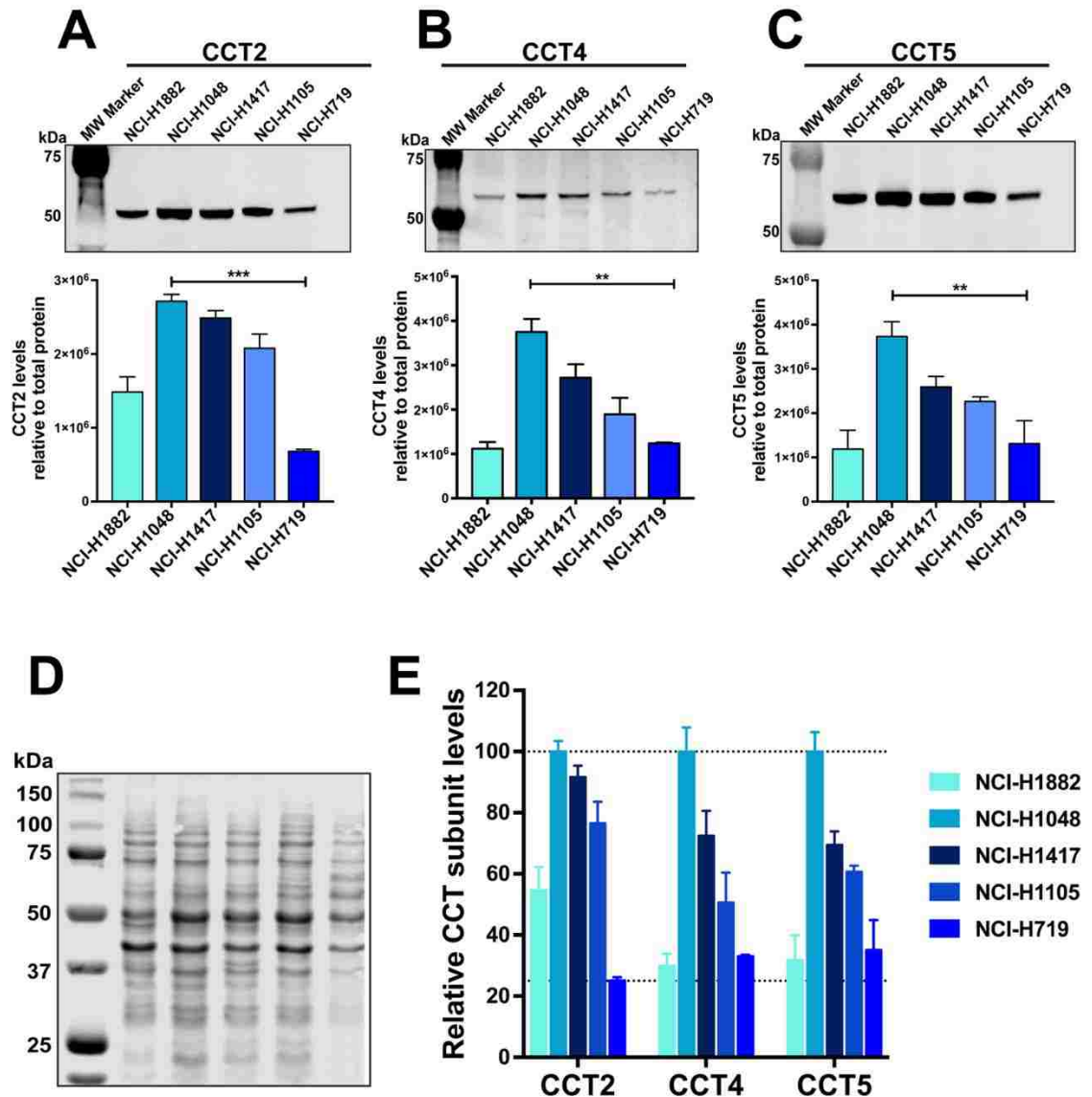
Figure 8: Levels of CCT subunits are detected in SCLC cell lines

Lysates corresponding to five SCLC cell lines were subject to immunoblot analysis for (A) CCT2, (B) CCT4 and (C) CCT5. The bar graphs below each corresponding blot, shows their relative levels for all five cell lines. Relative quantification was calculated by normalizing antibody specific signal to signal obtained from total protein. (D) PVDF membrane stained for total protein using Revert (LI-COR). (E) Graph showing relative values of the three assayed CCT subunits in each SCLC cell line. $* = p < 0.05$, $** = p < 0.01$, $*** = p < 0.001$, $**** = p < 0.0001$. Blot images are representative

Table 3: Sample sizes for lung tissue cores analysis

	Classification	Sample size
	Normal	20
	Adenocarcinoma	76
	Carcinoid	11
	Small cell carcinoma	82
Lung	Squamous cell carcinoma	67
	SqCLC T1/T2	52
	SqCLC T3/T4	15
	SCLC T1/T2	67
	SCLC T3/T4	15

Table 4: Sample sizes for liver, colon and prostate tissue cores analysis

	Classification	Sample size
Liver	Normal hepatic tissue	20
	Cholangiocellular carcinoma	30
	Hepatocellular carcinoma	147
	HCC - grade 1	19
	HCC - grade 2	111
	HCC - grade 3	12

	Classification	Sample size
Colon	Normal colon tissue	7
	Adenocarcinoma	23
	Mucinous adenocarcinoma	8
	Signet cell ring carcinoma	7

	Classification	Sample size
Prostate	Normal prostate tissue	9
	Adenocarcinoma	131
	Adenocarcinoma - stage II	33
	Adenocarcinoma - stage III	10
	Adenocarcinoma - stage IV	27
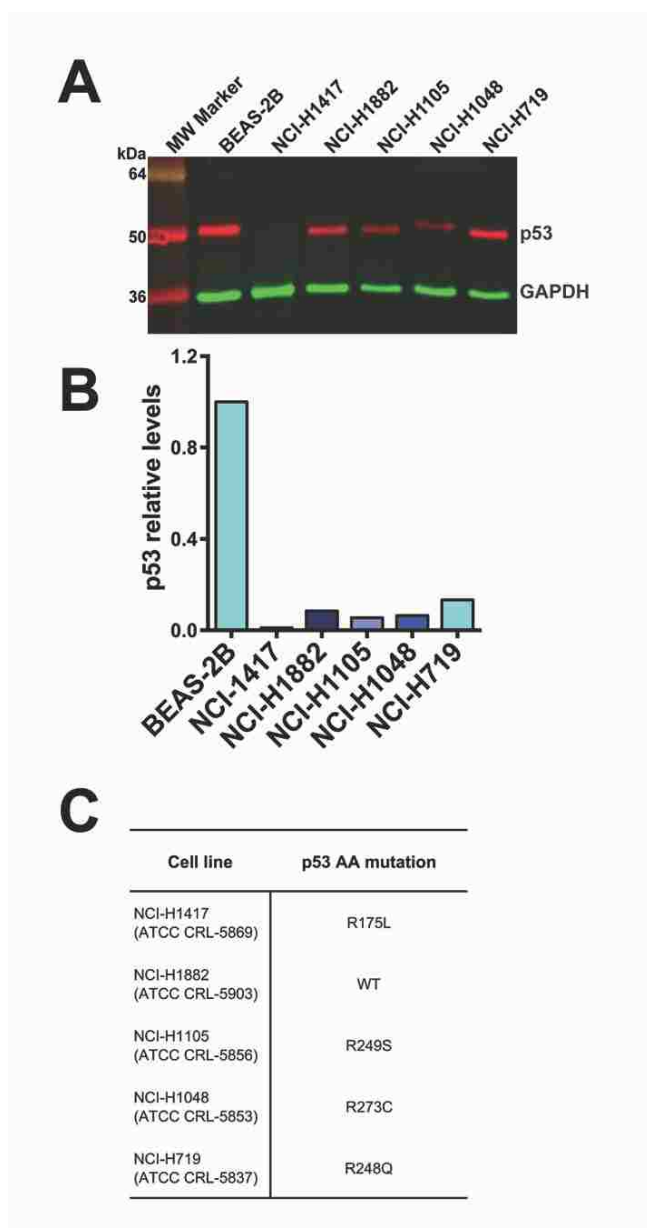
Figure 9: Levels of p53 in SCLC cell lines

Cell lines from the ATCC SCLC p53 Hotspot mutation panel, used in this study, were assayed for p53 levels as quality control. (**A**) Total soluble lysate corresponding to indicated cell lines (five human SCLC cell lines and an immortalized lung breast epithelial cell line) were assayed for p53 levels (red band). GAPDH was used as loading control (green band). (**B**) Bar graph showing relative quantification of p53 levels which were normalized to GAPDH levels as described in Supplemental Methods and Materials. (**C**)Amino acid change due to genomic mutations found in TP53 for each cell line. All mutations resulted in "loss of function"
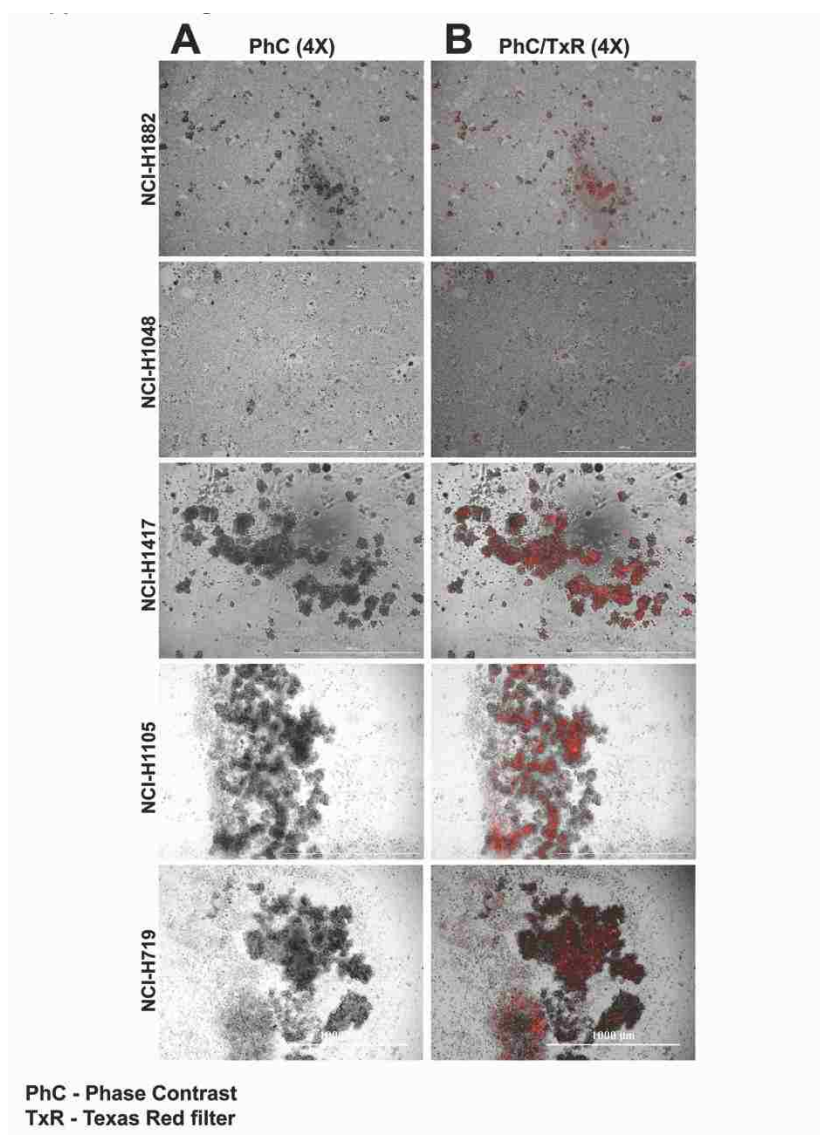
Figure 10: CT20p NPs co- localize with SCLC cells

DiI dye (1,1'-Dioctadecyl-3,3,3',3'-Tetramethylindocarbocyanine Perchlorate) encapsulated in HBPE-nanoparticles were delivered to viable SCLC cells as described in Materials and Methods. Cells were imaged after 24 hours for fluorescent signal indicative of nanoparticle uptake. Column (**A**) Phase contrast images(4X) (**B**) Phase contrast(4X)/ TexasRed merged image.
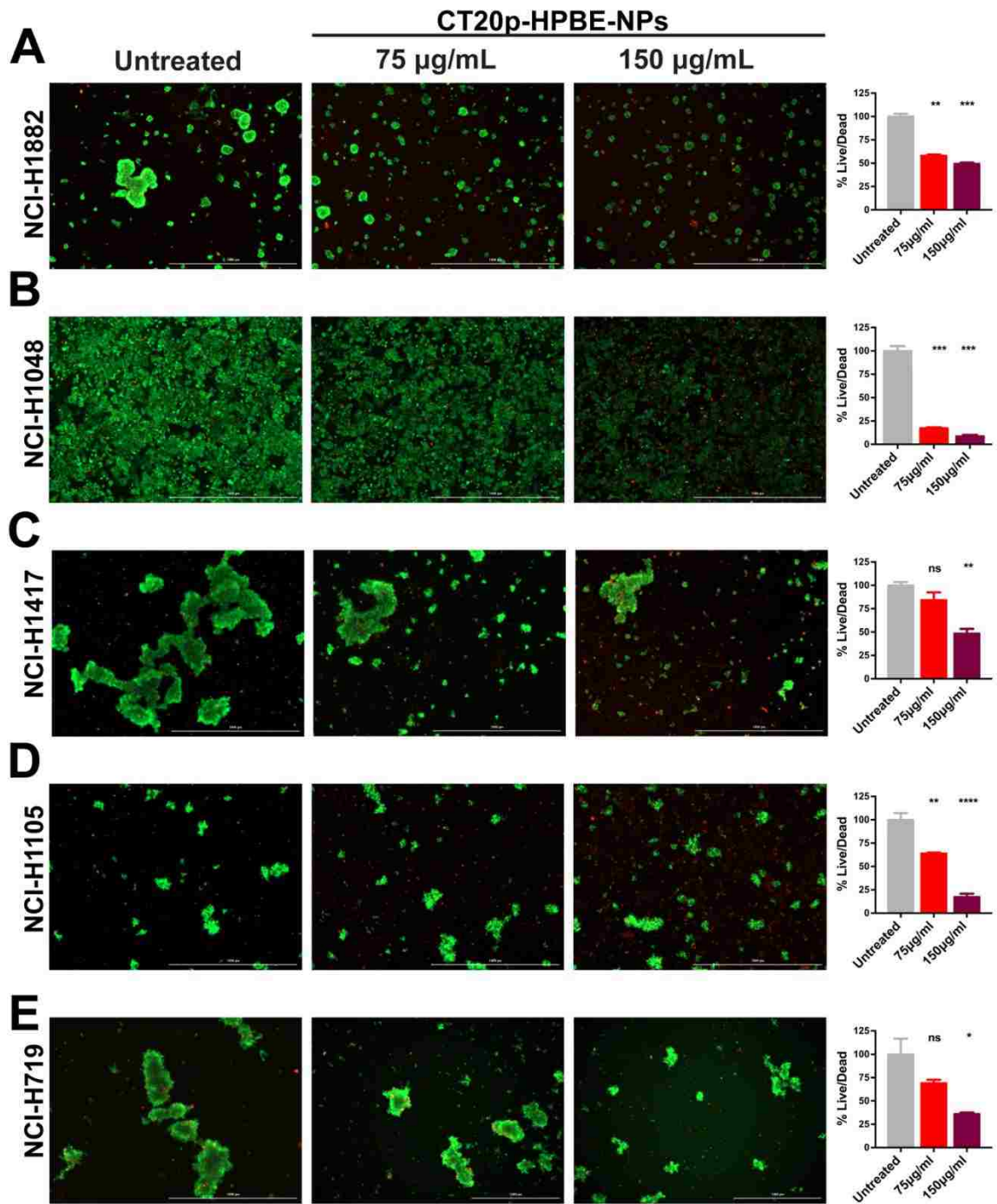
Figure 11: CT20p is cytotoxic to SCLC cell lines

Five SCLC cell lines were subject to CT20p treatment at 75 µg/ml or 150 µg/ml for 48 hrs as described in Methods and Materials. Untreated control received medium only. Calcein-AM and ethidium homodimer were added to cell cultures prior imaging to indicate live (green) and dead (red) cells respectively. Representative images of (A) NCI-H1882, (B) NCI-H1048, (C) NCI-H1417, (D) NCI-H1105 and (E) NCI-H719 are shown for untreated control and the two doses used. Signal obtained using GFP filter (indicative of live cells) was divided by signal detected using TexasRed filter (indicative of dead or damaged cells) for each cell line. Bar graphs adjacent to each corresponding cell line show the normalized ratios (%live/dead). Cytotoxic effects can be observed by an overall decrease in green signal concomitantly to an increase in red signal. * = p<0.05, ** = p<0.01, *** = p<0.001, **** = p<0.0001
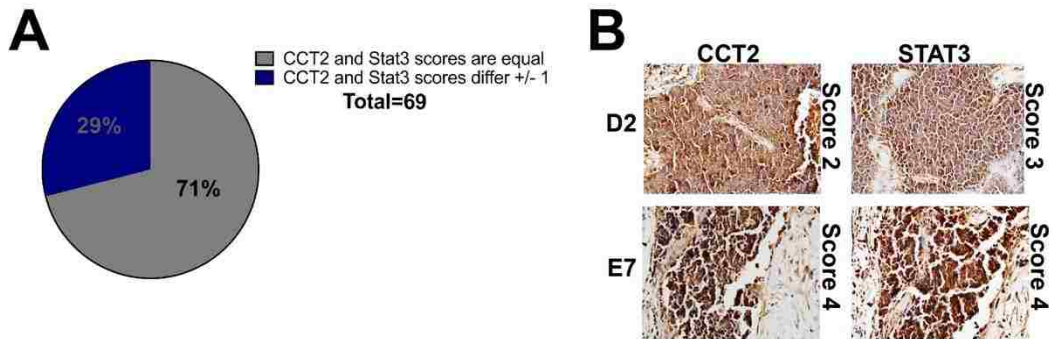
Figure 12: In SCLC patient tissue, levels of CCT2 correlate with levels of client protein Stat3

(A-B) TMA containing human SCLC tissue was stained for CCT2 and Stat3 in parallel as described in Methods and Materials. Tissue cores were analyzed by a pathologist according to stain intensity as described previously. (A) Pie chart indicates the number of cores which received equal scoring for CCT2 and Stat3 staining, as well as cores which received scores that differed by 1 (no cores received scores that differed by more than 1). (B) Representative images of corresponding CCT2 and Stat3 stained TMA cores D2 and E7 respectively. Images were provided by the pathologist at 200X (D2 pair) and 400X (E2 pair).
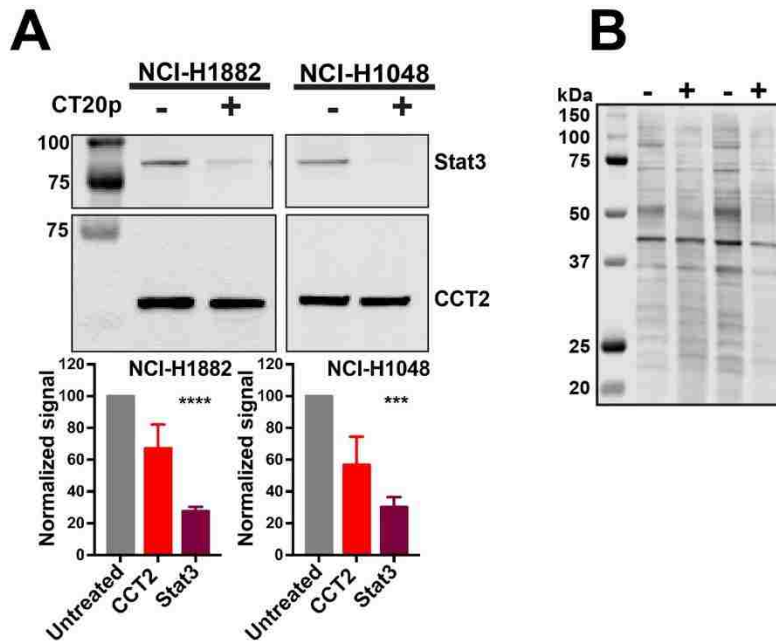
Figure 13: CT20p treatment decreases levels of Stat3 in SCLC cell lines

(A) Cell lines NCI-H1882 and NCI-H1048 were treated with 75 μg/ml CT20p-NPs for 16 hours and 6 hours respectively, at which point cells were trypsonized and lysates made. Soluble lysates of untreated cells (cultured in parallel with treated cells and lifted at the same time) were immunoblotted for CCT2 and Stat3. Bar graphs indicate relative levels of CCT2 and Stat3 in control and treated cells calculated as in Figure 8A-C. (B) Image of stained PVDF membrane showing total protein corresponding to the samples blotted. Signal obtained from total protein was used to normalize CCT2 and Stat3 signal. * = p<0.05, ** = p<0.01, *** = p<0.001, **** = p<0.0001

A STAT3

B Stat3 Inhibitor IV

49
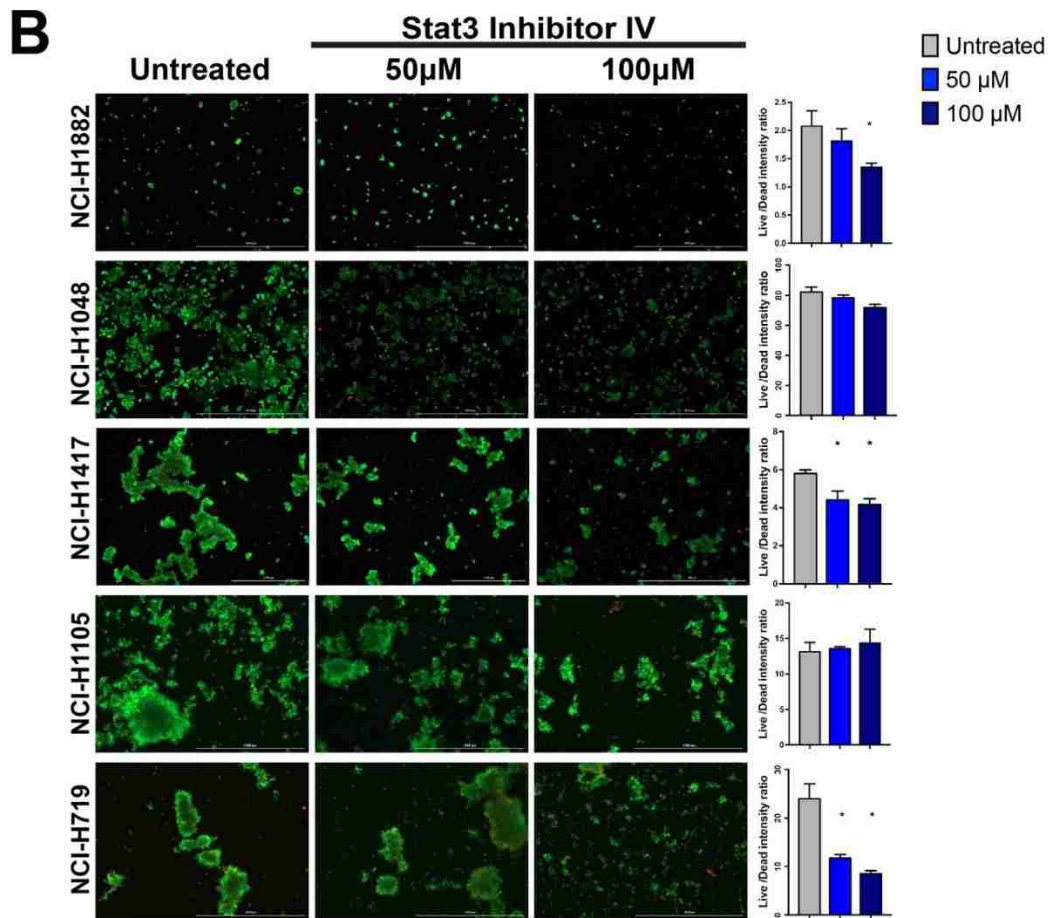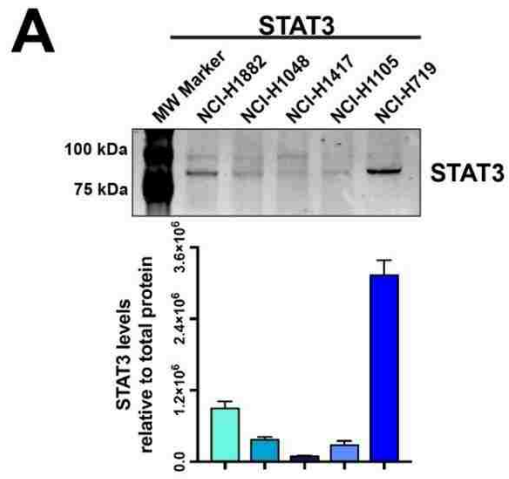
Figure 14: SCLC cell lines Stat3 inhibition

(A) Immunoblot showing relative levels of Stat3 in the five SCLC cell lines. Levels of Stat3 shown were normalized to total protein. Calculations are described in Methods and Materials. (B) Five SCLC cells lines were treated with Stat3 inhibitor IV at 50μM and 100μM as described in materials and methods. The cell line the highest levels of Stat3, NCI-H719, had the most significant response. Analysis was performed by averaging triplicates and significance was calculated as described in Methods and Materials. * = $p<0.05$, ** = $p<0.01$, *** = $p<0.001$, **** = $p<0.0001$
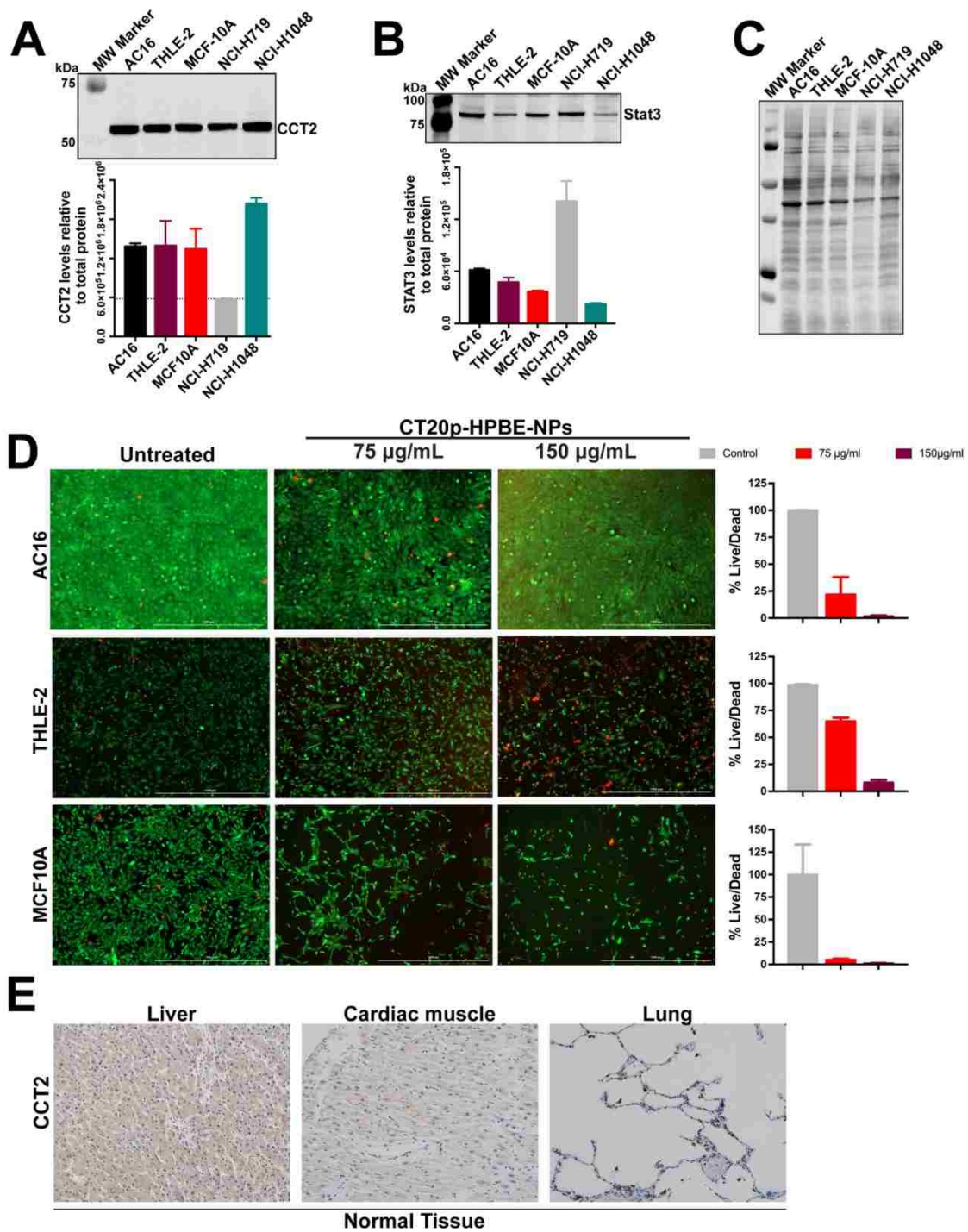
Figure 15: Immortalized cell lines are high expressers of CCT2

(A-B) Immunoblot of the indicated immortalized cell lines alongside two SCLC cell lines for (A) CCT2 and (B) STAT3. (C) PVDF membrane stained for total protein, used for normalization of band intensity after antibody probing. (D) Viability of immortalized cell lines after 48 hours treatments with CT20p-NPs at indicated and control was assessed using Calcein-AM and ethidium homodimer to indicate live and dead cells respectively. (E) The levels of CCT2 were assayed in tissue from normal organs by IHC as described in Materials and Methods. Representative images of stained TMAs of liver, heart and lung shows minimal levels of CCT2 detected.
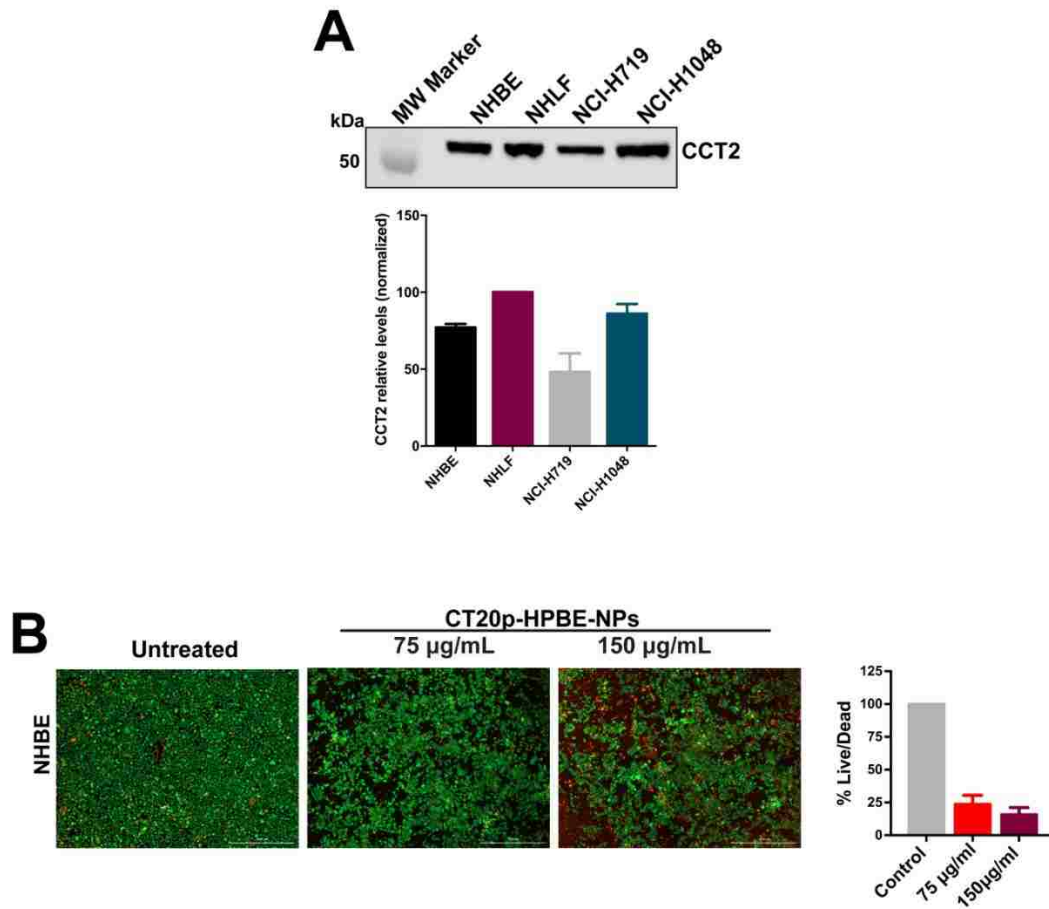
Figure 16: Primary lung cells have high levels of CCT2

Normal human bronchial epithelial cells (NHBE) as well as normal human lung fibroblasts (NHLF) were assayed for levels of CCT2 and susceptibility to CT20p. (**A**) Levels of CCT2 in primary lung cells were high compared to SCLC cell lines. Levels are shown as percent of the highest signal (HNLF) and normalization was performed as described previously. (B) NHBE cells were treated with CT20p as described in Methods and Materials and cytotoxicity detected using Live/Dead (Promega). Signal from 3 wells were averaged as means and standard error. Per well, four overlapping quadrants were imaged and stitched using Gen5 software. Images shown are representative of the experiment.

A

HBPE-CT20p treated
Control

Reference Clinic Chemistry Values

	Unit	Mouse
Glucose	mg/dl	62 - 175
Cholesterol	mg/dl	-
Creatinine	mg/dl	0.2 - 0.9
BUN	mg/dl	8 - 33
T. Bilirubin	mg/dl	0 - 0.9
Albumin	g/dl	2.5 - 3
Total Protein(serum)	g/dl	3.5 - 7.2
AST	U/L	54 - 298
ALT	U/L	17 - 77
ALP	U/L	35 - 96

B

C

Urinalysis

Day	pH	Leukocytes	Protein	Glucose	Blood
3-5	6	Trace	Trace	Normal	-
10-11	5	-	Trace	Normal	-
18-22	5	Trace	Trace	Normal	-
26	6	Trace	Trace	Normal	-

D

Liver   Kidney

Figure 17: Results from blood chemistry, urinalysis, weight and histology from mice treated with CT20p-NPs

Three male and three female nude mice (6-8 weeks old) were treated with five doses (2.4 mg/kg, 4.8 mg/kg, 9.6 mg/kg, 19.2 mg/kg, 38.4 mg/kg) of CT20p-NPs over a two week period. Treatments were performed on Days 0, 3, 7, 10 and 14 and mice were euthanized 14 days after the last treatment. (A) Serum of treated mice was sent to Idexx for testing for the chemical chemistry panel which assesses kidney and liver function. No statistical differences were observed between control and NP-treated mice. Reference table contains normal clinical chemistry values adapted from the Animal Care Website at the University of Arizona. (B) The weight of mice during treatment was determined at the specified time points. (C) Urine analysis was performed using dipstick during treatment at four time points as indicated in the table. Results from a representative mouse are shown. (D) Histology of treated mice liver and kidney showing no signs of necrosis. Representative images are shown.

Table 5: Information on cell lines used in this study:

	Cell line	Tissue	Source	Key characteristics/ mutations	Lot number
Small Cell Lung Cancer	NCI-H1882 (ATCC CRL-5903)	Lung	Metastatic site:Bone marrow	Adherent cell line/ RB1 mutation	58136167
	NCI-H1048 (ATCC CRL-5853)	Lung	Metastatic site: Pleural effusion	Adherent cell line - cells grow in colony and can form clusters/ RB1, TP53 mutations	62784665
	NCI-H1417 (ATCC CRL-5869)	Lung	Primary	Suspension cells - grow in floating clusters/ RB1, TP53 mutations	62007515
	NCI-H1105 (ATCC CRL-5856)	Lung	Metastatic site: Lymph node	Suspension cells - grow in floating clusters/ TP53 mutations	63374473
	NCI-H719 (ATCC CRL-5837)	Lung	Metastatic site:Bone marrow	Suspension cells - grow in floating clusters/ RB1, TP53 mutations	62007616
Normal Tissue Immortalized	THLE-2 (ATCC CRL-2706)	Liver	Liver	Epithelial cells transformed with SV40 large T antigen [1].	64258509
	MCF-10A (ATCC CRL-10317)	Breast	Breast epithelial	Breast epithelial cells, derived from human fibrocystic mammary tissue spontaneously immortalized [2].	64066742
	AC16 (SCC109)	Heart	Cardiomyocyte	Primary cells from human ventricular tissue, were fused with SV40 transformed, uridine auxotroph human fibroblasts, devoid of mitochondrial DNA [3].	RD1606008

Table summarizes information pertaining to cell lines used in the experiments in the main manuscript. Information about tissue of origin, source (primary versus metastatic sites for tumor derived cell lines), key characteristics and lot number are provided. Relevant publications regarding the immortalized cell lines used are provided.

Table 6: Comparison of CCT2 levels, CT20p susceptibility, tumor source, and key genes mutated

	CCT2 Levels	CT20p susceptibility	Source	Culture type	Mutations
NCI-H1048 (ATCC CRL-5853)	↑↑↑	↑↑↑	Metastatic site: Pleural effusion	Adherent	RB1, TP53
NCI-H1417 (ATCC CRL-5869)	↑↑↑	↑	Primary	Suspension	RB1, TP53
NCI-H1105 (ATCC CRL-5856)	↑↑↑	↑↑	Metastatic site: Lymph node	Suspension	TP53
NCI-H1882 (ATCC CRL-5903)	↑↑	↑	Metastatic site:Bone marrow	Adherent	RB1, TP53
NCI-H719 (ATCC CRL-5837)	↑	↑	Metastatic site:Bone marrow	Suspension	RB1, TP53

	CCT2 levels: based on normalized levels (Fig.2E)	CT20p susceptibility
	Normalized CCT2 levels making levels obtained for H1048=100%	Extrapolated IC50 concentrations based on results otained from the two doses tested (linear regression)
↑↑↑	> 70%	< 75 µg/mL
↑↑	< 69% and > 30%	> 76 µg/mL and < 120 µg/mL
↑	< 30%	> 121 µg/mL
	% of signal	µg/mL of nanoparticle

This table summarizes results on experiments using the five SCLC cell lines obtained from CCT2 blots found in Figure 2, CT20p susceptibility found in Figure 3, tumor source, culture type (suspension versus adherent) and key genes containing mutations. The criteria for "high, medium and low levels" are summarized on the table itself. In short, for CCT2 levels, figure 2E was used. Cell lines with signal about 70% were classified as "high", and below 30% as low, if in between, they were considered "medium". For CT20p susceptibility, average values obtained for untreated, 75µg/ml and 150µg/ml were plotted in prism and using linear regression, the IC50 value for each cell line was determined. If the extrapolated IC50 was below 75µg/ml, susceptibility was considered high, if above 121µg/ml, susceptibility was determined to be low, if in between, cells were considered partially susceptible to CT20p treatment.

Discussion

In this study, tissues and cells from various cancers and normal organs were used to investigate CCT as a potential biomarker and therapeutic target in cancer treatment. We assessed CCT2 subunit protein levels across prostate, liver, and lung cancer tissue specimens and found that CCT2 expression levels correlated with disease progression in liver and prostate cancers, and CCT2 levels were significantly higher in lung carcinomas as compared to normal lung tissue independent of disease stage. We also showed that CCT2 levels were low in normal heart, liver, and lung tissues. These findings build upon our previous discoveries in breast and prostate cancer in which CCT2 levels were elevated as compared to non-disease tissues. Using SCLC cell lines, we demonstrated susceptibility to killing by our putative CCT inhibitor, CT20p, which proved more effective than a STAT3 inhibitor, and the resulting reduction of CCT client proteins (e.g., STAT3) in part addressed the mechanism of action for CT20p.

CCT belongs to the family of group II chaperonins that are found in eukaryotic cells and archaea and consists of eight paralogous subunits that differ mainly at the apical domains [61]. Unique to CCT is the formation of hetero-oligomeric complexes and the use of an ATP-dependent conformational change to control the opening/closing of a built-in lid [22, 61]. Hence, subunit diversity and sequential substrate binding generates multiple substrate binding sites that, when coupled to the lid closing mechanism, endow CCT with a flexibility to fold many more proteins than its bacterial counterparts [26]. This broad range of protein substrates means that 5-10% of newly synthesized proteins

may require CCT for folding [24], but also that only part of the CCT interactome has been discovered. Given our findings of elevated CCT expression across cancer types, it is likely that CCT is responsible for folding more of the cell proteome in cancer or transformed cells than in normal cells. There also seems to be a selectivity for CCT subunits based on cancer types. For example, CCT3 and CCT8 were overexpressed in hepatocellular carcinoma (HCC) [39, 72, 79, 80] and the proteins were detected in the plasma from patients, suggesting that CCT3 could be used as a biomarker for screening HCC. We and others found that CCT2 was elevated in breast cancer [18, 41] as well as in gall bladder carcinoma [70]. In the current study, in addition to HCC and prostate cancer, we also found that CCT2 was increased in SCLC and in advanced stages of SqCLC. Understanding why cancers are selective for CCT subunits may require a better understanding of the basis of CCT substrate recognition as well as the discovery of new classes CCT substrates, such as those up-regulated in cancer cells.

As a possible CCT inhibitor, CT20p is one of the first. While arsenic was shown to inhibit CCT function and impair both actin and tubulin filaments [81], other than CT20p, only N-iodoacetyl-tryptophan (I-Trp), a synthetic small molecule, has been found to disrupt the interaction between CCT and tubulin, causing apoptosis through an ER stress-dependent mechanism [82, 83]. In contrast to I-Trp, CT20p does not cause death through a traditional apoptotic mechanism [14], which can be downregulated in cancer cells; rather, its inhibitory effects could extend to multiple client proteins that are essential for cancer progression [84]. Hence, inhibitors of protein folding have therapeutic value since their inhibition can decrease the pool of oncoproteins that cancer cells depend on. As an example, inhibitors of the heat shock protein family (HSPs),

Hsp90 or Hsp70, showed significant efficacy in pre-clinical studies [85]. The Hsp90 inhibitor, Ganetespib, proved effective in SCLC cell lines, causing cell cycle arrest and caspase-3 dependent apoptosis [86]. However, human clinical trials in non-small cell lung cancer (NSCLC) with molecularly unselected patients were disappointing. While some promising results were observed in a cohort of patients with ALK-rearrangements, HSP inhibitors overall did not perform as expected from the pre-clinical data. The reasons for this could be that inhibition of HSPs may trigger a protective heat shock response through activation of heat shock transcription factor 1 (HSF1) and GRP78, which blocks the apoptosis of cancer cells. Alternatively, the level of HSP inhibition achieved in patients could have been insufficient to kill tumor cells [87]. Patients also developed resistance to Hsp90 inhibition due to activation of RAF/MEK/ERK or PI3K/AKT/MTOR pathways, requiring the need for combination approaches to make Hsp90 inhibitors work [88]. We anticipate that inhibition of CCT with CT20p may not result in similar problems because we have no evidence of induction of a heat shock response, such as the membrane translocation of GRP78 (data not shown). Further, the use of nanoparticles to deliver CT20p to tumors can achieve therapeutically relevant doses [14, 15, 19]. Our data also suggest that CT20p could knock out pathways—such as those induced through STAT3—that are linked to growth and survival signaling; hence, resistance activated by these pathways may not develop.

STAT3, which regulates the expression of genes involved in cancer progression, is an attractive target for inhibition in SCLC since it is found in primary SCLC tissues and in SCLC cell lines [89]. While a number of STAT3 inhibitors have been developed, most either inhibit the kinases that phosphorylate and activate STAT3 or they prevent the

formation of STAT3 dimers through disruption of the protein's SH2 domains. Drugs, like the antibiotic doxycycline, inhibit STAT3 in lung cancer cells at the cost of severe side effects in patients like nausea, vomiting and diarrhea, rash and sensitivity to sun [90]. While there are many STAT3 inhibitors, few have moved into clinical trials and none to the clinic. Reasons for this failure are unknown but could be explained by the fact that most STAT3 inhibitors target the dimerization or phosphorylation domains; therefore, unphosphorylated STAT3 is unaffected and available for activation [91]. Since CCT is essential for the synthesis, refolding, and activity of STAT3 [28], inhibitors of CCT should also reduce the levels of total STAT3. Our data show that in SCLC cell lines, CT20p reduced STAT3 levels, while these same cell lines were resistant to killing with a STAT3 inhibitor. In fact, only one SCLC cell line was susceptible to the STAT3 inhibitor and also had the highest levels of STAT3. This cell line was also killed by CT20p, likely due to the loss of STAT3 along with other CCT client proteins.

Cancers like SCLC are challenging diseases to treat and are typically diagnosed at advanced stages. Systemic treatments are not curative [43]. Molecular targeted therapies are promising, despite requiring patients to be pre-screened, but only a few targets, like ALK, are associated with clinically relevant inhibitors (e.g., Crizotinib) and patients frequently relapse [87]. Our research suggests that therapeutically targeting CCT with inhibitors like CT20p could have benefits for SCLC patients. As shown in our studies, CCT subunits are overexpressed in SCLC as well as in advanced stages of other cancers. We anticipate that each patient will likely have their own unique CCT interactome based on the oncogenes that drive their cancer. The products of many of these oncogenes—such as STAT3, KRAS, or MYC—are CCT substrates; hence, each

62

patient whose cancer overexpresses CCT could be treated without the need of molecular subtyping the downstream substrates. So whether a patient's tumor is driven by STAT3, MYC, Notch or a combination, they could still be treated with a CCT inhibitor since the chaperonin is essential for these proteins to reach functional status. Our approach, using the nanoparticle platform to deliver CT20p, has the potential to reach therapeutic doses in tumors and minimize off-site accumulation. CT20p treatment also has promising use in combination approaches with other drugs. Trials with checkpoint inhibitors in SCLC resulted in some durable responses [9], generating interest in agents like CT20p that could make cancers immunogenic or sensitive to radiation therapy

CHAPTER 3: THE EFFECT OF CHAPERONIN CONTAINING TCP1, SUBUNIT 2, ON TUMORIGENICITY OF BREAST CANCER

Preface

Material presented in this chapter is part of the manuscript "The Effect of Chaperonin Containing TCP1, Subunit 2, on Tumorigenicity of Breast Cancer" currently in preparation for submission to NPJ Breast Cancer, a SpringerNature journal. The author of articles published by SpringerNature do not usually need to seek permission for re-use of their material as long as the journal is credited with initial publication. Ownership of copyright in in original research articles remains with the Author.

Ana C. Carr*[1], Anne Showalter*[1], Amr S. Khaled, Orielyz Flores, and Annette R. Khaled
* These authors contributed equally to this work

Breast cancer is one the most commonly diagnosed cancer types and the second leading cause of death in women [42]. Tissue biopsy is typically used to confirm diagnosis and classify the tumor according to histological grade, using parameters such as the Nottingham Histologic Score and pathologic staging (TMN). Such classification, while needed for prognosis, does not always provide information on useful markers that can guide targeted therapies. In contrast, molecular classification of breast cancer allows for a patient specific treatment plan, which yields improved patient outcome. There are five breast cancer molecular subtypes, which are classified according to the levels of estrogen receptor (ER), progesterone receptor (PR), human epidermal growth factor receptor 2 (HER2), claudin and EGFR: claudin-low, basal-like/triple negative, Her2 enriched, luminal A and luminal B [92]. Cancers with such markers can be treated with drugs like Tamoxifen that blocks the effects of estrogen or Herceptin (trastuzumab) which works against HER-2 positive cancers. While these treatments are successful, the need still exists for the discovery of new therapeutic targets for cancers lacking hormone receptors or to improve the use of current therapies in combination approaches.

Triple negative breast cancer (TNBC) tumors are aggressive and are associated with poorer prognosis compared to the ER-positive subtypes [93]. TNBC is marked by the absence of ER, PR and Her2 receptor, therefore, patients diagnosed with this type of breast cancer are not eligible for hormone therapy or anti-HER2 agents. TNBC represents about 17% of all breast cancer cases and is marked by genomic instability, heterogeneity,

high recurrence rates and increased risk of metastasis. Patients diagnosed with TNBC have limited therapeutic options and a much lower survival rate. To address this issue, we previously reported the development and efficacy of CT20p, a cancer specific cytotoxic peptide [18]. In the same work, we provided compelling evidence that the intracellular target of CT20p is the chaperonin containing TCP1 (CCT) or T-complex 1 ring protein (TRiC). CCT is a macromolecular, evolutionarily conserved complex composed of two stacked rings, back-to-back, with each ring being comprised of eight distinct subunits CCT1-CCT8 or CCTα-θ [94]. All eight subunits share the same basic structure containing an equatorial ATP binding domain, an apical substrate binding domain and an intermediate domain, linking the other two domains [62]. CCT substrates are sequestered into a central chamber, formed by the two stacked rings, where protein folding occurs in an ATP-dependent fashion [62, 63]. About 10% of the proteome is thought to interact with CCT [24] including CCT's obligate clients, the cytoskeletal proteins actin and tubulin, and cell cycle regulators Cdc20 and Cdh1 [22, 94, 95]. Other client proteins include, PLK1 [96], cyclin E [34], the von Hippel Lindau tumor suppressor [31], Stat3 [28], p53 [33] and MYC [26]. Considerable evidence suggests that CCT has a role in oncogenesis and tumor progression [97]. The genes coding for the eight CCT subunits are amplified in a variety of cancers [64]. CCT1 and CCT2 are essential for breast cancer cell survival and are linked to driver oncogenes responsible for tumorigenesis in breast cancer [41]. Our previous work shows that CCT2 is significantly overexpressed in invasive ductal breast carcinoma (IDC), in TNBC cell lines, such as MDA-MB-231 and MDA-MB-436 [18], and in prostate cancer cell lines [19], which suggests that CCT2 levels could indicate increased disease severity.

For the work presented here, we further investigated the role of CCT2 in tumorigenesis to better understand its contribution to cancer progression. Using the CRISPR/Cas9 system, we generated breast cancer cell lines with partial inhibition of CCT2 (full inhibition was lethal) and using a lentiviral over expression system, we produced breast epithelial cells with increased levels of CCT2. As a result, we detected changes in tumorigenicity and key CCT client proteins like STAT3. These findings indicated that CCT could be a driver of breast cancer through selective expression of subunits like CCT2 that confer increase protein folding activity to provide essential client proteins needed by cancer cells to survive, grow and transform. Hence CCT2 could be a new molecular marker for breast cancer and target for novel cancer therapies.

Materials & Methods

Cell lines and culture conditions

Cell lines used were MDA-MB-231 (ATCC HTB-26) triple negative breast cancer cells and MCF10A (ATCC CRL-10317™) breast epithelial cells. MDA-MB-231 cells were low passage cells cultured in Dulbecco's Modified Eagle's Medium (DMEM) (Corning) supplemented with 10% FBS (Gemini) and 1% Penicillin-Streptomycin (Corning). MCF10A cells were low passage cells cultured in Mammary Epithelial Basal Medium (MEGM-Lonza) supplemented with bovine pituitary extract (BPE), human epidermal growth factor (hEGF), hydrocortisone (all from MEGM bullet kit - Lonza) and 1% Penicillin-Streptomycin (Corning). MDA-MB-231 transfected with CRISPR gRNA 3 plasmid (GenScript) were cultured in the same medium as WT MDA-MB-231 with the addition of 0.5 μg/mL puromycin dihydrochloride (ThermoFisher). The MCF10A cells transfected with the lentiviral plasmid were cultured in the same medium as the WT MCF10A with the addition of 1 μg/mL puromycin dihydrochloride (ThermoFisher). All cells were grown in a humidified incubator at 37° C with 5% carbon dioxide.

Immunohistochemistry

Small cohort tissue microarray (TMA) was obtained from Florida Hospital (IRBNet# 748165). Large cohort TMAs containing normal breast tissue and breast cancer tissue at various disease stages were commercially acquired (BR8013 and BR8017, US

Biomax) and contained associated information about the tissue type, TNM score, tumor grade, and stage. TMAs were stained for CCT2 using anti-CCTβ antibody (LS-B4861; LifeSpan Biosciences) and for STAT3 using anti-Stat3 antibody (ab32500; Abcam). Antibodies were diluted 1:100 in Antibody Diluent (Leica). Staining of tissue arrays was performed using a Bond-Max Immunostainer (Leica), with an epitope retrieval buffer of EDTA pH 9.0 (Leica). Polymer Refine Detection reagents (Leica) were used, which include a hematoxylin counterstain. Scoring of staining was performed by a surgical pathologist as previously published [18].

Plasmids and primers

The CRISPR knockout CCT2 CRISPR guide RNA 3, Clone ID: C27761, Vector: pSPCas9 BB-2A-Puro (PX459) v2.0 was purchased from GenScript. The lentiviral plasmid pLV[Exp]-EGFP:T2A:Puro-EF1A>{hCCT2[ORF023792]*/FLAG} for CCT2 overexpression was purchased from Vector Builder by Cyagen Biosciences. Envelope vector pMD2.G (Addgene 12259) and packaging vector psPAX2 (Addgene 12260) were provided by Didier Trono through Addgene plasmid repository. PCR primers used for CCT2 knockdown efficiency were Forward CACTGCCCCTTTAACTGTCA and Reverse AGCTGCTGGATTGTCAACAC from Eurofins.

Lentiviral transduction

Lentiviral plasmid pLV[Exp]-EGFP:T2A:Puro-EF1A>{hCCT2[ORF023792]*/FLAG} for CCT2 overexpression (Cyagen Biosciences), envelope vector pMD2.G (Addgene 12259),and packaging psPAX2 (Addgene 12260) were transfected into 293T cells using transfection solution (105 μM Tris, water, 98 mM CaCl2, and 1X HEPEs-buffered saline). Supernatants containing the virus were harvested 24 and 48 hours post-transfection. The virus was concentrated in 15 mL Beckman Ultraclear tubes at 4° C 70000 x g for 1.5 hours then resuspended in RPMI 1640 (Corning). MCF10A cells were plated in 6 well plates and transduced with 50X virus stock the following day in MEBM as described above with 8 μg/mL polybrene (Millipore). The following day cells were washed twice with 1X phosphate-buffered saline (Corning) and medium replaced with MEBM containing 1 μg/mL puromycin. CCT2 overexpression was monitored by tracking GFP signal in the transduced cells.

CRISPR/Cas9 MDA-MB-231 CCT2 knockdown cell line generation

CRISPR knockout CCT2 CRISPR guide RNA 3, Clone ID: C27761, Vector: pSPCas9 BB-2A-Puro (PX459) v2.0 was designed by the Zhang lab and purchased through GenScript. The plasmid was transformed into DH5α E. coli and maxiprepped using Invitrogen PureLink HiPure Plasmid Filter Purification Kit Catalog #K2100-15 and Invitrogen PureLink HiPure Precipititator Module Kit Catalog #K2100-21 following the included protocol. MDA-MB-231 cells were plated in 6 well plates overnight and transfected the following day using Mirus Trans-IT® X2 Transfection reagent. 48 hours

following transfection the cells were split and placed under selection with 0.5 μg/mL puromycin in DMEM.

CCT2 knockdown efficiency

Measurement of CCT2 genomic cleavage performed using Life Technologies GeneArt Genomic Cleavage Detection Kit (Cat# A24372) following the included protocol. MDA-MB-231 CCT2 Knockout cells were collected and pelleted for each sample and lysed according to protocol. Using the lysate, PCR was performed around the region of interest using primers: Forward CACTGCCCCTTTAACTGTCA and Reverse AGCTGCTGGATTGTCAACAC. The PCR product was confirmed to be present and of the correct size by running on 1.5% agarose gel with control primers to validate the kit. Next the PCR product underwent cleavage assay according to the protocol and the final product run on a 1.5% agarose gel. Intensity of each band was analyzed using ImageJ software to measure relative intensities. The gel image was captured as a TIF and converted to an 8-bit black and white image. A histogram of each lane was generated and the area of the curve and percent intensity was captured using the wand tool. The relative density was calculated by relative density = % of sample/ % of standard.

Immunoblots

Antibodies for immunoblots include: anti-TCP-1 beta (Millipore,clone F39 P7 F11 MAB10050 mouse monoclonal (1:1000 WB) , Abcam anti-TCP-1 delta ERP8495(B) ab129072 rabbit monoclonal (1:1000 WB), Abcam anti-TCP-1 epsilon EPR7562

ab129016 rabbit monoclonal (1:1000 WB), Abcam anti-STAT3 antibody E121-21 ab32500 rabbit monoclonal (1:1000 WB), Santa Cruz anti-p38α (C-20) rabbit polyclonal (1:1000 WB), LI-COR IRDye 680 CW Goat anti-Rabbit IgG (1:10000 WB)and LI-COR IRDye 800 CW Goat anti-Mouse IgG (1:10000 WB). For lysate preparation, cell pellets were washed in 1X PBS prior freezing and stored at -80° C for at least 30 minutes. Cells were lysed by resuspending in ice-cold NP-40 Lysis Buffer (50 mM K+ HEPES pH 7.5, 150 mM NaCl, 1% NP-40, 1 mM EDTA) containing 1X protease inhibitors (ThermoScientific) on ice for 10-15 minutes. Lysates were centrifuged at 12000 x g for 15 minutes at 4° C to pellet cellular debris. Supernatant recovered was mixed with 4X Orange G loading dye (LI-COR) supplemented with 10% β-mercaptoethanol (Gibco) and heated at 99° C for 10 minutes. Proteins were resolved by SDS-PAGE and transfered to PVDF membrane (Immobilon-FL Millipore IPFL00010). Before membrane blocking, total protein was measured using the REVERT Total Protein Stain (LI-COR) and detected by NIR fluorescence at 700 nm (LI-COR Odyssey). The membrane was blocked for 1 hour (1% fish gelatin in TBS-T with 0.1 mM EDTA) followed by overnight incubation with primary antibody, at 4° C. The membrane was incubated with secondary antibody for 1 hour at room temperature then imaged on the LI-COR Odyssey. Quantification was performed using LI-COR Image Studio software and signal normalized to total protein signal. Normalization was calculated by dividing the total protein signal of each lane by the lane with the highest signal to gain the Lane Normalization Factor (LNF). The quantified signal for each protein band was divided by each LNF to gain the normalized signal. Each sample had three technical replicates.

Migration assay

Cellular migration was measured using Oris Migration Assembly Kit (Platypus Technologies). Stoppers were placed in each well and cells seeded around the stoppers. The stoppers were removed after 2 hours and wells were imaged on the Cytation 5 (Biotek). The cells were incubated for an additional 15 hours. The control cells were stained using CellTrace CFSE stain (ThermoScientific) for 20 min at 37° C then all cells were imaged as previously. The images were analyzed using Gen5 Software for mean GFP signal within the plug. The wells were quantified by subtracting the pre-migration signal from the post-migration signal.

In vivo experiments

Female nude (nu/nu) mice used in these experiments were obtained from Charles River Laboratories. Mice were allowed to acclimate for one week after arrival, prior undergoing orthotopic implantation of cells. Each mouse received 800,000 cells into the right mammary fat pad in a 50:50 solution of PBS and Matrigel Matrix (Corning Cat# 354248). One group of mice received MDA-MB-231 cells (n=3) (tumor control mice) and another group of mice (n=3) received MDA-MB-231 CCT2 knockout cells. Mice were monitored for 60 days and once the tumor was large enough to be detected, caliper measurements were taken three times per week. The formula used for tumor volume measurements was length (mm) x width (mm) x 0.5). All animal work followed the study

protocol approved by the Institutional Animal Care and Use Committee (IACUC) at the University of Central Florida

Statistical analysis and data mining

For scoring analysis of TMAs one-way ANOVA was used to compare mean scoring between the different groups defined by various tissue parameters. Tukey's multiple comparison test was used to compare significance between individual groups. Survival data was analyzed using Sidak's multiple comparison test. Calculations were performed with GraphPad Prism software (GraphPad). Statistical significance was defined as $p < 0.05$. Breast cancer patient survival data in the current study is available in the Kaplan-Meier Plotter (KMPlot) repository [67, 68] at:

http://kmplot.com/analysis/index.php?p=service&cancer=breast

Results

Increased CCT expression correlates with lower overall survival in breast cancer patients

There are eight genes (*cct1-8*) that encode the subunits that form the CCT protein folding complex. To determine whether breast cancer patient survival correlated with increased gene expression of individual CCT subunits, we interrogated the breast cancer database available in the Kaplan-Meier plotter (n=3951). We found that while increased expression of all the subunits correlated with decreased patient survival, the most

statistically relevant results (p< 0.0026) were achieved for CCT2 (Fig. 18A-B). A difference in survival of over 44 months was noted for patients that were high expressors of CCT2 compared to low expressers of CCT2 (Table 7). These results support our previous findings using The Cancer Genome Atlas (TCGA) database that increased expression of the CCT2 subunit is associated with decreased breast cancer patient survival [18] .We also found that CCT2 copy is increased across cancer cells lines (Project Achilles) and that CCT2 is an essential gene (Fig. 19A-C).

CCT2 levels are higher in tissues of breast cancer patients when compared to normal breast tissue and correlate with levels of STAT3.

We next examined a small cohort of archival tumor tissues (n=20) from patients with invasive ductal carcinoma (IDC) from a local hospital for protein levels of CCT2 as well as one of the CCT client proteins, STAT3. While CCT levels varied from low to high irrespective of cancer grade or stage, an almost 100% correlation between CCT2 and STAT3 levels was observed (Fig. 20A). We expanded this study to include commercially available tumor tissues from patients with advanced breast cancer, stage II or greater (n=160). Tumor tissues representative of scoring for CCT2 and STAT3 staining are shown in Figure 20D. We observed that CCT2 and STAT3 levels were low in normal tissues and increased in stage II or III breast cancer (Fig. 20B-C). When directly comparing CCT2 and STAT3 staining, we found that over 50% of the tumors had equal scores, that 37.6% of the tumors has scores that differed by only 1 score point and that 11.4% of the tumors differed by 2 or more score points (Fig. 20E). This indicated that

88.6% the tumors had comparable levels of both CCT2 and STAT3, suggesting that more CCT2 could confer increased protein folding activity and provide more client proteins like STAT3 to cancer cells.

Decreased levels of CCT2 leads to decreased levels of STAT3, while increase in CCT2 leads to increased STAT3

Based on the studies showing that CCT2 is an essential gene for cancer cells (Fig. 19B-C), we opted for a knockdown of CCT2 in MDA-MB-231 breast cancer cells using CRISPR-CAS-9 technology. We previously showed that these cells had high levels of CCT subunits as compared to the breast epithelial cell line, MCF-10A [18]. Using a genomic cleavage assay, we achieved a 32% decrease in CCT2. This cell line showed a corresponding decrease in CCT2 protein and as well as a decrease in STAT3 (Fig. 21B). Next, using a lentiviral system, we generated a stable MCF-10A cell line that overexpressed FLAG-tagged CCT2. We confirmed both expression of the FLAG tag and increased CCT2 in the cell line and observed an increase in STAT3 (Fig. 22). Together these results, support that CCT2 is driving the levels of client proteins like STAT3 and could underlie the mechanism by which CCT promotes cancer progression.

Increased expression of CCT2 stimulated cell migration, while decreased levels of CCT2 reduced tumor growth in mice

The overexpression of CCT2 in the non-tumorigenic breast epithelial cells, MCF10A, increased migration capabilities in these cells (Fig. 23A-B). MCF10A cells are immortalized but they are unable to form tumors in mice, these cells are sensitive to

77

confluency, nutrients and environment and can undergo spontaneous epithelial-to-mesenchymal (EMT) transitions, a process that can also be induced by treatment with TGF-beta [98]. MDA-MB-231 cells are highly tumorigenic in mice. To determine if decreasing levels of CCT2 in the MDA-MB-231 influenced tumorigenicity, we used CRISPR/Cas9 with a gRNA targeting CCT2 to partially inhibit gene expression (Fig. 21). Cells were injected orthotopically in the mammary fatpad of female nude mice and tumor growth compared between wild-type (WT) MDA-MB-231 cells and CCT2 inhibited MDA-MB-231 cells. We found that tumors lacking CCT2 grew slower by 14 days (Fig. 25) and were 2-5 fold smaller after 8 weeks (Fig. 25). These results show that even a partial loss (~32%) of a single CCT subunit, like CCT2, is sufficient to significantly impair tumor cell migration and tumor growth, indicating that inhibiting this protein folding complex could be an effective therapeutic approach.
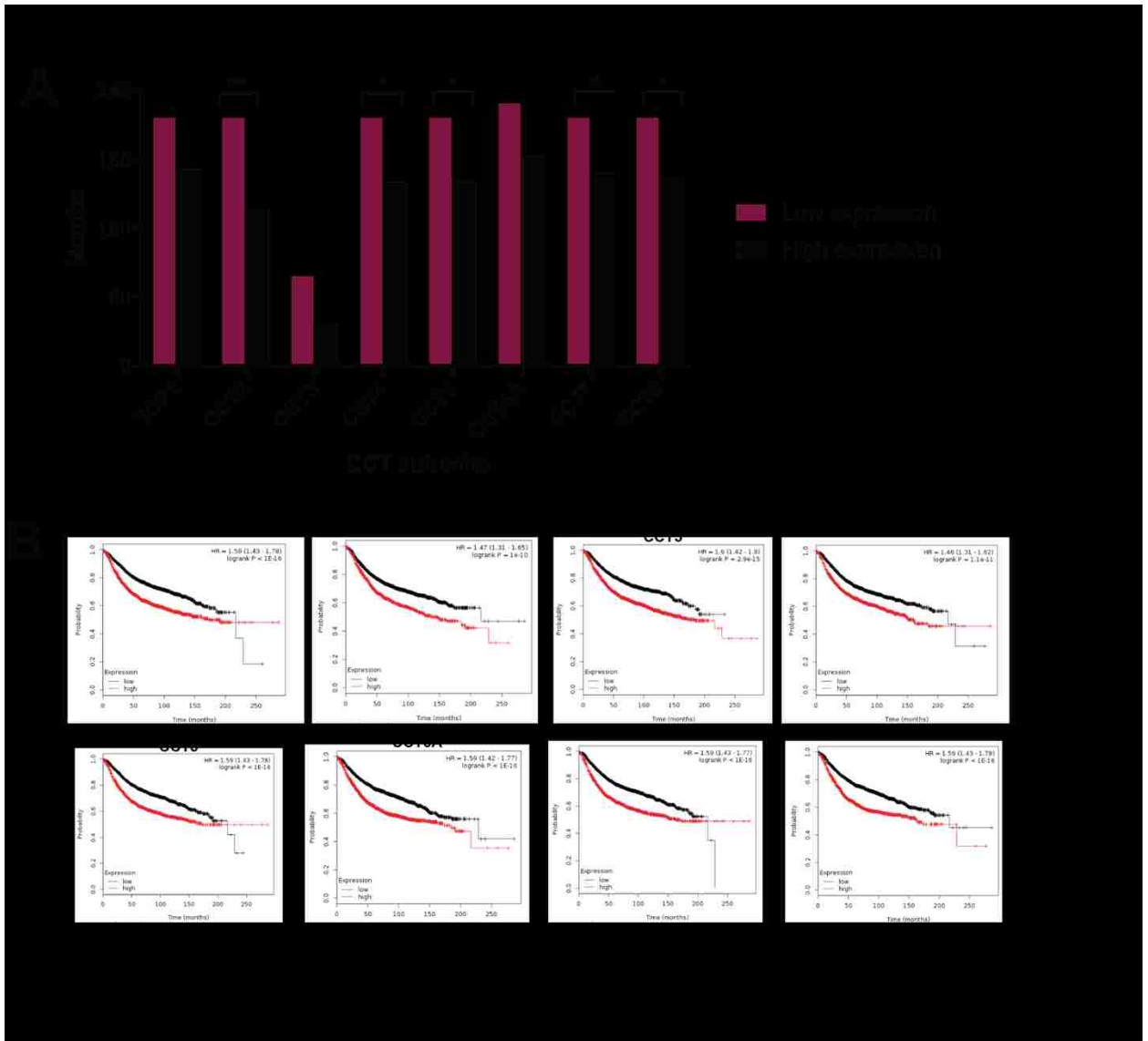
Figure 18: High CCT expression levels significantly decrease survival in breast cancer patients

Survival data in breast cancer patients showing that higher expression of all CCT subunits correlates with lower survival rates. (A) Bar graph of survival data showing that CCT3 levels have the highest effect on overall survival, but CCT2 levels have the most significance between high and low levels. (B) Kaplan-Meier plots of breast cancer patients based on the expression level of each CCT subunit. Numbers used to generate data is also on table 7. The survival graph was generated using publicly available database. Cohort size: 3951 patients (KM plotter; www.kmplot.com).

Table 7: Effect of high and low expression of each CCT subunit in survival of breast cancer patients

CCT subunits	Low expression cohort (months)	High expression cohort (months)	Significant?	Summary	Adjusted P Value
TCP1	216.7	171.43	No	ns	0.0594
CCT2	216.7	137	Yes	**	0.0026
CCT3	78.48	38.4	No	ns	0.1032
CCT4	216.7	160.28	Yes	*	0.0194
CCT5	216.7	161.43	Yes	*	0.0216
CCT6A	228.85	184.04	No	ns	0.0624
CCT7	216.7	168.5	Yes	*	0.0438
CCT8	216.7	163.46	Yes	*	0.0264

Numbers used to generate data shown in Figure 18.
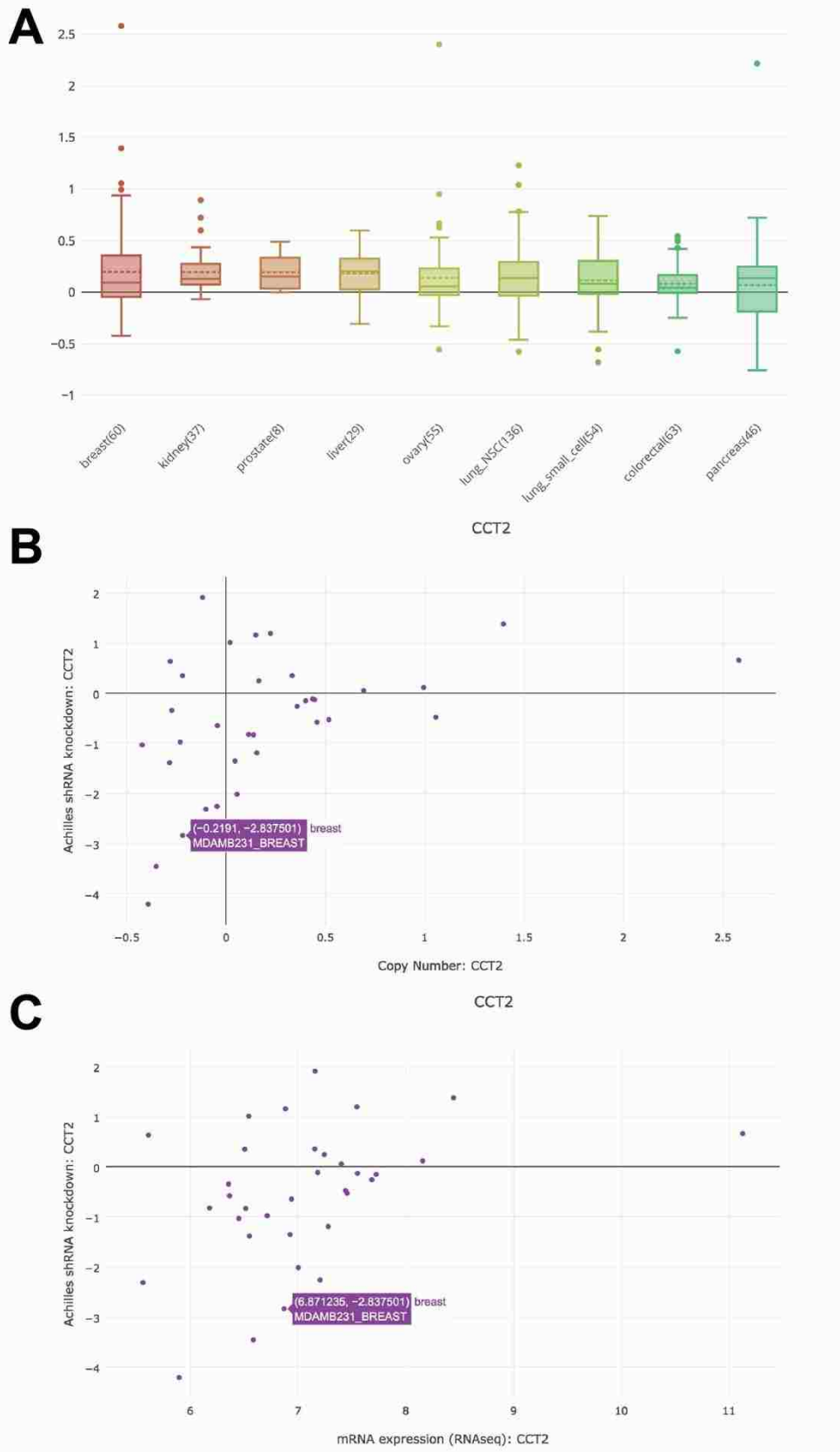
Figure 19: CCT2 copy number and CCT2 essentiality in MDA-MB-231 cells

Data and graphs obtained using publicly available databases (A) CCT2 copy number in cancer cell lines. Data from the Cancer Cell Line Encyclopedia (CCLE). Breast cancer cell lines have the highest copy number. (B-C) Data on CCT2 and essentiality in common cell lines (B) Achilles knockdown of CCT2 vs copy number and (C) Achilles knockdown of CCT2 versus mRNa expression showing essentiality of MDA-MB-231 cells [99]. Entrez ID: 10576 https://figshare.com/articles/AguirreMeyers/3420907

Figure 20: CCT2 levels are significantly higher in breast cancer tissues than normal breast tissue and significantly correlates with STAT3 levels

Human tissue derived from breast cancer patients were stained for CCT2 and Stat3 using immunohistochemistry. (A) Bar graph showing a strong correlation between levels of CCT2 and Stat3 on breast cancer tissue. Data obtained from local cohort samples (n=20). (B-C) Breast cancer containing medium to advanced stage breast cancer TMAs were purchased from USBiomax (cohort n=160). (B) CCT2 and (C) Stat3 staining scores. Tissue cores were analyzed by a pathologist according to stain intensity and given a score between 0-4 as previously published in Bassiouni et al (2016). (D) Graph of staining score results. Representative images of breast cancer TMA stained for CCT2 and Stast3 indicating scores of 0, for normal breast tissue and scores of 1-3 for tumor tissue. All images were taken using 400X magnification. (E) Pie chart with percentage of scores that were identical (51%), differed by 1 point (37.6%) and by 2 or more points (11.4%). Significance indicated in graphs are in reference to normal tissue.). * = $p<0.05$, ** = $p<0.01$, *** = $p<0.001$, **** = $p<0.0001$
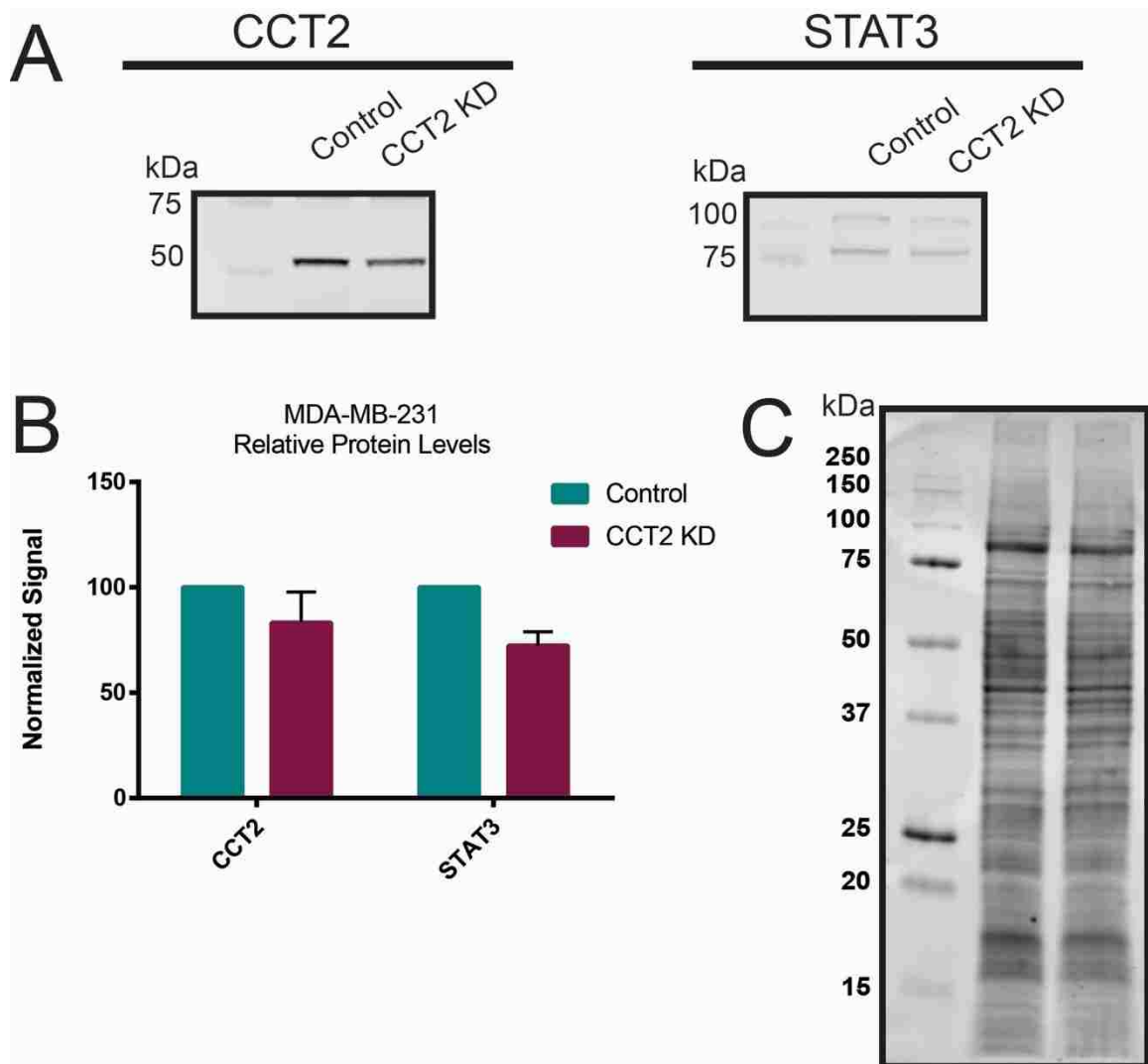
Figure 21: Knockdown of CCT2 in MDA-MB-231 cells

(A) The levels of CCT2 are reduced after stable transfection with CRISPR/Cas9 plasmid guide RNA 3. (B) Bar graph showing relative protein levels. CCT2 and stat3 levels are decreased after CRISPR/Cas9 (C) Total protein used for normalization. (CRISPR/Cas9 by A. Showalter and blots by the author)
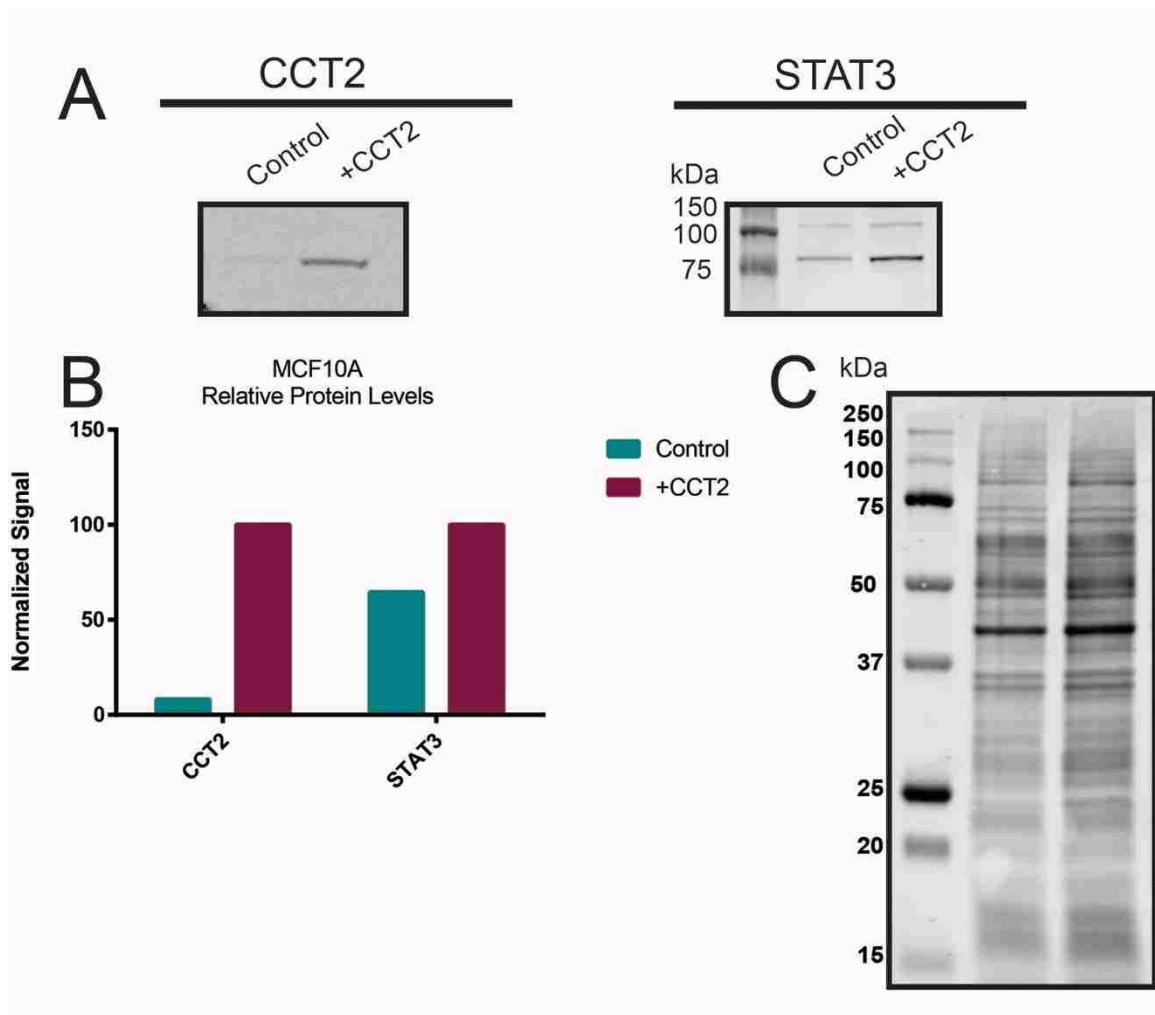
Figure 22: Overexpression of CCT2 increases the levels of CCT client protein STAT3.

Representative CCT2 and STAT3 blots of the control parental line and CCT2 overexpression line show increased protein levels under normal growth conditions (n=1). (B) The relative protein levels of CCT2 and STAT3 are both increased after normalizing the signal to total protein. (C) Representative blot of the total protein used to normalize the CCT2 (left) and STAT3 (right) blots. (Transfection performed by A. Showalter and blots performed by the author)
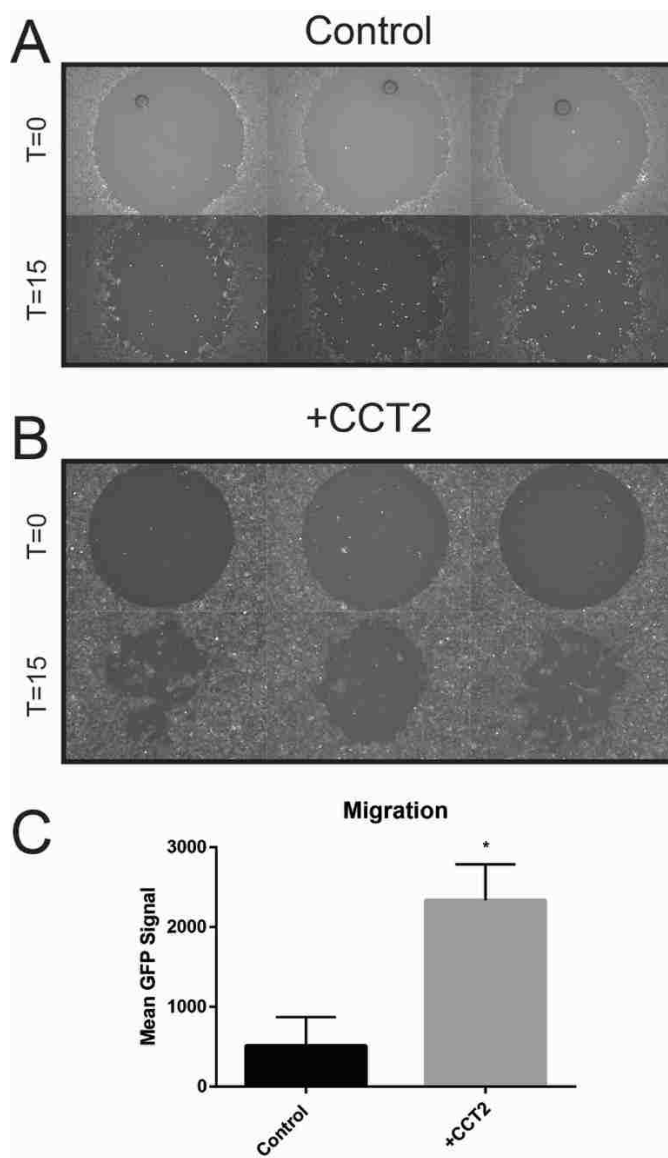
Figure 23: CCT2 overexpression cells migrate faster than the control line

Cells were plated around 2mm plugs and allow to adhere for 2 hours. The plugs were removed and the cells were allowed to migrate for 15 hours before imaging. Reference wells for T=0 had the plugs removed prior to staining with CFSE and subsequent imaging. Fluorescent images of the reference wells were taken for T=0 and samples wells for T=15. (A) Control cells (n=4 wells) showed some migration after 23 hours. (B) CCT2 overexpressing cells (n=4 wells) showed significantly more migration than the control cell line. (C) The mean GFP signal of cell within the 2 mm plug was measured with Gen5 software using the following formula: (signal post-migration – signal pre-migration). The results were analyzed using Graphpad Prism with a paired T test with p<0.05. (By A. Showalter)
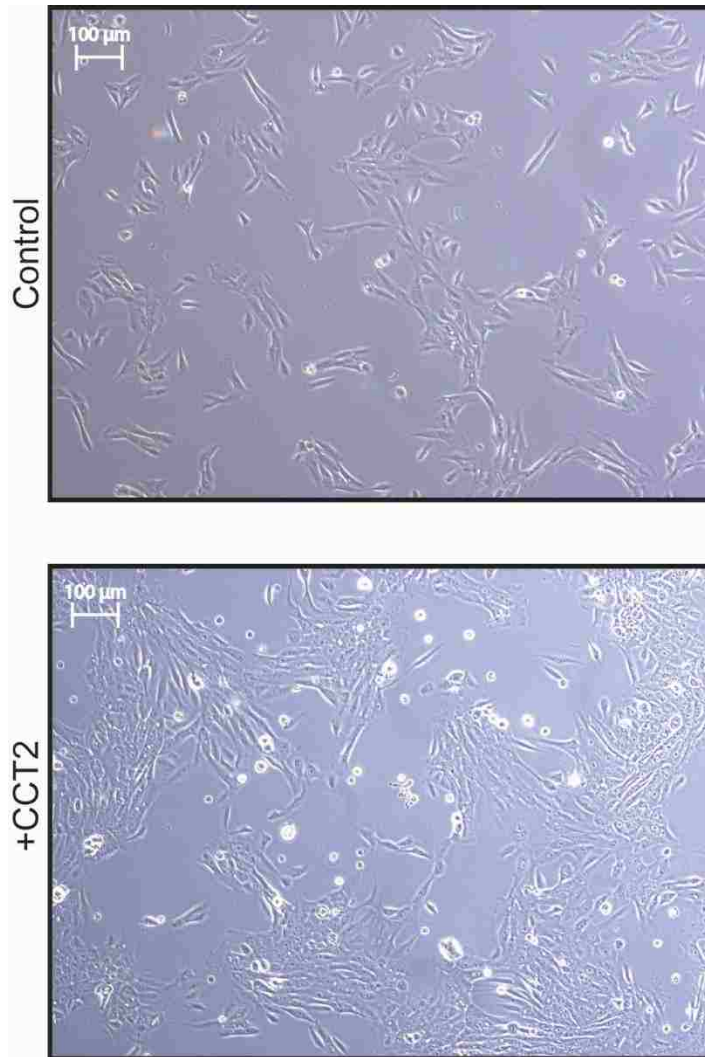
Figure 24: Overexpression of CCT2 in normal breast epithelial cells induces a change in morphology

Representative images taken by Zeiss Axio Imager by phase contrast at 10X magnification. (A) MCF-10A, normal breast epithelial cells grow in small patches and remain mostly elongated. (B) CCT2 overexpression cells, as indicated by +CCT2, become more cuboidal and grow in a more confluent monolayer.
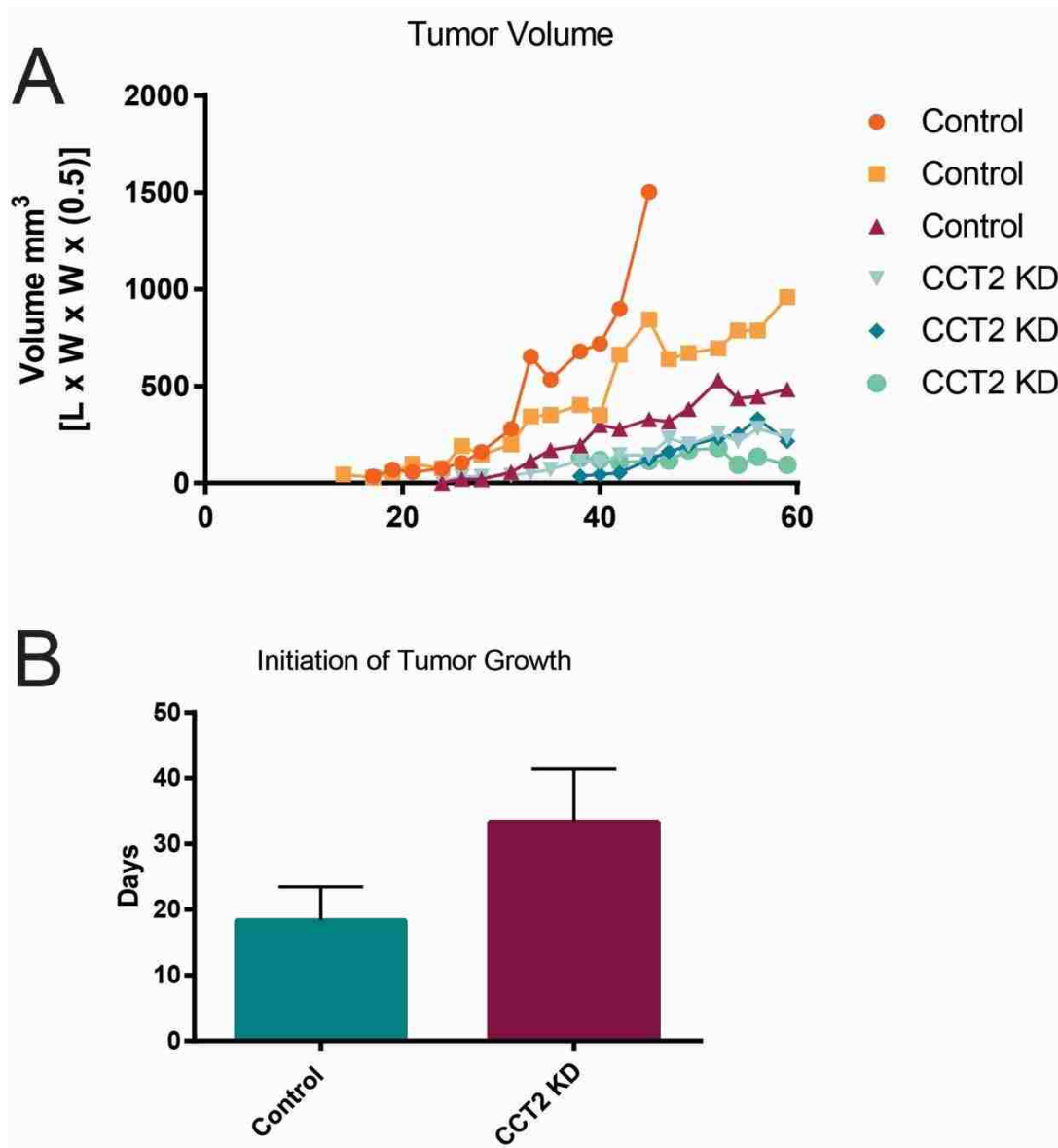
Figure 25: Knockdown of CCT2 decreases tumorigenicity of MDA-MB-231 cells in mice

Female *nu/nu* mice received either control (n=3) or CCT2 knockdown cells (n=3) injected into the mammary fat pad. Tumors were allowed to grow and were measured by calipers three times a week starting once the tumor was palpable. (A) Over a period of 60 days post-surgery, the control tumors grew large, with one being terminated early following the protocol. The CCT2 knockdown (KD) tumors remained smaller than the controls throughout the experiment. (B) The control tumors started to grow significantly earlier than the CCT2 knockdown tumors. Control tumors started to grow approximately 18 days post-surgery while CCT2 knockdown tumors did not start growing until approximately 30 days post-surgery.

Discussion

Using tools for genetic engineering, we generated cell lines in which expression of *cct2* was inhibited or increased to show that the CCT protein folding complex was essential for the process of tumorigenesis. Full loss of CCT2 in breast cancer cells was lethal, and a partial loss resulted in reduced client proteins like STAT3 and decreased tumor growth in mice. Increased expression of CCT2 altered the morphology of breast epithelial cells, increased STAT3 levels, and promoted a migratory phenotype. In support of CCT2 as a promising therapeutic target, we observed increased levels of CCT2 protein in tumor tissues from patients with advanced breast cancer, which highly correlated with STAT3 levels. In contrast, CCT2 levels were undetectable to low in normal breast tissues. Increased gene expression of CCT2 also correlated with decreased breast cancer patient survival. These findings support further investigation of CCT2 as a promising biomarker for breast that could have diagnostic as well as prognostic potential.

Group II chaperonins like CCT are found in the cytosol of archaea (e.g. thermosomes) and eukaryotes. CCT is evolutionarily conserved with multiple gene duplication events producing the eight subunits that form the two-ring complex[100] Each subunit has a unique position in the ring and substrates recognition is likely mediated through combinations of hydrophilic and hydrophobic interactions. What remains poorly understood is the level of redundancy or moonlighting for each CCT subunit. We observed that loss or overexpression of a single subunit, CCT2, was sufficient to alter the activity of the complex as reflected by the levels of client proteins like STAT3 and functional consequences such as migration and tumorigenicity. These

results suggest that individual CCT subunits are unique and could have multi-functions that are exploited by cancer cells. In support, others have shown that mutations in individual CCT complexes have divergent effects on cells. For example, mutation of CCT2 in yeast cells resulted in slower growth that was associated with a cell cycle defect, while mutations in CCT7 resulted in protein aggregations [101]. Such studies indicate that CCT subunits may each have unique roles related to substrate specificity but also the possibility that each subunit may have "moonlighting" functions independent of the complete complex. This is supported by our previous work and those of others using small interfering RNAs to inhibit individual CCT (iCCT) subunits, which suggested that iCCT subunits may have roles beyond protein folding, such CCT4 (epsilon) in the polymerization of F-actin [102] or CCT2 in promoting cancer cell growth [18, 41]

That CCT has a prominent role in oncogenesis is evident in the increasing number of reports documenting the activity of the protein folding complex in the signaling pathways critical to malignancy such as the STAT family of transcription factors [28] as we show herein. Other CCT substrates important for cancer cell growth include cycle regulators and cytoskeletal proteins as well as proteins directly related to oncogenesis such as VHL and p53 Hence distinct CCT subunits are overexpressed in different cancers. In addition to our findings that CCT2 is highly expressed in advanced breast cancer, others have found CCT2 elevated in gall bladder carcinoma [70], colorectal adenocarcinoma [103] and heptacellular carcinoma [40]. Several groups found that CCT3 expression was diagnostic in hepatocellular carcinoma [72, 79, 80], as well as CCT8 [39]. While this list is not extensive, it clearly demonstrates the growing trend that individual

91

CCT subunits are highly expressed in different cancers and could be important therapeutic targets.

The discovery of CCT's role in cancer progression has significant clinical implications in the development of personalized medicine for cancer therapy. Our data indicates that the CCT2 subunit could be a new biomarker for breast cancer that may be prognostic and help reveal when cancers progress and it could also be used as a companion or complementary diagnostic to guide therapies. In this regard, our lab developed a CCT inhibitor based on the capacity of an amphipathic peptide called CT20p [14, 104] to impair the chaperonin's activity. Much of the functional consequences of loss of CCT2 that are reported herein, such as decreased tumorigenicity, also result upon treatment with CT20p [15, 18]. Hence being able to manipulate the levels of CCT2 in cells, as we have shown, not only establishes the importance of this protein folding complex in oncogenesis but also provides a tool by which we can further address the pressing questions on the roles of individual CCT subunits and the possible consequences (or lack of) of CCT inhibition upon normal, healthy cells. The biology of chaperonins like CCT is complex but its understanding could reveal new targeted approaches for breast cancer therapy.

CHAPTER 4: SMALL MOLECULE SCREEN DEVELOPMENT USING TRIPLE-NEGATIVE BREAST CANCER CELLS

<u>Preface</u>

The first complete draft of this chapter was written by A.C.C. Comments from A.K were incorporated as it appears here.

Manuscript in preparation

Introduction

High throughput screens (HTS) are the backbone of drug discovery in the pharmaceutical industry as well as among academic researchers [105]. This type of screen encompasses testing a large number of compounds on a daily or weekly basis, for their biological effects. There are many types of HTS libraries including small peptides, small molecules, natural products and synthetic building blocks. In a target based approach, four crucial steps need to be considered in HTS design: target selection and validation; chemical hit and lead generation; lead optimization to identify a clinical drug candidate; and finally hypothesis-driven, biomarker-led clinical trials [106]. However, phenotypic screens are also used in instances where the target in unknown or targeted assays are not conducive with HTS.

Based on data previously published by our lab, the mammalian chaperonin-containing TCP1 (CCT) is an ideal candidate for target based drug discovery. We have showed that CCT is the intracellular target for CT20p, a cytotoxic peptide discovered by our lab [15, 18, 84, 107]. CCT is a macromolecular complex, composed of two rings stacked back-to-back, forming a barrel-like structure in which unfolded substrates are sequestered away from the cytosol until they reach their native conformation [62]. Each ring is composed of eight distinct, paralogous, subunits (CCT1-8). We identified targets of CT20p in a pull-down assay using biotin-CT20p. Proteomic analysis indicated CT20p interacts with seven out the eight CCT subunits [18]. We have also showed that in breast cancer cells, CT20p cytotoxicity correlates with CCT levels [18]. In addition, CCT levels have been shown to be higher in multiple cancers when compared to normal tissues [64]

94

The approach we developed and report here does not directly screen for CCT inhibitors, but it can be classified as target driven/phenotypic hybrid. Our primary, in cell assay uses a triple-negative (TNBC) cell line that stably expresses luciferase, therefore, decrease in luminescence can be caused by CCT inhibition, luciferase folding inhibition by direct interaction with the compound or cell death by an unrelated mechanism. Regardless of the MOA of the compound, every compound that met our luminescence signal decrease threshold (> 70% signal loss) criteria was selected as a hit compound and moved to the next screen.

In this manuscript, we report the results for a pilot screen involving a 2100 compound library focusing on assay development, optimization, hit compounds and lead identification.

Materials and Methods

Cell culture and conditions

MDA-MB-231/Luc cell line was purchased from Cell Biolabs, Inc. (AKR-231) and MDA-MB-231 cells were obtained from ATCC. The firefly luciferase gene was stably transfected into the cell line and placed under the CMV promoter. Cells were cultured in Dulbecco's Modified Eagle Medium (DMEM) supplemented with 10% FBS (Gemini). MCF-10A (ATCC CRL-10317) cells were cultured in Mammary Epithelial Cell Growth Media using MEGM bullet kit (Lonza). All media contained 1% antibiotic

antimycotic solution (Corning). Cells were grown in a humidified 37°C incubator with 5% carbon dioxide.

Reagents and small molecule library

D-luciferin (Goldbio) was dissolved in 1X PBS at 15 μg/ml, filter sterilized using 0.22 μm filter (Millipore) and stored in small aliquots in -20°C. Staurosporine InSolution (Calbiochem) stock concentration was 1mM, in DMSO.

The 2100 compounds were purchased from Asinex and distributed in a 384 plate format. Compounds were in DMSO and the stock concentration was 10mM. Plates were stored in -80°C.

Assay format, optimization and z'factor calculation

Cell seeding density: The screen was performed using 96 well plates (white, PerkinElmer). To determine optimal seeding density and signal linearity, MDA-MB-231/luc cells were seeded in two sets of triplicates at 1500, 3000 and 5000 cells per well. After 24 hours, spent medium was replaced with fresh medium containing 0.1μg/mL D-luciferin. Plate was wrapped in aluminum foil and luminescence signal measured after 10 minutes. This was repeated at the 48 hour time point as well.

Controls: For this pilot screen, the positive control for luminescence signal loss was staurosporine, used at 0.5μM final concentration (Fig. 27A)

Assay validation: The z' factor determines the quality of the assay, taking into account only the controls used in the assay [108]. The z' factor values range from 0 to 1,

values above 0.5 are considered excellent. We have determined the z' factor to be 0.611 for our assay.

Secondary screen: To determine the effect of hit compounds on non-tumorigenic cells, MCF10A cells were seeded at 10,000 cells per well and treated with 10μM for 48 hours. Viability was determine using CellTiter-Glo (Promega).

Results

Primary screen identified 24 hits in a 2100 compound library

Using a library composed of 2100 small molecules, we developed and optimized an in cell assay selecting for molecules that decreased luminescence signal by 70% or more in MDA-MB-231/luc cells. Compounds were tested at 10μM in duplicate wells. Each test plate contained duplicates of positive and negative controls and signal from test compounds were normalized to internal controls (Fig. 27B).

Both luciferase and luciferin are CCT clients, if the compound inhibits CCT, luciferase and luciferin will not fold properly and there will be a decrease in luminescence compared to the untreated control. Figure 28 summarizes the rationale for the assay. We identified 24 compounds that met the criteria.

Secondary screen

For a hit to move to the next phase of testing, it cannot have cytotoxic effects on normal cells. For that, we tested the 24 hit compounds on the non-tumorigenic MCF-10A cell line using the same concentration as in the primary screen. Only minimal cytotoxic effects were observed (Fig. 30A).

Lead compound

To identify the lead compound, we tested each of the 24 hits using an extended dose range from 2.5µM-40µM. Standard MDA-MB-231 (non-luc) cells were seeded as described in materials and methods. Only one "hit", the lead compound, killed the 231 cells in a dose dependent manner with and IC50 ~5µM (Fig. 30B).
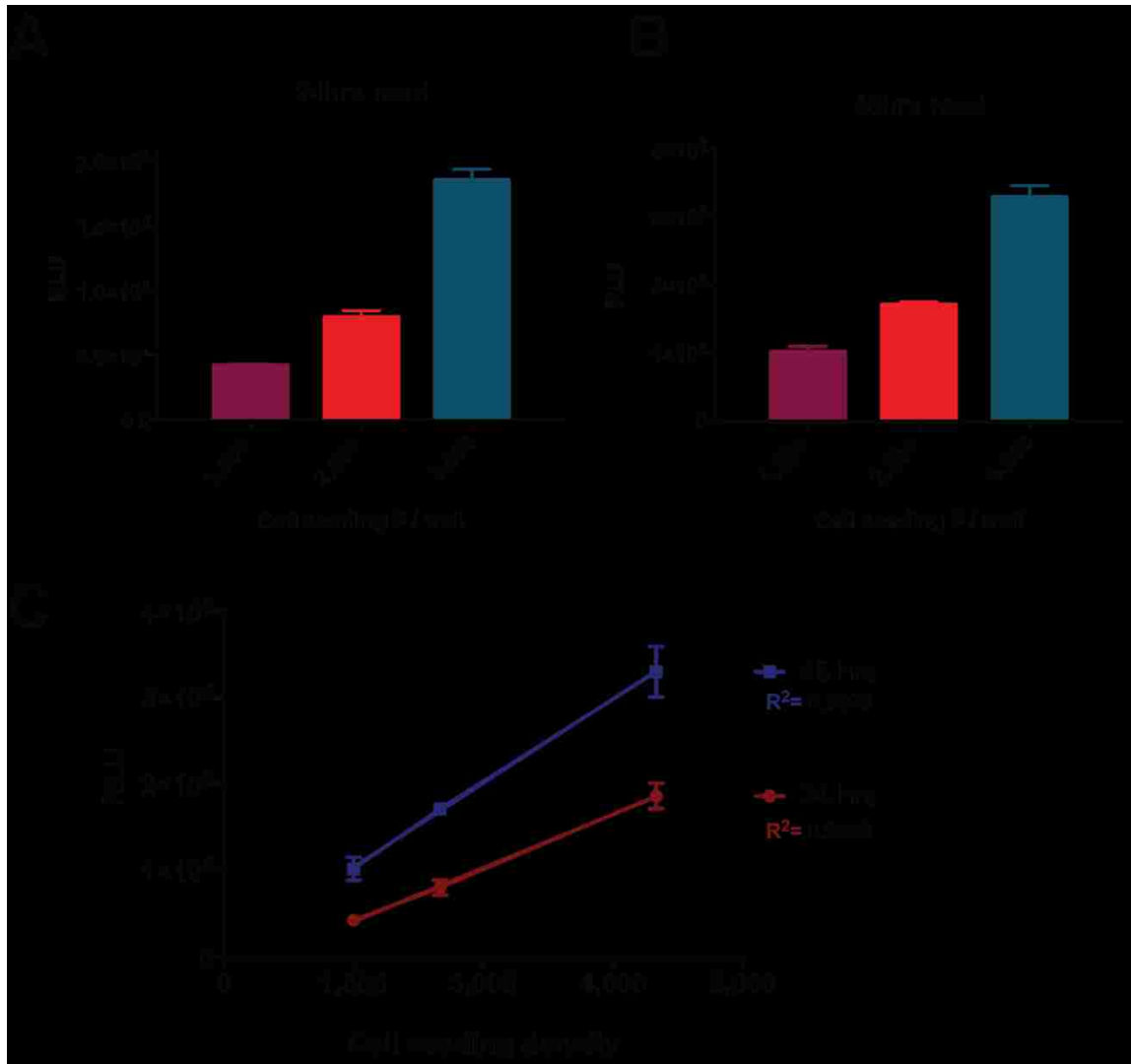
Figure 26: MDA-MB-231 cell seeding density optimization

On a 96 well white plate 1500, 3000 and 5000 cells per well were seeded in triplicates. Luciferin was added and signal measured (A) 24 hours or (B) 48 hours. (C) Graph showing linear relationship between cell number and signal detected using our approach.
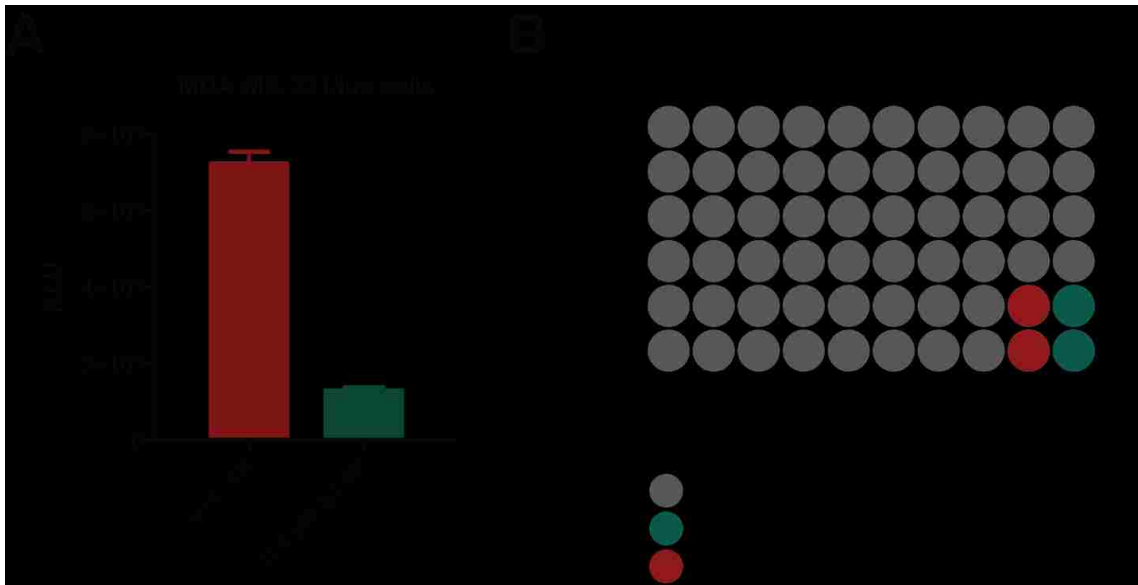
Figure 27: Assay plate set up showing position of positive and negative controls

(A) Signal from negative (untreated cells) and positive (staurosporine) controls. Staurosporine is a protein kinase inhibitor and it causes cell death through a canonical apoptotic pathway. (B) Only the inside wells were used for this assay to avoid edge effects. The plate set up includes both controls in every plate so data normalization is performed per plate.
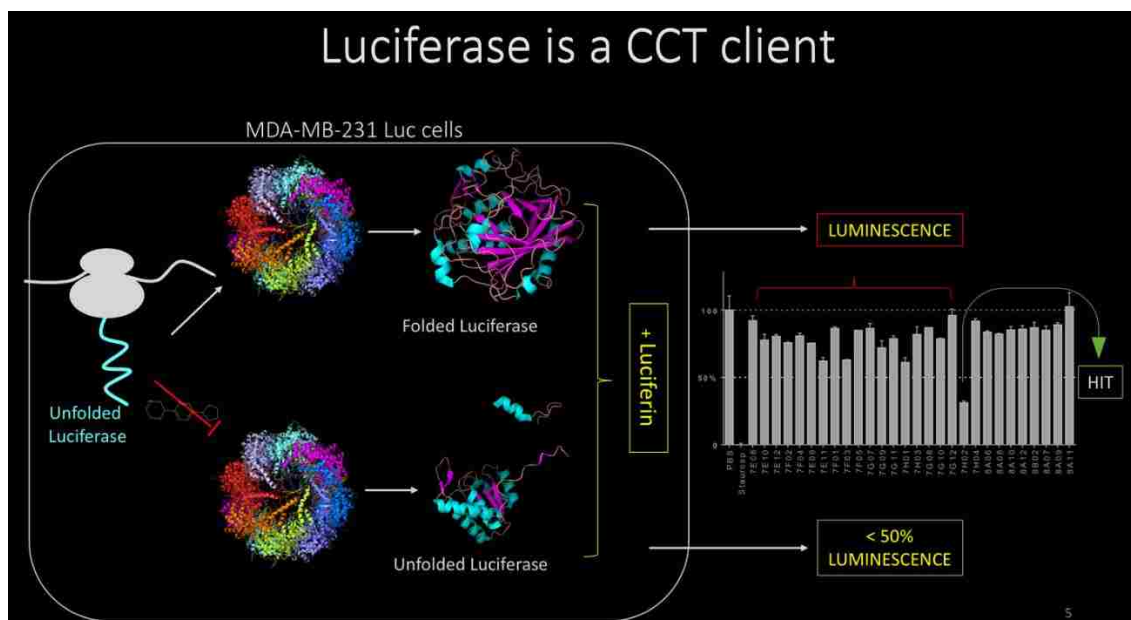
Figure 28: Summary of the assay rationale

The TNBC cell line, MDA-MB-231/luc stably expresses luciferase. Both luciferin and luciferase are folded by CCT. If CCT is inhibited by the small molecule in the screen, it will not fold luciferase properly and luminescence signal will be low. Each plate has both the positive and negative controls. The data is normalized to the internal controls per plate. Small molecules that caused luminescence signal loss by >70% we considered hits.
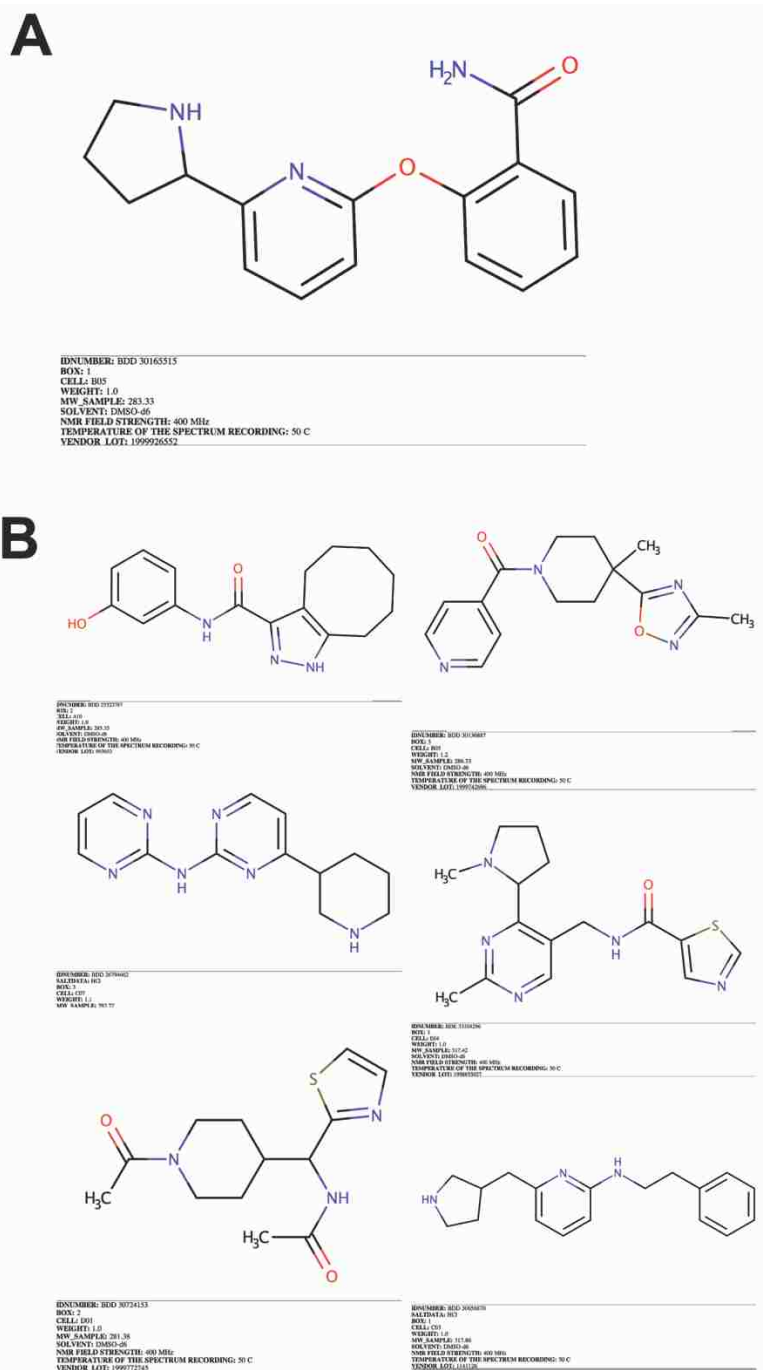
Figure 29: Representative structures identified in the screen.

A) Structure identified as the lead compound B) Six of the 24 compounds identified in the screen.
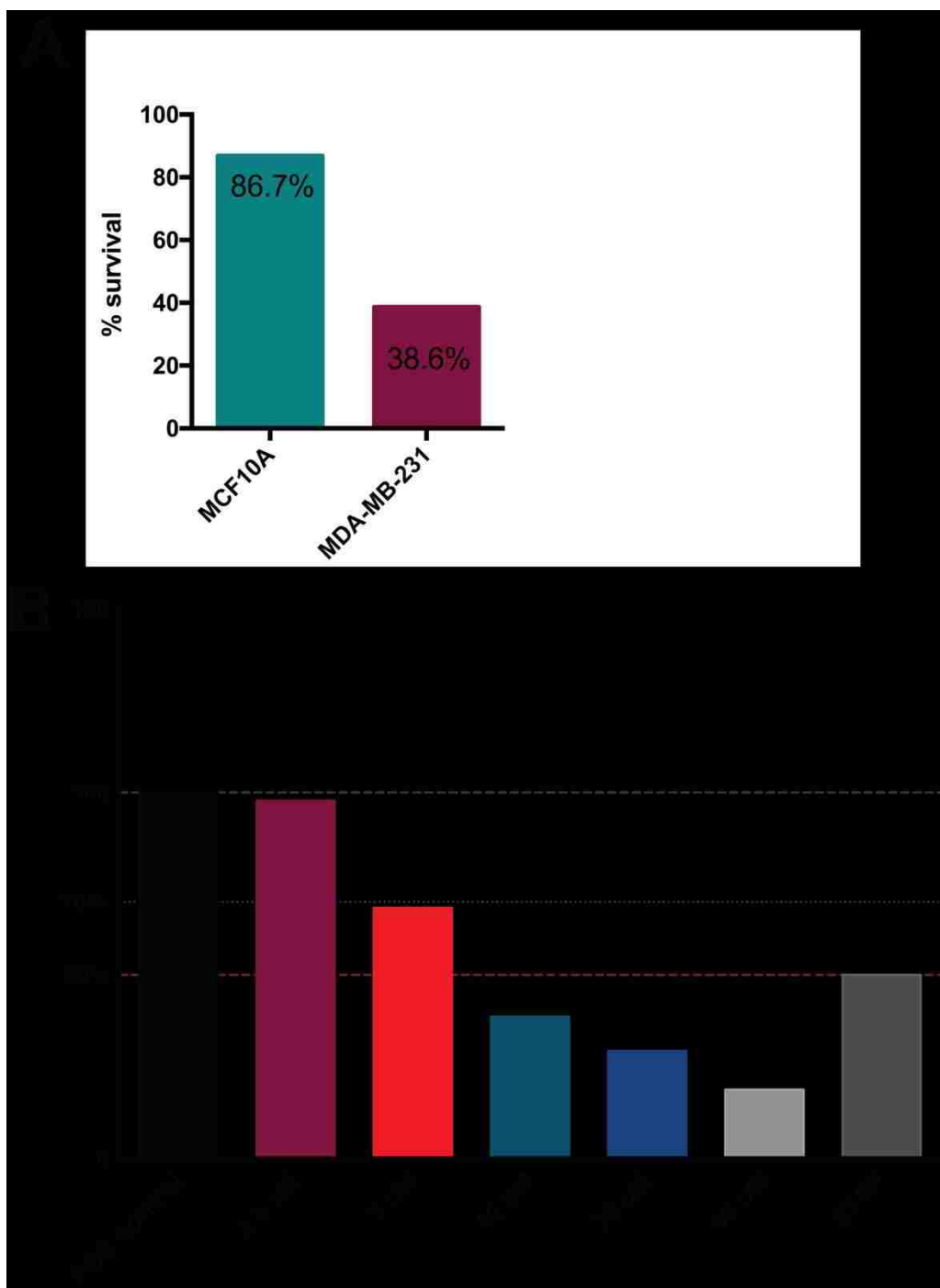
Figure 30: Lead compound secondary assays results

(A) Bar graph showing the percent survival of normalized signal of lead compound effects at 10μM, on control and TNBC cell lines using CellTiterGlo (B) Dose response of lead compound on MDA-MB-231/luc cells

Discussion

Our drug screening strategy to identify novel CCT inhibitors was validated using a pilot 2100 compound library. We rationalized that because both luciferase and luciferin are known to be folded by CCT, although they are not obligate clients [94], if the compound inhibits CCT, we will observe a decrease in luminescence compared to the untreated control. The initial screen identified 24 hit compounds , equivalent to ~10% of the library [109], based on loss of luminescence. We expected that a few of these could be chaperonin inhibitors. Secondary screens revealed which of these compounds was not toxic to immortalized breast epithelial cells but still killed triple negative breast cancer cells. Counter screens showed which of these compounds did not induce a heat shock response but did trigger the membrane translocation of calreticulin (not shown). Based on these assays, we identified one hit that matched our criteria for a possible CCT inhibitor.

To date, other than our CT20p peptide, no general use CCT inhibitors have been identified. There are only a few reports of CCT inhibitors based on hindering a specific interaction with a known client (e.g. tubulin [81, 82]) that have limited application. Hence our study would be the first to discover a CCT inhibitor that could have clinical use for multiple cancers. Disrupting molecular chaperones as a form of cancer therapy was first explored for HSP90. Hsp90 has received the most attention as a possible therapeutic target because it is upregulated during oncogenesis [83, 86, 88]. A number of small molecules and natural product inhibitors of HSP90 advanced to clinical trials. The best known of these are geldamycin derivatives [110]. However, problems with induction of protective heat shock response and the inability to achieve therapeutic doses hampered

these trials [111]. Another approach for targeting proteins essential for cancer cells, is to inhibit the proteasome. Pathways for protein folding and ubiquitin-mediated proteolysis have a number of points of commonality. Proteasome inhibitors, like Veldcade, are currently used in the treatment of multiple myeloma [112]. Benefits were also observed with combination approaches of protein folding and proteasome inhibition, hence, our CCT inhibitor could be used to improve existing therapeutics in combination approaches.

The typical screens used to identify agents that impair molecular chaperones are cell-based and involve loss of a chaperone-dependent activity. In one study, a v-src-luciferase fusion was used as reporter and hits included HSP90 inhibitors, ubiquitin pathway inhibitors, histone deacetylase inhibitors and others, revealing one of the challenges of this approach when seeking an inhibitor that could impact many downstream substrates [113]. Hence, it becomes important to generate a strategy, as we described herein, to move from a general screen to one that is more specific for CCT. As example, one group developed a method to purify the complete human CCT complex (all eight subunits) from HeLa cells. To confirm activity of the complex, a luciferase refolding was performed [114]. However, a more rigorous test was needed to ensure that the complex being isolated was indeed CCT, so an assay to measure aggregation suppression was also included [94]. However, this assay is tedious and time consuming and does not lend itself to high throughput. Our solution was based on characterizing the biological effects of CCT inhibition observed upon treatment with CT20p, such as the membrane translation of CRT and absence of GRP78 membrane translation, which can be assessed by flow cytometry. The latter was especially important as a counter screen, because most HSP90 inhibitors can cause GRP78 membrane exposure as part of

protective heat shock response. Future screens could also incorporate use cell lines that stably overexpress or inhibit CCT subunits as well as employ in silico drug screen technology to identify classes or families of compounds that can dock at the substrate bindings sites of CCT.

CHAPTER 5: CONCLUSIONS

<u>Preface</u>

This chapter was composed entirely by A.C.C.

CCT2 levels are significantly higher in prostate, hepatocellular, breast and lung cancers compared to normal tissues, indicating CCT as a potential biomarker in these cancers. CT20p is cytotoxic to SCLC cells but not normal lung tissue, therefore targeting CCT with CT20p in SCLC is a promising therapeutic approach. CCT levels are high in immortalized cell lines or cells lines that have undergone EMT, but the same is not observed in normal human tissue, therefore immortalized or transformed cell lines cannot be used as control for CT20p experiments. When CCT is inhibited, levels of client proteins, such as STAT3 decreases, indicating CCT targeting has the potential to inhibit many pathways involved in oncogenesis. Partially knocking out CCT2 in MDA-MB-231 cells, a highly tumorigenic triple negative cell line, is sufficient to decrease tumorigenicity potential in nude mice. Overexpressing CCT2 in immortalized breast cells, increases migration and causes morphology to change, two characteristics of cells that have undergone EMT and causes levels of client proteins, such as STAT3, to increase.

CCT2 levels is a biomarker in many cancers

Using patient tissue microarrays containing 80-120 cores each, we determined CCT2 levels in a large number of samples in prostate, colon, liver, breast and lung cancers by immunohistochemistry. We were also able to correlate CCT2 levels with stage, severity, and histological characteristics in these TMAs, allowing us to conduct a broad analysis of CCT2 in the most common cancers affecting the population today. We found that CCT was significantly higher in advanced tumors when compared to normal

tissue. SCLC stood out by having the highest CCT2 levels among the cancers analyzed in our study. We used publicly available genomic databases and found that all CCT subunits are expressed at higher levels in breast cancer and that higher levels correlate with decreased survival. The CCT subunit with the most significant effect on patient survival was CCT2, which indicates that this subunit has an essential role in breast cancer progression, which is validated by previous work published by us and others [18, 41, 70].

Targeting CCT with CT20p in SCLC is a promising therapeutic approach

Using five SCLC cell lines, we showed that CT20p is cytotoxic in a dose dependent manner and that cytotoxicity levels vary among cells lines, indicating that there's a therapeutic window which allows for effective eradication of tumor cells while sparing non- cancerous ones.

Client proteins, such as STAT3, also respond to CCT inhibition to different degrees in a cell line dependent fashion. Targeting CCT is a rational approach because cancer cells express and rely on the chaperonin more heavily than normal cells. Rapidly proliferating cells, such as during development and spermatogenesis, have higher levels of CCT than non-proliferating cells, as it has been shown in a previous study done using mice [115, 116]. Using siRNA to deplete CCT causes cell cycle arrest in Swiss 3T3 mouse fibroblasts indicating CCT has an essential role in cell cycle progression[102]. In this same study, CCT's folding activity was modulated by using an antibody against CCT5 which caused loss of cell motility and cytoskeletal disorganization [102]. Similar effects were observed in studies by our lab on CT20p effects on breast cancer cells [18].

Other CCT inhibitors include arsenic and N-iodoacetyl-tryptophan (I-Trp) [81]. Arsenic inhibits CCT and impairs actin and tubulin filaments [81, 85]. I-trp is a synthetic small molecule derived from iodoacetamide capable of interrupting the constitutive β-tubulin/CCT2 interaction eliciting caspase-dependent signaling which leads to cellular apoptosis [82, 83]. An advantage of CT20p, is that cell death is caused independently of the canonical apoptotic pathway [14], which is often downregulated in tumor cells, instead, CT20p prevents folding of many tumor essential proteins therefore, halting tumor progression [84]. Targeting CCT, a chaperonin responsible for folding many oncogenic proteins, is advantageous in the sense it decreases the pool of essential proteins required for tumor progression.

CCT2 plays a role in oncogenesis

The TNBC cell line MDA-DB-231 is a highly tumorigenic and commonly used to investigate growth and metastasis of human breast cancer *in vivo*, by xenograft transplantation in immunocompromised mice [117]. By partially knocking out CCT2 using CRISPR/Cas9, tumor development was delayed by about 2 weeks compared to control cells. We were unable to obtain complete CCT2 knock out cell lines because full loss of CCT2 in this cell line was lethal. In addition to decreasing tumor growth in mice, partial loss of CCT2 also resulted in reduced client proteins like STAT3. These results agree with previous work that found CCT to be overexpressed in cancer cells compared to non-cancerous cells, with notably high expression in MDA-MB-231 cells [64], suggesting this cell line has a higher CCT dependency for growth and survival.

Overexpressing CCT2 in immortalized, untransformed breast epithelial cells induced morphological changes and increased migration, a phenotype also observed in this cell line when it undergoes EMT, suggesting that CCT could have a role as a driver of oncogenesis.

The role of CCT complex in oncogenesis has not been extensively explored yet, but there is an increasing trend in recently published work suggesting that CCT's role in cancers could be cancer specific. In addition to our findings on CCT2 overexpression in breast cancer, others have reported CCT2 to be elevated in gall bladder carcinoma [70], colorectal adenocarcinoma [103] and hepatocellular carcinoma [40]. Also in HCC, CCT3 was determined to be diagnostic in hepatocellular carcinoma [72, 79, 80], as well as CCT8 [39, 40]. Together, these data suggest that there might be a CCT subunit/cancer type correlation that should be further explored since understanding this relationship would help elucidate the process of oncogenesis and ultimately lead to better therapies.

The search for small molecules inhibitors of CCT

We developed an *in cell,* luminescence based assay for rapid screen of small molecules able to inhibit CCT and/or luciferase folding in TNBC cells. The assay was considered optimal based on the high z'factor obtained (z'factor =0.6) [108]. In a period of 2 months, 2100 small molecules were screened, in duplicates, yielding 24 hits. The number of hits obtained by this assay further validates our approach, since robust HTS assays are expected to yield 10% of the total number of screened molecules as hits. Secondary screens identified one lead compound which caused cell death in a dose

dependent manner in TNBC cells but only minimally affected immortalized breast epithelial cells. Unfortunately, the structure associated with the lead compound was inaccurate and we were unable to continue further characterizing of the lead molecule. Nonetheless, in this study, we developed and validated a high throughput screen assay that is relatively simple, cost effective and scalable, consequently establishing a new platform for the screening of larger libraries for potential inhibitor of CCT. Future studies will focus on developing an *in vitro* companion and/or secondary assay focused on CCT activity. Luciferase folding assay is commonly used to test CCT activity [61, 94], as a companion assay, it would be possible to screen for CCT inhibitors by combining results from the *in vivo* with the *in vitro* components by setting more lax thresholds and only considering the compounds above both thresholds as "hits". Alternatively, the *in vitro* component would serve as a secondary assay, for inhibitors of CCT that directly contact at least one of the eight subunits, thus, only true CCT inhibitors would continue further characterization. The approach we used to screen for CCT inhibitors *in vivo* using TNBC cell lines that stably express luciferase can be adapted to any cancer cell line capable of stably expressing luciferase, thus, the impact of this work expands well beyond breast cancer and could impact an array of different cancer types.

Concluding remarks

The discovery of CCT's role in cancer progression has crucial clinical implications in the development of personalized medicine for cancer therapy. TNBC and SCLC, both aggressive, highly metastatic cancers that currently lack efficient treatments, have the potential of being detected earlier by using CCT2 levels in biopsies and treated

effectively by targeting CCT as a therapeutic approach. Other cancers, such as prostate and hepatocellular can also benefit from CCT targeted therapies. Therefore, the findings presented in this dissertation provide a broad impact in the cancer field of research which can be translated into the clinic and ultimately on patients affected by these cancers. Because CCT subunits have different specificities and reports have shown they have different roles in several different disease states, understanding the role of each CCT subunit in normal cells as well as their role in different cancers is imperative and it will allow for rational drug design, tailored to each cancer type, with improved targeting capabilities and decreased off target effects. As an alternative, the development of medium and high- throughput screens aimed to identify CCT inhibitors in many cancers, such as the one presented in this dissertation which used TNBC cells, could yield novel therapeutics in a faster time-scale. Altogether, the work presented in this dissertation demonstrates the feasibility of CCT as a biomarker in many cancers, especially SCLC, the use of CT20p as a cancer therapeutic and that CCT2 has an essential role in cancer progression, significantly contributing to overall body of knowledge in the cancer field. Future work is focused on elucidating the inhibitory mechanism of CT20p at the cellular level and further exploring CCT as a molecular target for therapeutics.

APPENDIX A: CLINICAL CANCER RESEARCH
COPYRIGHT RELEASE

This Agreement between University of Central Florida -- Ana Carr ("You") and American Association for Cancer Research ("American Association for Cancer Research") consists of your license details and the terms and conditions provided by American Association for Cancer Research and Copyright Clearance Center.

License Number	4223190358971
License date	Nov 06, 2017
Licensed Content Publisher	American Association for Cancer Research
Licensed Content Publication	Clinical Cancer Research
Licensed Content Title	Chaperonin Containing TCP-1 Protein Level in Breast Cancer Cells Predicts Therapeutic Application of a Cytotoxic Peptide
Licensed Content Author	Rania Bassiouni,Kathleen N. Nemec,Ashley Iketani,Orielyz Flores,Anne Showalter,Amr S. Khaled,Priya Vishnubhotla,Robert W. Sprung,Charalambos Kaittanis,Jesus M. Perez,Annette R. Khaled
Licensed Content Date	Mar 24, 2016
Type of Use	Thesis/Dissertation
Requestor type	academic/educational
Format	print and electronic
Portion	figures/tables/illustrations
Number of figures/tables/illustrations	5
Will you be translating?	no
Circulation	1
Territory of distribution	North America
Title of your thesis / dissertation	Chaperonin Containing TCP1 (CCT) as a Target for Cancer Therapy
Expected completion date	Nov 2017
Estimated size (number of pages)	150
Requestor Location	University of Central Florida 6900 Lake Nona Blvd

ORLANDO, FL 32827 United States Attn: Annette Khaled |
| Billing Type | Invoice |
| Billing Address | University of Central Florida 6900 Lake Nona Blvd

ORLANDO, FL 32827 United States Attn: Annette Khaled |

115

REFERENCES

1. Global Burden of Disease Cancer, C., et al., *Global, Regional, and National Cancer Incidence, Mortality, Years of Life Lost, Years Lived With Disability, and Disability-Adjusted Life-years for 32 Cancer Groups, 1990 to 2015: A Systematic Analysis for the Global Burden of Disease Study.* JAMA Oncol, 2017. **3**(4): p. 524-548.

2. Howlader N, N.A., Krapcho M, Garshell J, Miller D, Altekruse SF, Kosary CL, Yu M, Ruhl J, Tatalovich Z, Mariotto A, Lewis DR, Chen HS, Feuer EJ, Cronin KA (eds), *SEER Cancer Statistics Review, 1975-2012.* based on November 2014 SEER data submission, posted to the SEER web site, April 2015, National Cancer Institute. Bethesda, MD: http://seer.cancer.gov/csr/1975_2012/,.

3. Society, A.C. *Cancer Facts & Figures 2017.* [cited 2017 08/04/2017].

4. Society, A.C., *Breast Cancer Facts & Figures 2017-2018.* American Cancer Society 2017.

5. Siegel, R.L., K.D. Miller, and A. Jemal, *Cancer Statistics, 2017.* CA Cancer J Clin, 2017. **67**(1): p. 7-30.

6. *American Cancer Society. Cancer Facts & Figures 2015.* 2015, American Cancer Society: Atlanta.

7. Demes, A.F.-E.a.M., *Neuroendocrine Tumors of the Lung.* Cancers 2012.

8. Carter, B.W., et al., *Small cell lung carcinoma: staging, imaging, and treatment considerations.* Radiographics, 2014. **34**(6): p. 1707-21.

9. Tartarone, A., et al., *Progress and challenges in the treatment of small cell lung cancer.* Med Oncol, 2017. **34**(6): p. 110.

10. Thomas N. Seyfried, a.L.C.H., *On the Origin of Cancer Metastasis.* Crit Rev Oncog, 2013: p. 43–73.

11. Bramati, A., et al., *Efficacy of biological agents in metastatic triple-negative breast cancer.* Cancer Treat. Rev., 2014. **40**(5): p. 605-613.

12. Cox, K., B. Alford, and H. Soliman, *Emerging Therapeutic Strategies in Breast Cancer.* South Med J, 2017. **110**(10): p. 632-637.

13. Kamb, A., S. Wee, and C. Lengauer, *Why is cancer drug discovery so difficult?* Nat Rev Drug Discov, 2007. **6**(2): p. 115-20.

14.   Boohaker, R.J., et al., *Rational Development of a Cytotoxic Peptide To Trigger Cell Death.* Mol.Pharm., 2012. **7**(9): p. 2080-2093.

15.   Lee, M.W., et al., *The CT20 peptide causes detachment and death of metastatic breast cancer cells by promoting mitochondrial aggregation and cytoskeletal disruption.* Cell Death Dis, 2014. **5**: p. e1249.

16.   Santra, S., C. Kaittanis, and J.M. Perez, *Cytochrome C encapsulating theranostic nanoparticles: a novel bifunctional system for targeted delivery of therapeutic membrane-impermeable proteins to tumors and imaging of cancer therapy.* Mol.Pharm., 2010. **7**(4): p. 1209-1222.

17.   Santra, S., C. Kaittanis, and J.M. Perez, *Aliphatic hyperbranched polyester: a new building block in the construction of multifunctional nanoparticles and nanocomposites.* Langmuir, 2010. **26**(8): p. 5364-5373.

18.   Bassiouni, R., et al., *Chaperonin Containing TCP-1 Protein Level in Breast Cancer Cells Predicts Therapeutic Application of a Cytotoxic Peptide.* Clin Cancer Res, 2016. **22**(17): p. 4366-79.

19.   Flores, O., et al., *PSMA-Targeted Theranostic Nanocarrier for Prostate Cancer.* Theranostics, 2017. **7**(9): p. 2477-2494.

20.   HARTL, F.U., *Molecular chaperones in cellular protein folding.* Nature, 1990.

21.   Leitner, A., et al., *The molecular architecture of the eukaryotic chaperonin TRiC/CCT.* Structure, 2012. **20**(5): p. 814-25.

22.   Spiess, C., et al., *Identification of the TRiC/CCT substrate binding sites uncovers the function of subunit diversity in eukaryotic chaperonins.* Mol Cell, 2006. **24**(1): p. 25-37.

23.   Reissmann, S., et al., *A gradient of ATP affinities generates an asymmetric power stroke driving the chaperonin TRIC/CCT folding cycle.* Cell Rep, 2012. **2**(4): p. 866-77.

24.   Yam, A.Y., et al., *Defining the TRiC/CCT interactome links chaperonin function to stabilization of newly made proteins with complex topologies.* Nat Struct Mol Biol, 2008. **15**(12): p. 1255-62.

25.   Thulasiraman, V., *In Vivo newly translated polyptides are sequestered in a protected folding environment.* 1999.

26.   Joachimiak, L.A., et al., *The structural basis of substrate recognition by the eukaryotic chaperonin TRiC/CCT.* Cell, 2014. **159**(5): p. 1042-55.

27.   Shuin, T., et al., *Frequent somatic mutations and loss of heterozygosity of the von Hippel-Lindau tumor suppressor gene in primary human renal cell carcinomas.* Cancer Res, 1994. **54**(11): p. 2852-5.

28.   Kasembeli, M., et al., *Modulation of STAT3 folding and function by TRiC/CCT chaperonin.* PLoS Biol, 2014. **12**(4): p. e1001844.

29.   Lopez-Barneo, J., R. Pardal, and P. Ortega-Saenz, *Cellular mechanism of oxygen sensing.* Annu Rev Physiol, 2001. **63**: p. 259-87.

30.   Gossage, L., T. Eisen, and E.R. Maher, *VHL, the story of a tumour suppressor gene.* Nat Rev Cancer, 2015. **15**(1): p. 55-64.

31.   D.E. Feldman, V.T., R.G. Ferreyra, J. Frydman, *Formation of the VHL-elongin BC tumor suppressor complex is mediated by the chaperonin TRiC.* Mol Biol Cell, 1999.

32.   Vogelstein, B., Sur, S. & Prives, C. , *p53: The Most Frequently Altered Gene in Human Cancers.* Nature Education 2010.

33.   Trinidad, A.G., et al., *Interaction of p53 with the CCT complex promotes protein folding and wild-type p53 activity.* Mol Cell, 2013. **50**(6): p. 805-17.

34.   K.A. Won, R.J.S., G.W. Farr, A.L. Horwich, S.I. Reed, *Maturation of human cyclin E requires the function of eukaryotic chaperonin CCT.* Mol Biol Cell, 1998.

35.   A. Camasses, A.B., A. Shevchenko, W. Zachariae, *The CCT chaperonin promotes activation of the anaphase-promoting complex through the generation of functional Cdc20.* Mol Biol Cell, 2003.

36.   Paul, D., et al., *Cdc20 directs proteasome-mediated degradation of the tumor suppressor SMAR1 in higher grades of cancer through the anaphase promoting complex.* Cell Death Dis, 2017. **8**(6): p. e2882.

37.   Dang, C.V., *MYC on the path to cancer.* Cell, 2012. **149**(1): p. 22-35.

38.   Kamran, M.Z., P. Patil, and R.P. Gude, *Role of STAT3 in cancer metastasis and translational advances.* Biomed Res Int, 2013. **2013**: p. 421821.

39.   Huang, X., et al., *Chaperonin containing TCP1, subunit 8 (CCT8) is upregulated in hepatocellular carcinoma and promotes HCC proliferation.* APMIS, 2014. **122**(11): p. 1070-9.

40.   Yokota, S., et al., *Increased expression of cytosolic chaperonin CCT in human hepatocellular and colonic carcinoma.* Cell Stress Chaperones, 2001. **6**(4): p. 345-50.

41. Guest, S.T., et al., *Two members of the TRiC chaperonin complex, CCT2 and TCP1 are essential for survival of breast cancer cells and are linked to driving oncogenes.* Exp Cell Res, 2015. **332**(2): p. 223-35.

42. Howlader, N., et al., *SEER Cancer Statistics Review, 1975-2014.* 2016: National Cancer Institute. Bethesda, MD, https://seer.cancer.gov/csr/1975_2014/, based on November 2016 SEER data submission, posted to the SEER web site, April 2017.

43. Waqar, S.N. and D. Morgensztern, *Treatment advances in small cell lung cancer (SCLC).* Pharmacol Ther, 2017.

44. Arnedos, M., et al., *Triple-negative breast cancer: are we making headway at least?* Ther Adv Med Oncol, 2012. **4**(4): p. 195-210.

45. Sorensen, M., et al., *Small-cell lung cancer: ESMO Clinical Practice Guidelines for diagnosis, treatment and follow-up.* Ann Oncol, 2010. **21 Suppl 5**: p. v120-5.

46. Demedts, I.K., K.Y. Vermaelen, and J.P. van Meerbeeck, *Treatment of extensive-stage small cell lung carcinoma: current status and future prospects.* Eur Respir J, 2010. **35**(1): p. 202-15.

47. Roviello, G., N. Sobhani, and D. Generali, *Bevacizumab in small cell lung cancer.* Ann Transl Med, 2017. **5**(17): p. 361.

48. Ma, X., et al., *Bevacizumab Addition in Neoadjuvant Treatment Increases the Pathological Complete Response Rates in Patients with HER-2 Negative Breast Cancer Especially Triple Negative Breast Cancer: A Meta-Analysis.* PLoS One, 2016. **11**(8): p. e0160148.

49. Stratigos, M., et al., *Targeting angiogenesis in small cell lung cancer.* Transl Lung Cancer Res, 2016. **5**(4): p. 389-400.

50. Peifer, M., et al., *Integrative genome analyses identify key somatic driver mutations of small-cell lung cancer.* Nat Genet, 2012. **44**(10): p. 1104-10.

51. Santarpia, M., et al., *Targeted drugs in small-cell lung cancer.* Transl Lung Cancer Res, 2016. **5**(1): p. 51-70.

52. Tatematsu, A., et al., *Epidermal growth factor receptor mutations in small cell lung cancer.* Clin Cancer Res, 2008. **14**(19): p. 6092-6.

53. Kijima, T., et al., *Regulation of cellular proliferation, cytoskeletal function, and signal transduction through CXCR4 and c-Kit in small cell lung cancer cells.* Cancer Res, 2002. **62**(21): p. 6304-11.

54.   Maulik, G., et al., *Activated c-Met signals through PI3K with dramatic effects on cytoskeletal functions in small cell lung cancer.* J Cell Mol Med, 2002. **6**(4): p. 539-53.

55.   Maulik, G., et al., *Modulation of the c-Met/hepatocyte growth factor pathway in small cell lung cancer.* Clin Cancer Res, 2002. **8**(2): p. 620-7.

56.   Lee, J.H., et al., *Differential expression of heat shock protein 90 isoforms in small cell lung cancer.* Int J Clin Exp Pathol, 2015. **8**(8): p. 9487-93.

57.   Byers, L.A., et al., *Proteomic profiling identifies dysregulated pathways in small cell lung cancer and novel therapeutic targets including PARP1.* Cancer Discov, 2012. **2**(9): p. 798-811.

58.   Xu, L., et al., *A meta-analysis of combination therapy versus single-agent therapy in anthracycline- and taxane-pretreated metastatic breast cancer: results from nine randomized Phase III trials.* Onco Targets Ther, 2016. **9**: p. 4061-74.

59.   Komarova, N.L. and C.R. Boland, *Cancer: calculated treatment.* Nature, 2013. **499**(7458): p. 291-2.

60.   Narayanan, A., D. Pullepu, and M.A. Kabir, *The interactome of CCT complex - A computational analysis.* Comput Biol Chem, 2016. **64**: p. 396-402.

61.   Spiess, C., et al., *Mechanism of the eukaryotic chaperonin: protein folding in the chamber of secrets.* Trends Cell Biol, 2004. **14**(11): p. 598-604.

62.   Cong, Y., et al., *Symmetry-free cryo-EM structures of the chaperonin TRiC along its ATPase-driven conformational cycle.* EMBO J, 2012. **31**(3): p. 720-730.

63.   Meyer, A.S., et al., *Closing the folding chamber of the eukaryotic chaperonin requires the transition state of ATP hydrolysis.* Cell, 2003. **113**(3): p. 369-381.

64.   Boudiaf-Benmammar, C., T. Cresteil, and R. Melki, *The cytosolic chaperonin CCT/TRiC and cancer cell proliferation.* PLoS One, 2013. **8**(4): p. e60895.

65.   Zhao, X., X. Sun, and X.L. Li, *Expression and clinical significance of STAT3, P-STAT3, and VEGF-C in small cell lung cancer.* Asian Pac J Cancer Prev, 2012. **13**(6): p. 2873-7.

66.   Davidson, M.M., et al., *Novel cell lines derived from adult human ventricular cardiomyocytes.* J Mol Cell Cardiol, 2005. **39**(1): p. 133-47.

67.   Szasz, A.M., et al., *Cross-validation of survival associated biomarkers in gastric cancer using transcriptomic data of 1,065 patients.* Oncotarget, 2016. **7**(31): p. 49322-49333.

68. Gyorffy, B., et al., *An online survival analysis tool to rapidly assess the effect of 22,277 genes on breast cancer prognosis using microarray data of 1,809 patients.* Breast Cancer Res Treat, 2010. **123**(3): p. 725-31.

69. Lauwers, G.Y., et al., *Prognostic histologic indicators of curatively resected hepatocellular carcinomas: a multi-institutional analysis of 425 patients with definition of a histologic prognostic index.* Am J Sur Pathol, 2002.

70. Zou, Q., et al., *Clinicopathological features and CCT2 and PDIA2 expression in gallbladder squamous/adenosquamous carcinoma and gallbladder adenocarcinoma*
9. World J Surg.Oncol., 2013. **11**(1): p. 143.

71. D'Amico, D., et al., *High frequency of somatically acquired p53 mutations in small-cell lung cancer cell lines and tumors.* Oncogene, 1992. **7**(2): p. 339-46.

72. Zhang, Y., et al., *Molecular chaperone CCT3 supports proper mitotic progression and cell proliferation in hepatocellular carcinoma cells.* Cancer Lett, 2016. **372**(1): p. 101-9.

73. Lin, L., et al., *The STAT3 inhibitor NSC 74859 is effective in hepatocellular cancers with disrupted TGF-beta signaling.* Oncogene, 2009. **28**(7): p. 961-72.

74. Siddiquee, K., et al., *Selective chemical probe inhibitor of Stat3, identified through structure-based virtual screening, induces antitumor activity.* Proc.Natl.Acad.Sci.U.S.A, 2007. **104**(18): p. 7391-7396.

75. De Angelis, A., et al., *Doxorubicin cardiotoxicity and target cells: a broader perspective.* Cardio-Oncology, 2016. **2**(1).

76. Pfeifer, A.M., et al., *Simian virus 40 large tumor antigen-immortalized normal human liver epithelial cells express hepatocyte characteristics and metabolize chemical carcinogens.* Proc Natl Acad Sci U S A, 1993. **90**(11): p. 5123-7.

77. Meuwissen, R., et al., *Induction of small cell lung cancer by somatic inactivation of both Trp53 and Rb1 in a conditional mouse model.* Cancer Cell, 2003. **4**(3): p. 181-9.

78. Furukawa, M., et al., *Lung epithelial cells induce both phenotype alteration and senescence in breast cancer cells.* PLoS One, 2015. **10**(1): p. e0118060.

79. Cui, X., et al., *Overexpression of chaperonin containing TCP1, subunit 3 predicts poor prognosis in hepatocellular carcinoma.* World J Gastroenterol, 2015. **21**(28): p. 8588-604.

80. Qian, E.N., et al., *Expression and diagnostic value of CCT3 and IQGAP3 in hepatocellular carcinoma.* Cancer Cell Int, 2016. **16**: p. 55.

81.   Pan, X., et al., *Trivalent arsenic inhibits the functions of chaperonin complex.* Genetics, 2010. **186**(2): p. 725-34.

82.   Lin, Y.F., et al., *Intracellular beta-tubulin/chaperonin containing TCP1-beta complex serves as a novel chemotherapeutic target against drug-resistant tumors.* Cancer Res, 2009. **69**(17): p. 6879-88.

83.   Lin, Y.F., Y.F. Lee, and P.H. Liang, *Targeting beta-tubulin:CCT-beta complexes incurs Hsp90- and VCP-related protein degradation and induces ER stress-associated apoptosis by triggering capacitative Ca2+ entry, mitochondrial perturbation and caspase overactivation.* Cell Death Dis, 2012. **3**: p. e434.

84.   M.W. Lee, R.B., A. Iketani, O. Flores, J.M. Perez, A.R. Khaled, *The CT20 peptide: More than a Piece of Bax.* Cancer Cell & Microenvironment, 2014. **1**: p. e266.

85.   Zheng, Y., et al., *Arsenic trioxide (As(2)O(3)) induces apoptosis through activation of Bax in hematopoietic cells.* Oncogene, 2005. **24**(20): p. 3339-3347.

86.   Lai, C.H., et al., *HSP-90 inhibitor ganetespib is synergistic with doxorubicin in small cell lung cancer.* Oncogene, 2014. **33**(40): p. 4867-76.

87.   Gainor, J.F., et al., *Molecular Mechanisms of Resistance to First- and Second-Generation ALK Inhibitors in ALK-Rearranged Lung Cancer.* Cancer Discov, 2016. **6**(10): p. 1118-1133.

88.   Chatterjee, S., et al., *Acquired Resistance to the Hsp90 Inhibitor, Ganetespib, in KRAS-Mutant NSCLC Is Mediated via Reactivation of the ERK-p90RSK-mTOR Signaling Network.* Mol Cancer Ther, 2017. **16**(5): p. 793-804.

89.   Pfeiffer, M., et al., *Alternative implication of CXCR4 in JAK2/STAT3 activation in small cell lung cancer.* Br J Cancer, 2009. **100**(12): p. 1949-56.

90.   Qin, Y., et al., *Doxycycline reverses epithelial-to-mesenchymal transition and suppresses the proliferation and metastasis of lung cancer cells.* Oncotarget, 2015. **6**(38): p. 40667-79.

91.   Huang, W., et al., *Small-molecule inhibitors targeting the DNA-binding domain of STAT3 suppress tumor growth, metastasis and STAT3 target gene expression in vivo.* Oncogene, 2016. **35**(6): p. 802.

92.   Gautam K. Malhotra, X.Z., Hamid Band and Vimla Band, *Histological, molecular and functional subtypes of breast cancers.* Cancer Biology and Therapy, 2010.

93.   Fresia Pareja, F.C.G., Caterina Marchiò, Kathleen A Burke, Britta Weigelt and Jorge S Reis-Filho, *Triple-negative breast cancer: the importance of molecular*

and histologic subtyping, and recognition of low-grade variants. NPJ Breast Cancer, 2016.

94. Frydman, J., et al., *Function in protein folding of TRiC, a cytosolic ring complex containing TCP-1 and structurally related subunits.* EMBO J, 1992. **11**(13): p. 4767-78.

95. Gao, Y., et al., *A cytoplasmic chaperonin that catalyzes beta-actin folding.* Cell, 1992. **69**(6): p. 1043-50.

96. X. Liu, C.Y.L., M. Lei, S. Yan, T. Zhou, R.L. Erikson, *CCT chaperonin complex is required for the biogenesis of functional Plk1.* Mol Biol Cell, 2005.

97. Roh, S.H., et al., *Contribution of the Type II Chaperonin, TRiC/CCT, to Oncogenesis.* Int J Mol Sci, 2015. **16**(11): p. 26706-20.

98. Cichon, M.A., C.M. Nelson, and D.C. Radisky, *Regulation of epithelial-mesenchymal transition in breast cancer cells by cell contact and adhesion.* Cancer Inform, 2015. **14**(Suppl 3): p. 1-13.

99. Aguirre, A., Meyers, RM et al., *Genomic copy number dictates a gene-independent cell response to CRISPR-Cas9 targeting.* Cancer Discov, 2016.

100. Archibald, J.M., C. Blouin, and W.F. Doolittle, *Gene duplication and the evolution of group II chaperonins: implications for structure and function.* J Struct Biol, 2001. **135**(2): p. 157-69.

101. Amit, M., et al., *Equivalent mutations in the eight subunits of the chaperonin CCT produce dramatically different cellular and gene expression phenotypes.* J Mol Biol, 2010. **401**(3): p. 532-43.

102. Grantham, J., K.I. Brackley, and K.R. Willison, *Substantial CCT activity is required for cell cycle progression and cytoskeletal organization in mammalian cells.* Exp Cell Res, 2006. **312**(12): p. 2309-24.

103. Coghlin, C., et al., *Characterization and over-expression of chaperonin t-complex proteins in colorectal cancer.* J Pathol, 2006. **210**(3): p. 351-7.

104. Boohaker, R.J., et al., *The use of therapeutic peptides to target and to kill cancer cells.* Curr Med Chem, 2012. **19**(22): p. 3794-804.

105. Nathalie Malo, J.A.H., Sonia Cerquozzi, Jerry Pelletier & Robert Nadon, *Statistical practice in high-throughput screening data analysis.* Nature Biotechnology, 2006.

106.   Swen Hoelder, P.A.C., Paul WorkmanSwen Hoelder, Paul A. Clarke, Paul Workman, *Discovery of small molecule cancer drugs: Successes, challenges and opportunities.* Med Oncol, 2012.

107.   Boohaker, R.J., et al., *Rational development of a cytotoxic peptide to trigger cell death.* Mol Pharm, 2012. **9**(7): p. 2080-93.

108.   Ji-Hu Zhang, T.D.Y.C., Kevin R. Oldenburg, *A Simple Statistical Parameter for Use in Evaluation and Validation of High Throughput Screening Assays.* Journal of biomolecular screening 1999.

109.   Walters, W.P. and M. Namchuk, *Designing screens: how to make your hits a hit.* Nat Rev Drug Discov, 2003. **2**(4): p. 259-66.

110.   Miyata, Y., *Hsp90 inhibitor geldanamycin and its derivatives as novel cancer chemotherapeutic agents.* Current Pharmaceutical Design, 2005. **11**(9): p. 1131-1138.

111.   Sadikot, T., et al., *Development of a high-throughput screening cancer cell-based luciferase refolding assay for identifying Hsp90 inhibitors.* Assay Drug Dev Technol, 2013. **11**(8): p. 478-88.

112.   Chauhan, D., T. Hideshima, and K.C. Anderson, *Proteasome inhibition in multiple myeloma: therapeutic implication.* Annu Rev Pharmacol Toxicol, 2005. **45**: p. 465-76.

113.   Boschelli, F., et al., *A cell-based screen for inhibitors of protein folding and degradation.* Cell Stress Chaperones, 2010. **15**(6): p. 913-27.

114.   Knee, K.M., O.A. Sergeeva, and J.A. King, *Human TRiC complex purified from HeLa cells contains all eight CCT subunits and is active in vitro.* Cell Stress Chaperones, 2013. **18**(2): p. 137-44.

115.   Kubota, H., et al., *Structure and expression of the gene encoding mouse t-complex polypeptide (Tcp-1).* Gene, 1992. **120**(2): p. 207-15.

116.   Silver, L.M., et al., *Synthesis of mouse t complex proteins during haploid stages of spermatogenesis.* Dev Biol, 1987. **119**(2): p. 605-8.

117.   Christofori, A.F.a.G., *Mouse models of breast cancer metastasis.* Breast Cancer Research, 2006.